

Design and Fabrication of a High Precision Wafer Polishing Machine

by

Amir Torkaman

B.S., Mechanical Engineering, 1998
University of Florida

Submitted to the Department of Mechanical Engineering in partial fulfillment of the
requirements for the degree of

MASTER OF SCIENCE IN MECHANICAL ENGINEERING

at the
Massachusetts Institute of Technology
January 2000

[February 2000]

© Massachusetts Institute of Technology 2000. All rights reserved.

Signature of Author.....



Department of Mechanical engineering
January 30, 2000

Certified by.....



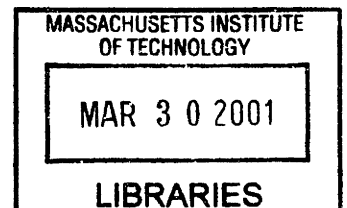
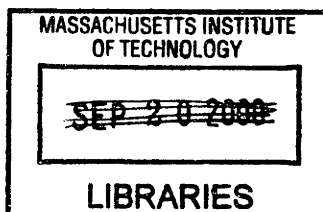
Ernesto Blanco
Adjunct Professor of Mechanical Engineering
Thesis Supervisor

Accepted by.....



Ain A. Sonin
Chairman, Department Committee on Graduate Students

ARCHIVES



Design and Fabrication of a High Precision Wafer Polishing Machine

By

Amir Torkaman

Submitted to the Department of Mechanical Engineering
On January 31, 2000 in Partial Fulfillment of the
Requirements for the Degree of

Master of Science in Mechanical Engineering

ABSTRACT

The objective of this project is to design and fabricate a full-scale Chemical-Mechanical Polishing machine, whose performance is much higher than that of the existing technology. The machine consists of a lower structure, an upper structure, and a polishing head. This thesis covers the design of the upper structure in detail. The machine was recently built and tested. The upper machine frame, which is the moving component of this polishing tool, was designed for maximum rigidity using FEA analysis. Vibrational analysis was also performed to design a mechanically quiet system. All of the associated components were designed with extreme precision in mind. In addition to the upper structure, a loading mechanism was also designed for the polishing head. Two high-precision linear drive mechanisms, the z-axis and the x-axis, were designed as the two major axes of motion for this machine tool. The z-axis applies the normal polishing force of 1500 lbs. This axis has a travel of 8", maximum velocity of 4 in/sec, resolution of 50 nm, and a repeatability of 0.0005". The z-axis applies the load using a pneumatic piston, in parallel with a "rotary" ball screw. The x-axis moves the upper machine structure, which weighs over 2000 lbs. The x-axis has a travel of 82", a maximum velocity of 12 in/sec, a maximum acceleration of 0.2g's, a resolution of 10 microns, and a repeatability of 0.002". The x-axis is driven on both sides with two separate motors and ball screws.

Thesis Supervisor: Ernesto Blanco

Title: Adjunct Professor of Mechanical Engineering

ACKNOWLEDGEMENTS

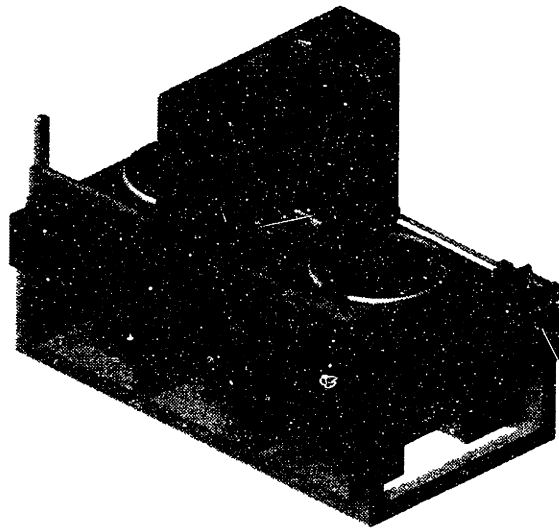
Once upon a time, a college freshman wrote his final English 101 essay about his future plans in life. He wrote about “graduating from MIT with a perfect GPA.” For him it was only a dream, which seemed absolutely ridiculous at the time. But the boy had a vision.... I was only 18 years old when I started my graduate studies at MIT. I am proud to say that I made it here 100% on my own, with no support. I took my chances, and it paid off.

There were three of us who started working on this research project at the same time: Jamie, Fardad, and myself. For the next two years we had the toughest time of our lives. *I loved MIT, and I loved my actual research project.* But lack of management, and personality conflicts turned this project into a nightmare! I have a lot of respect for my friend and lab-mate, Fardad, who ended up quitting this project after one year. I wish him the best of luck in life. Then there was Jason Melvin, the founder of the “Melvinistic” behavior: smart with an attitude! I still can’t figure out if I want to admire him or not! This kid is exceptionally talented, and I have learned more from him than anyone else ever.

I want to sincerely thank my family for their support. I couldn’t have done it without them. My father, my sister, and Lillian have always been there for me. I want to especially thank my brother who has always been my mentor. Furthermore, I want to dedicate this paper to my mom. I miss her, and I hope to be reunited with her soon.

I also want to thank my friends here at MIT: I really enjoyed watching Jamie and his best friend Dr. Saka “go at it” every week at our meetings. Farid is a teenager who’s

always looking for love! Fardad is the most annoying person I have ever met! But he is one hell of an intelligent person. Special thanks to my beautiful girlfriend Melissa, whom I feel very lucky to have met. I want to thank Lisa for putting up with all of our craziness. We owe you one Lisa! Finally, to the rest of my loser friends: Corey, Dave, Tang, Pankaj, Navid, Doug, etc. *get a life!*



I would like to sincerely thank the following faculty members for making this project possible:

- Prof. Jung-Hoon Chun
- Prof. Nam P. Suh
- Dr. Nannaji Saka

It was a pleasure for me to work with them on this project. I learned from them every single week. I would also like to specially thank my thesis supervisor Prof. Ernesto Blanco. He is an angel sent from the sky! I have learned a lot from his incredible experience and knowledge. I am honored to have had the pleasure of working with him.

TABLE OF CONTENTS

ABSTRACT	2
ACKNOWLEDGMENTS	3
TABLE OF CONTENTS	5
LIST OF FIGURES	9
CHAPTER 1: INTRODUCTION	11
1.1 BASIC DEFINITIONS.....	11
1.2 BACKGROUND ON CMP.....	12
1.3 COMPETITION: THE EXISTING TECHNOLOGY.....	14
1.4 DESIGN OF A SUPERIOR CMP MACHINE	16
1.4.1 <i>General Goals of the CMP Machine</i>	16
1.4.2 <i>Design Optimization</i>	17
1.4.3 <i>Performance Goals</i>	17
1.5 ESSENTIAL COMPONENTS OF THE CMP MACHINE	18
1.5.1 <i>The Velocity System</i>	19
1.5.1.1 [Within] Platen Motion System.....	20
1.5.1.2 Inter-Platen Motion System.....	20
1.5.2 <i>The Pressure Application System</i>	20
1.5.2.1 The Polishing-Head	21
1.5.2.2 The Force Application System.....	21
1.5.3 <i>End-Point Detection</i>	21
1.5.4 <i>Wafer Handling</i>	21
1.6 DESIGN OF THE TEST BED	22
1.7 OBJECTIVES OF THIS THESIS	23
CHAPTER 2: DESIGN OF THE Z-AXIS	25
2.1 BACKGROUND	25
2.2 CONCEPTUAL DESIGN	25
2.2.1 <i>Concept Generation</i>	25
2.2.1.1 Concept #1: Linear Motion.....	26
2.2.1.2 Concept #2: Rotary Motion	26
2.2.2 <i>Concept Selection</i>	27
2.3 DETAIL DESIGN OF THE Z-AXIS	28
2.3.1 <i>Supporting the Lateral Forces</i>	29
2.3.1.1 Conceptual Design.....	29
2.3.1.2 Selecting the Linear Guides	30
2.3.1.3 Mounting the Linear Guides	31
2.3.2 <i>Applying the Normal Polishing Force</i>	32
2.3.2.1 Conceptual Design.....	32

2.3.2.2	Selection of the Ball Screw.....	34
2.3.2.3	Buckling Analysis of the Z-Axis	34
2.3.2.4	Selection of the Pneumatic Cylinder.....	35
2.3.2.5	Selection of the Z-Axis Motor	35
2.3.2.6	Design of the Head Plate.....	35
2.3.2.7	Design of the Piston Attachment to the Head Plate.....	37
2.3.2.8	Design of the Z-Sensor Holder	38
2.3.2.9	Design of the Motor Timing Pulley	39
2.3.2.10	Design of the Ball Screw Timing Pulley	39
2.3.2.11	Selecting the Timing Belt	39
2.3.2.12	Design of the Z-Shaft Extender	39
2.3.2.13	Design of the Limit Switches.....	40
2.4	MODELING THE DYNAMICS OF THE Z-AXIS	40
CHAPTER 3: DESIGN OF THE X-AXIS.....		42
3.1	BACKGROUND	42
3.2	CONCEPTUAL DESIGN	42
3.2.1	<i>Concept Generation</i>	42
3.2.1.1	Concept #1: Linear Configuration	43
3.2.1.2	Concept #2: Rotary Configuration.....	43
3.2.2	<i>CONCEPT SELECTION</i>	44
3.3	DETAIL DESIGN OF THE X-AXIS	45
3.3.1	<i>Supporting the Lateral Forces</i>	45
3.3.1.1	Conceptual Design	45
3.3.1.2	Selection of the Linear Guides.....	46
3.3.1.3	Spacing of the Linear Guides.....	47
3.3.1.4	Mounting of the Linear Guides.....	48
3.3.2	<i>Applying the Driving Force for the X-Axis</i>	49
3.3.2.1	Concept Selection	49
3.3.2.2	Selection of the Ball Screws	51
3.3.2.2.1	Sizing the Ball Screws	51
3.3.2.2.2	Critical Velocity Calculations.....	52
3.3.2.2.3	End Machining of the Ball Screws	52
3.3.2.3	Selection of the Linear Encoder.....	54
3.3.2.4	Selection of the X-Axis Motor.....	55
3.3.2.5	Design of the Motor Bracket.....	56
3.3.2.6	Selection of the Flexible Coupling	57
3.3.2.7	Selection of the Ball Screw Bearings.....	57
3.3.2.8	Design of the Bearing Housing.....	58
3.3.2.9	Selection of the Oil Seals.....	59
3.3.2.10	Design of the X-Sensor Bracket	59
3.3.2.11	Design of the Bearing Mounting.....	60
3.3.2.12	Design of the Limit Switches.....	61
3.4	MODELING THE DYNAMICS OF THE X-AXIS.....	61
CHAPTER 4: DESIGN OF THE UPPER MACHINE STRUCTURE.....		62
4.1	BACKGROUND	62

4.2	CONCEPTUAL DESIGN	63
4.2.1	<i>Concept Generation</i>	63
4.2.1.1	Concept #1: The L-Shaped Structure.....	63
4.2.1.2	Concept #2: The Reduced-Footprint Design	64
4.2.1.3	Concept #3: The Gantry Structure	64
4.2.1.4	Concept #4: The Symmetrical Gantry Structure.....	65
4.2.2	<i>Concept Selection</i>	66
4.3	DETAIL DESIGN OF THE UPPER MACHINE STRUCTURE	67
4.3.1	<i>Exploded View of the Gantry Structure</i>	68
4.3.2	<i>Key Features & Tolerancing</i>	69
4.3.2.1	X-Reference Surface	69
4.3.2.2	Z-Reference Surface	69
4.3.2.3	Z-Reference Edge	70
4.3.2.4	Z-Ball Nut Mounting	70
4.3.2.5	Z-Motor Mounting.....	71
4.3.2.6	Z-linear Encoder Mounting.....	71
4.3.2.7	X-Ball nut mounting	72
4.3.2.8	X-linear encoder mounting	72
4.3.2.9	Cable Carriers and Wiring Holes.....	72
4.3.3	<i>Design of the Associated Components</i>	73
4.3.3.1	Design of the Spacer A	73
4.3.3.2	Design of the Spacer B	73
4.3.3.3	Selection of the Cable Carriers	74
4.3.3.4	Design of the Roof-Cover Plate.....	74
4.3.3.5	Design of the Side-Cover Plates	74
4.4	FABRICATION PROCESS	76
4.5	STRUCTURAL DESIGN USING FINITE-ELEMENT ANALYSIS	76
4.5.1	<i>Evolution to the Final Design</i>	77
4.6	VIBRATIONAL ANALYSIS OF THE UPPER STRUCTURE.....	79
CHAPTER 5: DESIGN OF THE LOAD/UNLOAD STATION		82
5.1	DESIGN SPECIFICATIONS	82
5.2	EXISTING TECHNOLOGY	83
5.3	DETAIL DESIGN OF THE LOAD/UNLOAD STATION	85
5.3.1	<i>Supporting Surface</i>	85
5.3.2	<i>Centering Mechanism</i>	86
5.3.2.1	Concept 1: Constraining the Wafer in a Repeatable Circle	86
5.3.2.2	Concept 2: Directly Touching the Edge of the Wafer	88
5.3.3	<i>Retraction Mechanism</i>	89
5.3.3.1	Concept 1: Separate Actuators.....	89
5.3.3.2	Concept 2: Belt Drive	90
5.3.3.3	Concept 3: Kinematic Linkage	90
5.3.4	<i>Wafer Holding Mechanism</i>	91
5.3.4.1	Concept #1: Vacuum.....	91
5.3.4.2	Concept #2: Vertical Motion of the Pins	92
5.4	OVERALL LOAD/UNLOAD STATION.....	93
5.5	DESIGN OF THE CONTROLS ALGORITHM.....	95

5.5.1	<i>Closed-Loop Kinematics Analysis</i>	95
5.5.2	<i>Application of Impedance Control in Impact Control</i>	96
5.5.3	<i>Dynamic Modeling of Impact</i>	98
5.5.4	<i>Matlab Simulations</i>	98
5.5.5	<i>Results and Discussion</i>	99
CHAPTER 6: AXIOMATIC DESIGN OF THE CMP MACHINE		102
6.1	INTRODUCTION TO AXIOMATIC DESIGN	102
6.2	AXIOMATIC DECOMPOSITION	103
6.2.1	<i>AXIOMATIC DECOMPOSITION OF THE Z-AXIS</i>	103
6.2.2	<i>AXIOMATIC DECOMPOSITION OF THE X-AXIS</i>	107
6.3	THE OVERALL CMP MACHINE.....	111
6.3.1	<i>Final Design</i>	111
6.3.2	<i>Upper Structure</i>	112
6.3.3	<i>Lower Structure</i>	112
6.3.4	<i>Polishing Head</i>	114
6.3.5	<i>End-Point Detection</i>	116
CHAPTER 7: FABRICATION AND DEBUGGING.....		117
7.1	DEBUGGING.....	117
7.2	ASSEMBLY	120
7.2.1	<i>Assembly of the Z-Axis</i>	120
7.2.2	<i>Assembly of the X-Axis</i>	122
7.2.3	<i>Assembly of the Upper Machine Structure</i>	124
7.2.4	<i>Assembly of the Load/Unload Station</i>	125
7.3	TESTING	126
7.3.1	<i>Velocity, Acceleration, and Smoothness</i>	126
7.3.1.1	<i>X-Axis Smoothness</i>	126
7.3.1.2	<i>Z-Axis Smoothness</i>	129
7.3.2	<i>Frequency Response Analysis</i>	131
7.3.3	<i>Accuracy, Resolution, and Repeatability</i>	132
7.3.3.1	<i>X-Axis Repeatability</i>	133
7.3.4	<i>Z-Axis Repeatability</i>	134
APPENDIX.....		136

LIST OF FIGURES

Figure 1.1: 200 mm Patterned Wafer	11
Figure 1.2: Semiconductor Wafer Processing	13
Figure 1.3: Previously Designed Test-Bed	23
Figure 2.1: Concept #1, Linear Motion	26
Figure 2.2: Concept #2, Rotary Motion	26
Figure 2.3: Internal Moments	28
Figure 2.4: Linear Guides	29
Figure 2.5: Forces Actin on the Wafer	30
Figure 2.6: Concept #1 and #2	33
Figure 2.7: Max. Deflection of Head Plate (3.2E-4m)	36
Figure 2.8: Max. Deflection of Head Plate (9.1E-6m)	37
Figure 3.1: Concept #1, The Linear Configuration	43
Figure 3.2: Concept #2: The Rotary Configuration	43
Figure 3.3: Natural Frequency of the Ball Screw	52
Figure 3.4: Driving End of the Ball Screw	53
Figure 3.5: Free End of the Ball Screw	54
Figure 3.6: Motor Bracket	56
Figure 3.7: Bearing Housing	58
Figure 4.1: Lower and Upper Structure of the CMP Machine (Concept)	62
Figure 4.2: concept #1	63
Figure 4.3: concept #2	64
Figure 4.4: Concept #3	64
Figure 4.5: Concept #4	65
Figure 4.6: Bending Moments Acting on the Upper Structure	66
Figure 4.7: Exploded View of the Gantry structure	68
Figure 4.8: Assembly View of the Upper Machine Structure	75
Figure 4.9: Meshed Model of the Gantry	77
Figure 4.10: Maximum Deflection of the Gantry Structure	78
Figure 4.11: Maximum Stress on the Gantry Structure	79
Figure 4.12: Natural Frequency of the Gantry	80
Figure 4.13: Maximum Deflection of the Gantry	81
Figure 5.1: Supporting Surface of the Load/Unload Station	86
Figure 5.2: Concept #1	87
Figure 5.3: Concept #2	88
Figure 5.4: Centering Mechanism	89
Figure 5.5: Retraction Mechanism	90
Figure 5.6: Wafer Handling Mechanism	92
Figure 5.7: Overall Load/Unload Station	93
Figure 5.8: Assembly Drawing of the Load/Unload Station	94
Figure 5.9: Four-Bar Linkage	96
Figure 5.10: Motor Angle vs. Arm Position	96
Figure 5.11: Closed-Loop Impact Control	97
Figure 5.12: Collision Model	98

Figure 5.13: Impact Force vs. Time	99
Figure 5.14: Open-Loop Impact	100
Figure 5.15: Closed-Loop Impact control	100
Figure 6.1: The CMP Machine	111
Figure 6.2: Lower Structure Assembly	113
Figure 6.3: Platen Assembly	114
Figure 6.4: Head Platen	115
Figure 6.5: Polishing Head Assembly	115
Figure 6.6: End-Point Detection Assembly	116
Figure 7.1: Z-Axis Assembly	122
Figure 7.2: X-Axis Assembly without the Actual Gantry	123
Figure 7.3: X-Axis Assembly	124
Figure 7.4: Upper Machine Structure Assembly	125
Figure 7.5: Load/Unload Station Assembly	126
Figure 7.6: X-Axis Position	127
Figure 7.7: X-Axis Velocity	128
Figure 7.8: X-Axis Acceleration	128
Figure 7.9: Z-Axis Position	129
Figure 7.10: Z-Axis Velocity	130
Figure 7.11: Z-Axis Acceleration	130
Figure 7.12: Frequency Response of the X-Axis	132
Figure 7.13: X-Axis Repeatability Measurements	133
Figure 7.14: Z-Axis Repeatability Measurements	134

CHAPTER 1: INTRODUCTION

1.1 *BASIC DEFINITIONS*

This thesis will cover the design of the x-axis, the z-axis, the upper machine structure, and the loading mechanism of a precision wafer-polishing machine. The goal of this project was to design and fabricate a CMP (Chemical Mechanical Polishing) machine to polish and planarize silicon wafers.

A chip, sometimes called an IC or integral circuit, is an incredibly complex, yet tiny module that stores computer memory or provides logic circuitry for microprocessors such as the Pentium microprocessors from Intel. A chip is manufactured from a silicon wafer (or in some special cases a sapphire wafer), which is first cut to size and then etched with circuits and electronic devices.

A wafer is a thin slice of semi-conducting material, such as a silicon crystal, upon which microcircuits are constructed by the diffusion and deposition of various materials. Millions of individual circuit elements, constituting hundreds of microcircuits, may be constructed on a single wafer. The individual microcircuits are separated by scoring and breaking the wafer into individual chips (dice).

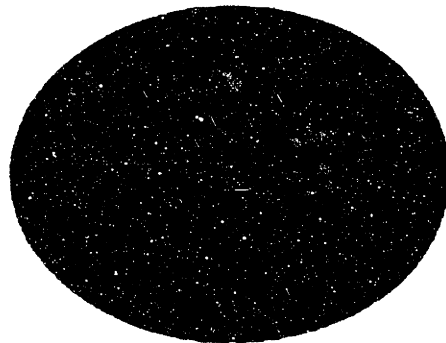


Figure 1.1 : 200 mm Patterned Wafer

As semiconductor manufacturing technology progresses, it is characterized by diminishing critical dimensions and tighter photo-lithographic depth of focus windows caused by the need to resolve these shrinking features. Previously inconsequential variations in the surface of the wafer, together with minimum required film thickness' and greater numbers of film layers, are shrinking the effective window of operation of the photolithography process. In sequence, process steps that apply and extend existing semiconductor manufacturing techniques have been introduced. Their sole purpose is to planarize the surface of a given thin film and try to reclaim some of the process window. However, these steps only affect relatively local regions of a film on a silicon wafer (Altman, Thesis-Abstract).

Chemical-Mechanical Polishing (CMP) is a method of achieving global film planarization, using technology adopted from the precision grinding and lapping industry. By polishing an entire wafer, it is possible to achieve an unprecedented degree of thin film smoothness. However, CMP is a process technology for which the underlying physical understanding is weak, and which has many control variables (Altman, thesis--Abstract).

1.2 **BACKGROUND ON CMP**

It has taken a long time for some U.S. chip makers to make the switch to CMP, or Chemical Mechanical Polishing. But now, they need major improvements in the process to turn out new generations of chips. For some emerging chip technologies, CMP will be absolutely required, according to process developers [Lineback 16].

In the beginning, wafer fab managers understandably were nervous about using CMP. It took plenty of nerve to place partly processed wafers face down in a solution of

silica or alumina and then grind them flat for the next process step. But it worked, and more and more fabs are now using CMP as device geometries shrink below a quarter micron and layers of interconnect grow [Lineback, 16]. CMP is usually the manufacturing process between metal deposition and lithography. The following figure shows how CMP fits into the whole IC manufacturing process.

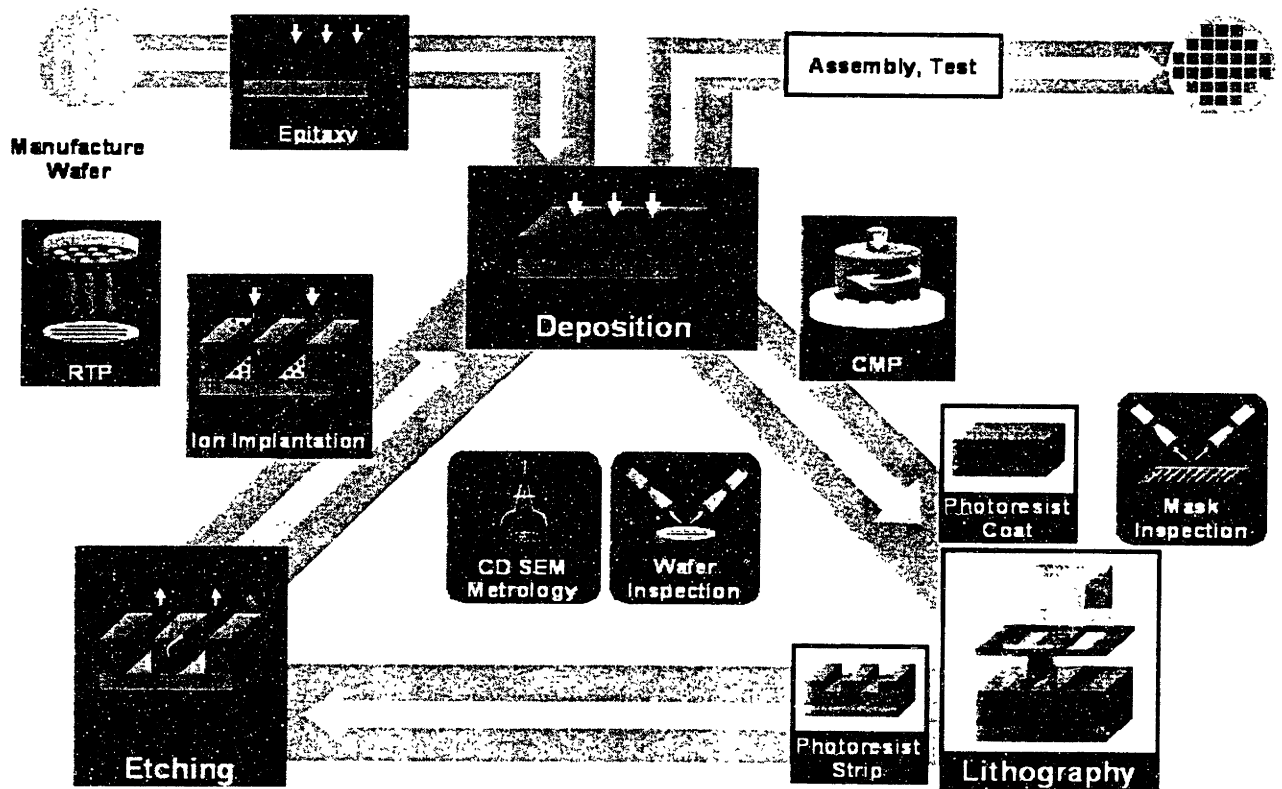


Figure 1.2: Semiconductor Wafer Processing

Planarization is becoming a critical factor in the photolithography steps for making transistors in front-end-of-the-line (FOEL) processes. With device feature sizes dropping to 0.18 micron and below, the depth of field in lithography also shrinks. This makes the ultra-smooth surfaces that CMP can turn out a crucial requirement in the fabrication of shallow-trench isolation structures and polygates [Lineback 16].

Chemical Mechanical Polishing is the fastest growing process technology in IC manufacturing. Over the past three years, worldwide sales have more than tripled. This places considerable demands on the growing number of manufacturers to increase overall productivity of their tool sets [DeJule 56].

1.3 **COMPETITION: THE EXISTING TECHNOLOGY**

As the industry gains confidence and learns more about CMP, tool suppliers are attempting to improve and fine tune the technology by changing the way these tools work. There are currently 20 CMP equipment suppliers, 12 from the Pacific Rim and 2 from Europe. The remainder are American. Five companies dominate the field with 90% of the market: Applied Materials (Santa Clara, Calif.), Ebara (Tokyo, Japan), IPEC Planar (Phoenix, Ariz.), Speedfam (Chandler, Ariz.) and Strasbaugh (San Luis Obispo, Calif.) [DeJule 57].

Polishing technologies typically use rotary, orbital, or linear mechanical motion coupled with an inert abrasive in a chemical solution. The different methods attempt to strike a balance among removal rate, planarization, and within wafer uniformity through a combination of pressure, speed, and pad hardness. Generally, a harder pad improves local (“within-die”) planarization; however, “within-wafer-uniformity” declines when the pad fails to conform to the surface. A softer pad promotes better global planarization. Similarly, a combination of high pressure and speed will increase removal rates, whereas when pressure is reduced, planarization improves, but uniformity declines [DeJule 57].

Most CMP technologies use rotary motion, and one IPEC Planar, uses a combination of orbital and rotational motion. The wafer head rotates in a circular path, while the polish head is orbital. The net effect is that each point on the pad traces a

spirographic trajectory. This configuration facilitates direct slurry delivery to the wafer surface while maintaining high relative velocities and a small overall tool footprint [DeJule 57].

The need for greater precision in tools is causing CMP suppliers to expand their options for end-point detection systems, real-time control, and in-situ metrology. The hope here is to be able to not only measure wafers as they complete CMP polishing but also to feed the results back to the control systems, which would help to adjust the tool setting for the next batch of wafers. Applied Materials Inc. recently added a second in-situ metrology option to its Mirra CMP systems that measure layer thickness while the wafers are still wet and inside the tool. They use an embedded system from Israel's Nova Measuring Instruments Ltd. A dry measurement system from Nanometric Inc. in Sunnyvale, Calif., is also available to compare pre- and post-polishing thickness [Lineback 19].

To meet the demands of the next-generation devices, toolmakers have implemented multi-step processing capabilities, new polishing head designs, end-point detection, and dry-in/dry-out platforms. More stringent requirements are also driving technologies such as belt polishing and slurry-less technologies [DeJule 57].

In the past two years, the considerable improvement seen in uniformity and edge exclusion is equally attributable to advances in consumables and the polishing tool. The most significant tool contribution was in carrier design [DeJule 57].

1.4 **DESIGN OF A SUPERIOR CMP MACHINE**

1.4.1 General Goals of the CMP Machine

The main requirement of the CMP machine is to maximize Return of Investment (ROI), where ROI is defined as,

$$\text{ROI} = (\text{Value Added} - \text{Cost of Operation})(\text{Net Wafers Per Hour})(\text{Machine Life}) / \text{Capital Investment}$$

Maximizing the *Value Added* can be achieved by having a flexible and integrated system. The requirement to maximize the Value Added is satisfied through customer perception, which is currently the integration of the polish, cleaning, and metrology in one station. Cost of Operation (COO) is defined as,

$$\text{COO} = \text{Materials} + \text{Operational Activities} + \text{Overhead}$$

Where Materials include, for example, slurry and the pad, the Operational Activities include the transport, manual operations, and setup of the machine. Overhead is the footprint of the machine. It is desired to minimize the Cost of Operation. Minimizing each individual element of the above formula does this.

Minimizing Investment requires a production-optimized machine design, which begins with a functionally complete machine and evolves the design, using cost reduction methods in particular, to reduce the manufacturing cost of the tool. Ultimately, this leads to reduced selling price. Net Wafers Per Hour is defined as,

$$\text{Net Wafers per Hour} = \text{Availability} * \text{Throughput} * \text{Yield}$$

Maximizing each individual element of the above formula will maximize Net Wafer per Hour. Using leading-edge technology in the quickly progressing production environment maximizes the Machine Life.

1.4.2 Design Optimization

A further study of each of the elements discussed above will result in the following general *design goals* for the CMP machine:

- Maximize throughput
- Minimize footprint
- Optimize consumable use
- Reliable, robust design
- Allow flexible user interface
- Minimize costs of design, manufacturing, maintenance and operation
- Allow automated operation
- Maximize availability/reliability
- Make tool serviceable (easy access for maintenance)
- Make tool “user-friendly”
- Process cycle time
- Reduce scrap

1.4.3 Performance Goals

Design goals must be optimized and constrained to satisfy the given *performance goals*. The superiority of this CMP machine lies in satisfying the required *performance*, while optimizing the *design* (throughput, footprint, etc.). The specified performance goals include the following:

- Increase Material Removal Rate (MRR)
- Planarize Surface – die scale flatness

- Improve Within Wafer Non-Uniformity
- Surface quality – scratches & roughness
- Wafer-to-wafer variation (< 2%)
- Minimize over-polish and reduce dishing
- Clear 100 % of the land area

1.5 *ESSENTIAL COMPONENTS OF THE CMP MACHINE*

The polishing of the wafer is done through the “three-body aberration” process, in which the material removal rate (MRR) obeys the following relation (the Preston Equation):

$$\text{MRR} = k \cdot P \cdot V$$

Where “P” is the pressure on the surface of the wafer, “V” is the relative velocity between the wafer and the pad, and “k” is the Preston constant. Therefore, the Abrasive Removal Process, which is used to polish the wafers, can be decomposed into the following sub-systems:

- Velocity System to create the relative velocity
- Pressure Application System to apply the normal pressure

The basic task of the CMP machine is to create a relative velocity between the pad and the wafer, and to apply a normal pressure on the wafer. The velocity system and the force application system must be designed in such a way as to optimize the design goals listed in the previous section. To summarize, the break-up of the main design tasks is as follows:

- Polishing Head
- Platen Motion System

- Inter-Platen Motion System
- Slurry Distribution System
- Force Application System
- End-Point Detection
- Wafer Handling
- Lower Machine Structure
- Upper Machine Structure
- User Interface
- Control Axis

1.5.1 The Velocity System

To increase the Material Removal Rate, it is necessary for the velocity system to create high relative velocities. However, the key design specification is to keep a “uniform” velocity profile over the surface of the wafer. This requirement provides three options for motion: rotary, linear, and orbital systems.

In the rotary system, the wafer and the pad both rotate (in opposite directions). In the linear system, the wafer rotates, but the pad has a linear motion (often created by having two large platens with a belt in between). In the orbital system, both the head and the wafer rotate, but the wafer is not stationary, and instead moves around the pad.

After carefully studying each system, the rotary mechanism was chosen. The orbital system is very complicated to build, and the collected data shows that it has no advantages over the other systems. The rotary and the linear systems were both designed and built, and after testing the two, it was proven that the rotary system is simpler to design, and it polishes faster and more uniformly.

1.5.1.1 [Within] Platen Motion System

In the rotary system, there are two platens rotating at the same velocity, and the wafer is at an offset distance from the center of one of the platens. This will provide the uniform relative velocity that is required for the polishing of the wafer. The bottom platen rotates the pad and the supporting structure, and the head platen rotates the polishing head that holds the wafer. The rotation of the two platens with respect to each other is called the Platen Motion System. The details of this mechanism will be explained further in the next chapter.

1.5.1.2 Inter-Platen Motion System

A requirement of the machine is to have two different pads, enabling the user to use different slurries, or to use one pad to polish and the other to planarize. The system that moves the polishing head from one platen to the next is called the Inter-Platen Motion System. The second essential task of this system is to provide Wafer-Offset Oscillation. As the wafer is being polished, it is desirable to have a slow radial motion to improve uniformity. This is sometimes referred to as the Sweep Motion, which exists in all of the current CMP machines.

1.5.2 The Pressure Application System

To increase the Material Removal Rate, it is necessary for the pressure application system to apply a high normal pressure on the wafer. However, perhaps the most important feature of this CMP machine, which distinguishes it from the existing CMP machines, is the ability to control the pressure profile behind the wafer. This can be used to solve the biggest problem with CMP: Within Wafer Non-Uniformity and Flatness over

the surface of the wafer. The basic concept is to apply less pressure on the areas that are over-polished, thereby creating a flat and uniform material removal rate across the wafer.

1.5.2.1 The Polishing-Head

This is the device that holds the wafer in place throughout polishing and applies normal pressure on the wafer. The retainer ring keeps the wafer from slipping out, and the separate pressure bellows are used to apply different pressures on the back of the wafer. The details of this mechanism will be explained further ahead.

1.5.2.2 The Force Application System

The net polishing force of the wafer is applied by this mechanism. The polishing head applies the pressure on the wafer, and the Force Application System supports the loads of the polishing head. The other task of this system is to provide a vertical motion for the purpose of loading and unloading the wafer into the head.

1.5.3 End-Point Detection

A unique feature of this CMP machine is the End-Point-Detection System, which is used to detect the end of the polishing process. This is done to avoid over-polishing of the wafer.

1.5.4 Wafer Handling

Wafer handling or wafer transfer, is the mechanism that transfers the wafers when they are not being polished. It can be thought of as the robot that moves the wafers from the cassette to the polishing head, to load and unload, and then moves them to the

cleaning station if necessary. The latter can be ignored for this particular CMP machine since it will not have a cleaning station.

1.6 ***DESIGN OF THE TEST BED***

The actual polishing process that happens at the interface of the wafer and the pad is an unknown phenomenon. Even though it is assumed to be a “three-body aberration” process, and it has been modeled by the Preston equation ($MRR = k.P.V$), there are still many unknown parameters involved. As it was previously mentioned, CMP is a process for which the physical understanding is weak, and there are many control variables.

In designing the CMP machine, some fundamental understanding of the process is necessary. The machine must be designed to satisfy the requirements of the polishing process (i.e $P_{max} = 10$ psi). For this purpose, the CMP research group was divided into a ‘design’ team and a ‘process’ team. The task of the process team was to run experiments and get information about the polishing process, so that the design team could build a machine to satisfy those specifications. For this purpose, the Test Bed--a smaller and simpler version of a CMP machine--was built so that the process team might run experiments with it.

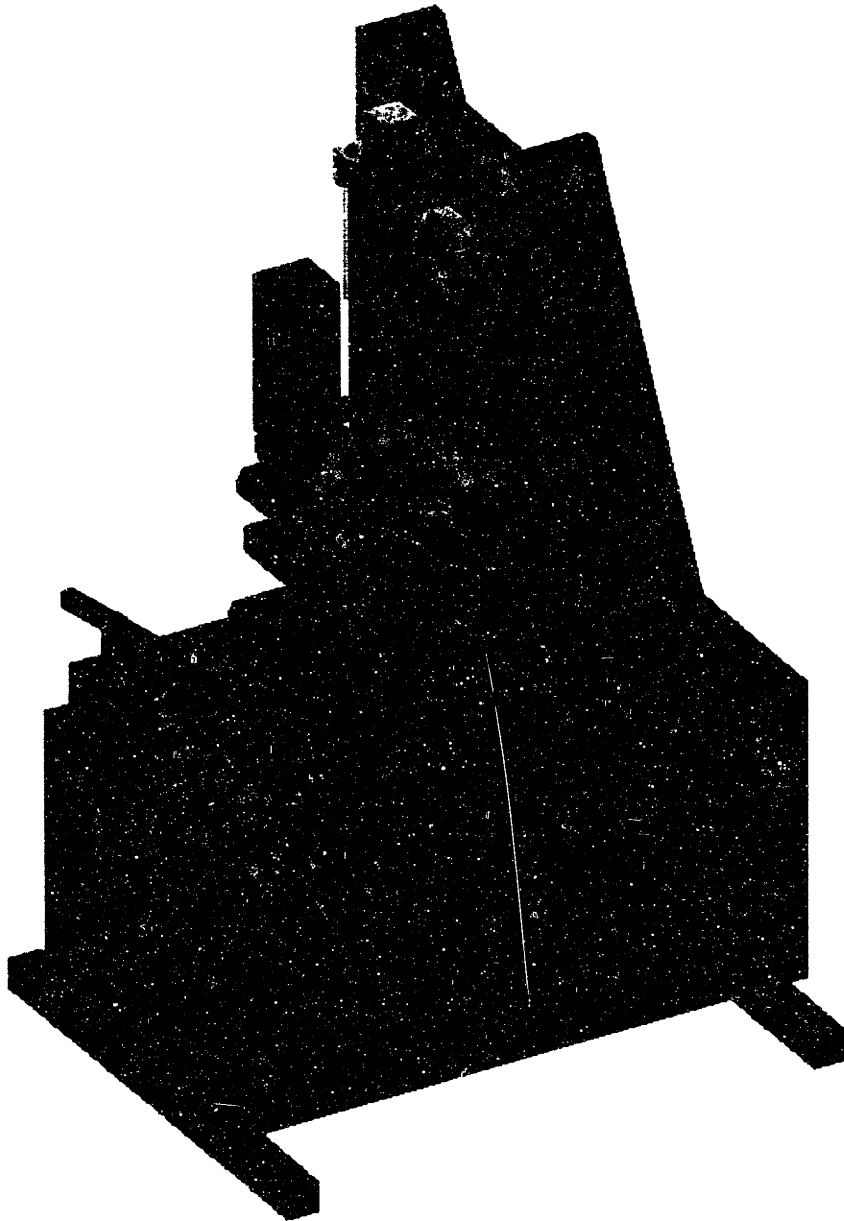


Figure 1.3: Previously Designed Test-Bed

1.7 OBJECTIVES OF THIS THESIS

This thesis will cover the design of the z-axis (Force Application System), x-axis (Inter-Platen Motion System), and the Load/Unload station. The other design tasks that were mentioned in the previous section will also be briefly discussed in the next few

chapters. It must be noted that all of the components must fit together to create one CMP machine, and therefore all of the design tasks are closely related. When designing a specific system, it is very important to consider the rest of the machine and to determine how each individual system will be integrated into the overall CMP machine. The final chapter of this thesis will cover the fabrication of the Upper Machine structure, the Inter-Platen Motion system, and the Force Application system. This chapter covers the physical assembly of the machine, the primary testings, the final testings and the debugging of individual components. This is referred to as the optimization process, which is the last step in completing the design of the machine.

CHAPTER 2: DESIGN OF THE Z-AXIS

2.1 BACKGROUND

The function of the z-axis, or the Force Application System, is to apply the normal polishing load, although the load is not directly applied to the back of the wafer. Since it is desirable to control the pressure profile behind the wafer, the polishing head must apply the pressure at different zones on the back of the wafer. The reaction force of the polishing head, which is the total polishing load, must be supported by the z-axis. The Force Application System is also responsible for directly applying the load on the retainer ring (the most outer ring) of the polishing head. The z-axis must allow enough movement in the vertical direction to load and unload the wafer into the polishing head, and to clear the conditioner when going from one platen to the next.

2.2 CONCEPTUAL DESIGN

2.2.1 Concept Generation

In designing the z-axis, two basic design concepts were generated at the early stages of determining the configuration and overall geometry of the machine. After carefully reviewing each one, the best concept was selected.

2.2.1.1 Concept #1: Linear Motion

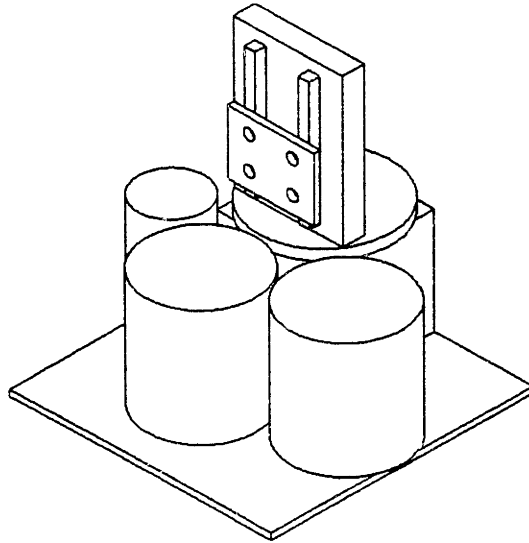


Figure 2.1: Concept #1, Linear Motion

In this concept the polishing head has a linear up and down motion, perpendicular to the surface of the pad.

2.2.1.2 Concept #2: Rotary Motion

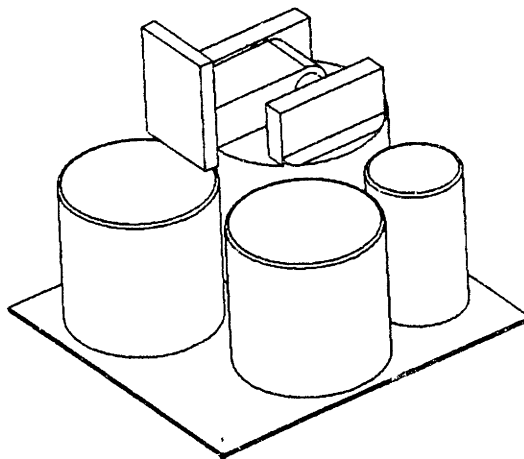


Figure 2.2: Concept #2, Rotary Motion

In this concept, the z-axis provides the vertical motion of the polishing head by rotating about a pivot-point in space.

2.2.2 Concept Selection

The advantage of concept #2 (rotary motion) is its simplicity. A motor and a gear head can apply the driving torque on a robotic arm, which is supported on a pair of bearings at its pivot-point. To assure that the polishing force at the end-effector is perfectly perpendicular to the pad, a gimbal mechanism (a universal joint) must be used. In concept #1 it is more difficult and more expensive to design linear actuators that can apply the required load.

The great advantage of concept #1, however, is that internal moments acting on the structure due to the normal polishing force can be minimized. In a rotary design, the reaction force acts at the center of the wafer, and it is supported at the pivot point of the robotic arm. This leaves a large distance between where the reaction load is applied and where it is supported, which leads to high internal moments acting on the upper structure. In a linear design, the load is applied at the center of the wafer, and it can also be supported directly above the center of the wafer. In other words, the applied normal load and its reaction are co-linear in space. This means that no internal moments will be created, and there will only be forces acting on the upper structure.

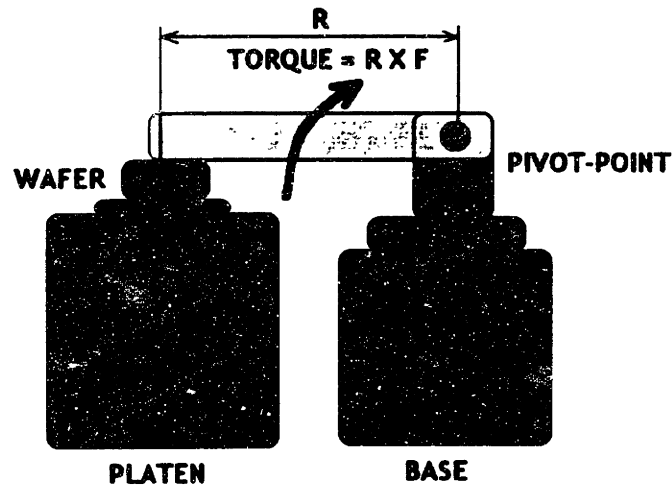


Figure 2.3: Internal Moments

If there are no internal moments acting on the upper structure, a number of advantages will be achieved. The motion of the z-axis can be controlled more accurately in such a case. The deflections of the structure will be significantly reduced since there are no bending moments present, and this will ultimately increase the precision of the machine. The rigidity of the structure is greatly increased, and the machine frame can be designed to be much less massive, which in turn reduces the cost and complexity of the system. The advantages offered by the linear motion in the Force Application System seem to be much greater than those of the rotary motion. Therefore, it was decided to make the Force Application System a linear axis of motion.

2.3 DETAIL DESIGN OF THE Z-AXIS

This system has two basic functions: applying the normal polishing force, and supporting the lateral forces and moments. This means that all of the other degrees of freedom must be constrained, and the system must be allowed to move *only* vertically.

2.3.1 Supporting the Lateral Forces

2.3.1.1 Conceptual Design

Since it was previously decided that the Force Application System must be a linear axis of motion, linear bearings must be used to support the lateral forces. The most important design goal here is to make the system as rigid as possible. The block of a linear guide sits on small circular balls that roll in the grooves provided on the rail. Since there is an actual physical contact between the balls and the rail, linear guides can offer tremendous stiffness in supporting normal forces. However, the stiffness of linear guides is not as high under bending moments, especially in the *roll* direction.

To improve the pitch and yaw stiffness of the system, usually *two blocks*, separated by a distance *A*, will be used for every rail. To improve the roll stiffness of the system, *two rails*, separated by a distance *B*, will be used. This is shown Figure 2.4.

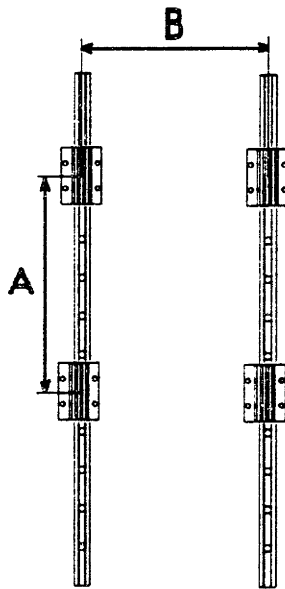


Figure 2.4: Linear Guides

The actuator must apply the driving force at the center of the two linear guides. In such a case, the guidance ratio of A/B becomes critical. For example, if B is much greater than A , the drive mechanism can possibly jam and get stuck, or the motion can have a lot of cogging. For such a mechanism, the ratio of A/B must be 1.5 to achieve the best motion. Anything lower may cause problems.

2.3.1.2 Selecting the Linear Guides

The next step is to calculate the loads acting on the linear guides. To do this, the external forces acting on the wafer must be first identified as shown in Figure 2.5.

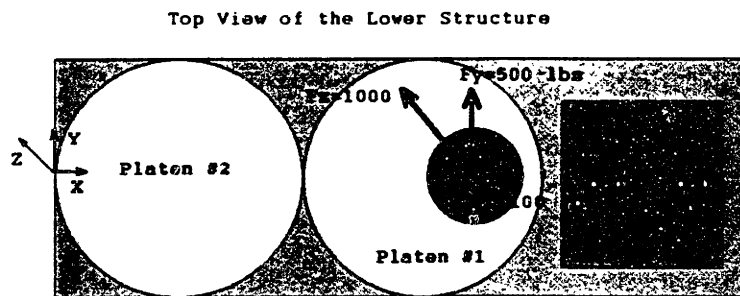


Figure 2.5: Forces Acting on the Wafer

The normal force is simply the maximum applied pressure (20-psi) multiplied by the surface area of an 8" wafer, which comes out to about 1000 lbs. The *magnitude* of the frictional force is calculated by multiplying the normal force by the coefficient of friction between the pad and the wafer, which is approximated to be 0.5. This is, of course, an overestimate of the coefficient of friction, which is usually about 0.2. This overestimation works as the safety factor for the load calculations. The *direction* of the frictional force is always in the direction of the relative velocity between the pad and the wafer. The relative velocity has one component along the y-axis, which is due to the

rotation of the two platens, and a smaller component along the x-axis, which is due to the *sweep motion* while polishing. After completing the analysis, the external forces that act on the wafer have been identified as:

- **$F_z = 1000$ lbs**
- **$F_y = 500$ lbs**
- **$F_x = 100$ lbs**

Using these forces, the loads and moments acting on the linear slides can now be approximated. Knowing these loads, the correct linear guides can be selected for the system. Detailed calculations are shown in the Appendix.

2.3.1.3 Mounting the Linear Guides

It is crucial for the linear guides to be *parallel* with each other, and *perpendicular* to the surface of the pad. To this end, the linear slides are both mounted on a flat reference plane, which is designed into the upper structure. This will assure the coplanarity of the two guides. The reference plane, which will be discussed in Chapter 4 “Design of the Upper Machine Structure,” is specified to be perpendicular to the surface of the pad. This assures that the two guides are perpendicular to the pad from the pitch direction (or the y-direction). To make them perpendicular in the remaining direction (the roll or x-direction), there will be a reference edge designed into the upper structure, which has been specified to be perpendicular to the surface of the pad. One of the linear slides can mount against this reference edge, and the other can be made parallel to it by moving the head-plate (which supports the upper platen) up and down several times and

tightening the bolts while doing so. The two guides will then be parallel to each other and perpendicular to the surface of the pad.

2.3.2 Applying the Normal Polishing Force

2.3.2.1 Conceptual Design

There are three basic linear *force* actuators that can be used to apply the normal force.

These actuators can also be used in parallel with each other to apply the load.

- Linear motor
- Pneumatic cylinder
- Motor and ball screw

To apply 1000 lbs, a large and extremely expensive linear motor would be required. A pneumatic cylinder alone would not have the positioning accuracy that is required for this system. Since the ultimate function of the z-axis is to hold the polishing head at a certain position during polishing, it must be able to support the polishing load as well. The positioning accuracy of the z-axis must be very high, and a pneumatic cylinder alone is not sufficient for position control. The z-axis will run a closed-loop control loop to hold the head at a constant offset from the pad. The pad has small bumps which act as disturbances on the system. The z-axis must have a very quick response time to account for the pad bumps, and a pneumatic cylinder does not have the required response time.

The only other possibility is to use a motor and a ball screw. This would be the easiest method of applying the load. A ball screw has a very high response time, and it is good for position control (whereas a pneumatic cylinder is good for force control).

Since the polishing load is very large, the motor would have to work continuously throughout the polishing period to keep a fixed position. This may lead to a lot of heat generation, and it may shorten the life of the motor. To solve this problem, a new concept was developed, in which a ball screw and a pneumatic cylinder are used in parallel to apply the load. The pneumatic cylinder would apply most of the load, and the ball screw would be used for fine tuning of the load, giving it the desired accuracy while not having to apply the entire load.

This concept was introduced right before freezing the final design. Because there are many unknowns about such a system, there was a great possibility that it would not work well. To avoid any problems later on, the design of the z-axis was focused on using a ball screw as the main force actuator. The motor and ball screw were sized to apply the entire polishing force. The pneumatic cylinder, however, was still integrated into the system to run experiments with the dual-actuator concept.

Furthermore, there are two possible methods of applying the load using a motor and a ball screw. Concept #1 would have the ball screw fixed and the nut moving, while concept #2 would have the nut fixed and the ball screw moving.

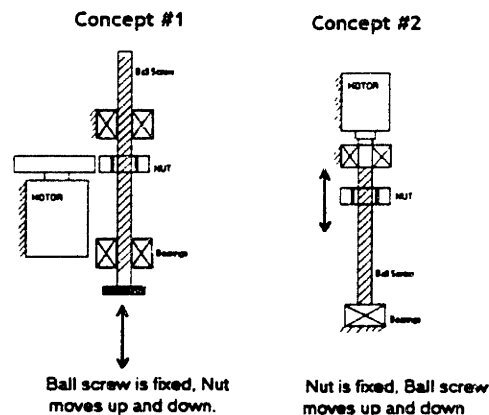


Figure 2.6: Concept #1 and #2

The main purpose of using a linear axis of motion was to eliminate bending moments. This can be achieved by applying the normal force along the same axis as that of the reaction force, which acts at the center of the wafer. To do this, concept #2 *must* be selected, since implementing concept #1 would require the ball screw to pass through the center of the head-plate, which is not possible. A ball screw drive mechanism in which the ball screw moves and the nut is held fixed is called a “rotary ball screw”. THK Inc. is one of the best manufacturers of such systems, in which the whole package has already been designed and can be readily purchased. The nut attaches to the fixed structure and the ball screw to the moving object. To turn the nut, two pulleys and a timing belt must be used. One pulley will be attached to the rotating nut, and the other to a motor. A timing belt transfers the torque between the two.

2.3.2.2 Selection of the Ball Screw

The ball screw was selected based on its axial load capacity. A ball screw with the smallest possible lead was desired so the motor could be downsized. The force and velocity calculations are shown in the Appendix. The ball screw was purchased from THK Inc.

2.3.2.3 Buckling Analysis of the Z-Axis

Since the axial load acting on the z-axis ball screw is very large (1500 lbs), and the diameter of the ball screw is relatively small (0.5”), there is a possibility that the ball screw may buckle under the load. This is not a concern for the x-axis, since the axial load is low and the ball screw is larger in diameter. The buckling analysis that was performed to assure the safety of the z-axis ball screw is shown in the Appendix.

2.3.2.4 Selection of the Pneumatic Cylinder

The available air pressure in a clean room for a CMP machine is about a 100 psi. Knowing the load applied on the pneumatic cylinder, the size of the piston was calculated to be about 3". This size, along with the range of motion of the z-axis, were used to select a pneumatic cylinder.

2.3.2.5 Selection of the Z-Axis Motor

Since this motor was to be placed on the roof of the upper structure, it was important for it to be as short as possible. For this purpose, Platinum XT motors from Kollmorgen were selected since they meet the height constraints. These motors also have great performance criteria, such as zero cogging torque and high smoothness. Using the load on the z-axis, the pitch of the ball screw, and the transmission ratio between the two pulleys, the torque on the motor was calculated. This was matched by the stall torque of a Platinum XT motor.

2.3.2.6 Design of the Head Plate

The head plate is the supporting structure for the head platen. The head platen consists of a frameless motor that spins the polishing head. The task of the head plate is to provide mounting for the motor. It must be attached to the linear guides from one side, and the ball screw must be able to push down on it.

The simplest concept was to have an L-structure, which is attached to the guides from the back and to the ball screw from the top. To add rigidity to the structure, two triangular flanges were added to the sides, connecting the top to the back. A quick FEA analysis was done to test for the deflections of this structure.

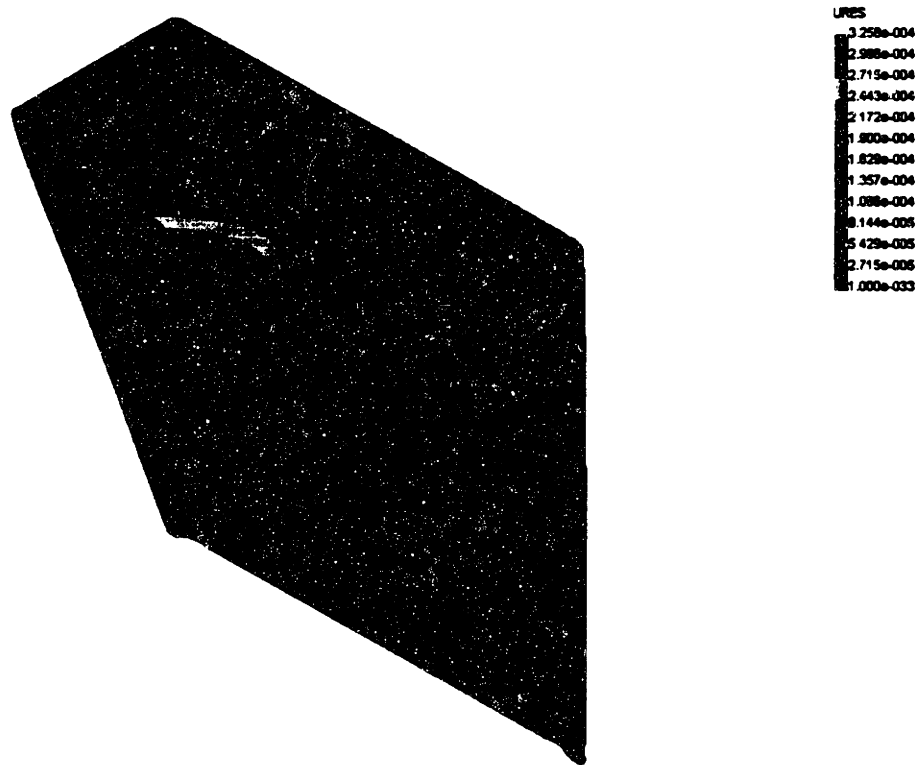


Figure 2.7: Max. Deflection of Head Plate (3.2E-4 m)

Even though the head plate was made of $\frac{1}{2}$ " thick stainless steel plates, the deflections were still too high, due to the large downward force applied by the ball screw. An additional 'lip' was therefore added to the front of the head plate to increase the moment of inertia of the structure in the direction that it was bending the most. The FEA analysis shows that the addition of the lip has significantly reduced the deflections of the structure.

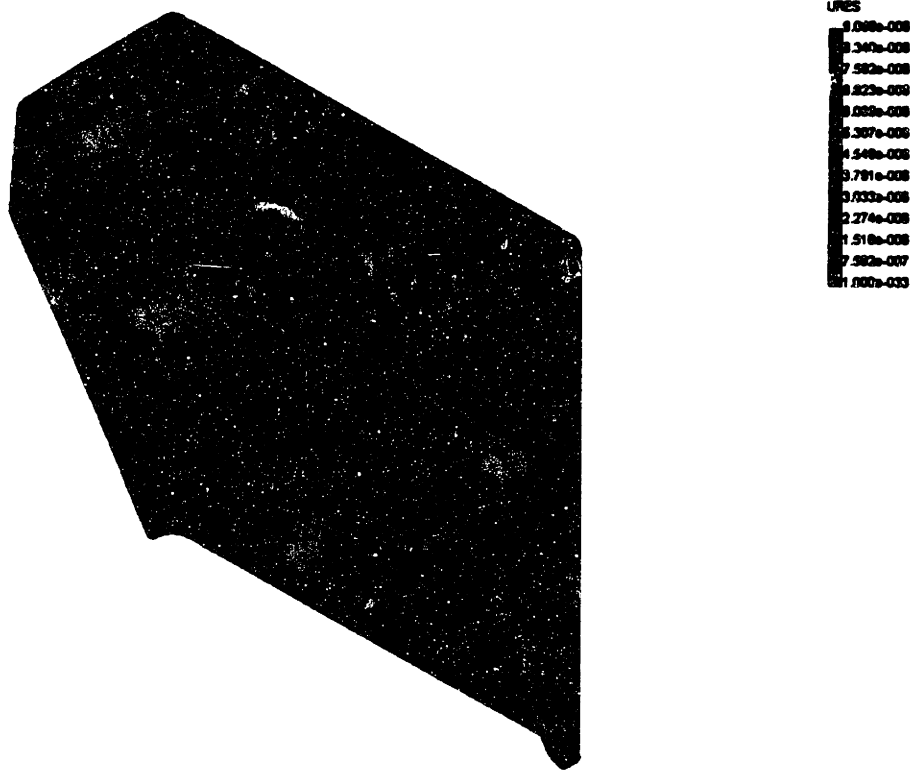


Figure 2.8: Max. Deflection of Head Plate (9.1E-6)

Appropriate bolt holes were created on the head plate for the mounting of the head platen. Three accurate dowel pins ensure the parallelism of the head platen with the head plate. A large hole was also created for the wires to pass through. Other features on the head plate include: taped holes for the attachment of the linear guides, the z-axis encoder, the piston mounting, and the ball screw.

2.3.2.7 Design of the Piston Attachment to the Head Plate

Unlike the ball screw, the pneumatic piston cannot apply the load to the top of the head plate. This is because the minimum length of the air piston is too long for it to be on top (it will stick up the top of the machine). Therefore, the piston must be behind the

moving head plate, between the two linear guides. From one side, the piston can be attached to the roof of the machine, and from the other side, the following bracket was designed to attach the end of the piston to the head plate.

Since it is be impossible to for the axis of the piston to be perfectly parallel with the axis of the ball screw, it was necessary for the piston to be attached by pin joints on each side that would allow it to rotate. Otherwise the system will be over-constrained, which will lead to large internal forces.

2.3.2.8 Design of the Z-Sensor Holder

The resolution of the z-axis must be very high, since it controls the position of the wafer relative to the pad. The motor encoder will not have the required resolution for this axis; therefore, an accurate linear encoder must be used. The linear encoder has a read-head that moves over a magnetic strip. The head must be attached to the head plate to move up and down with it, and the magnetic strip can be glued to the upper structure. The following bracket was designed to attach the encoder head to the head plate.

A small pocket was designed into the back of the head-plate for the z-sensor holder to sit in. The side of the z-sensor holder lines up against the edge of the pocket, making sure the read head is directly above the magnetic strip attached to the upper structure. The critical dimension here is the gap between the encoder head and the magnetic strip. The dimensions were toleranced accordingly to ensure the correct value for this gap.

2.3.2.9 Design of the Motor Timing Pulley

It is desirable to have the largest possible transmission ratio between the motor and the ball screw, so the motor can be downsized. For this purpose, the smallest timing pulley that would fit on the motor shaft was selected, and it was re-bored to fit the motor shaft. A set screw holds the pulley in place from the side.

2.3.2.10 Design of the Ball Screw Timing Pulley

A large pulley was selected to provide a $\frac{1}{4}$ transmission ratio between the motor and the ball screw. The pulley was then re-bored for the ball screw to pass through. The ball screw bearing is attached to the pulley through four bolts. The tapped holes are provided on the bearing, and the clearance holes were drilled on the pulley. An important assembly feature was to create a counter bore on the pulley for the bearing to sit on in order to keep the ball screw centered.

2.3.2.11 Selecting the Timing Belt

Since this is a precision axis of motion, it was important to select a belt with no stretching and no backlash. The timing belt selected for this application has steel cables going through it to reduce stretching, and it has a special tooth profile to eliminate backlash. The length of the belt was calculated through a given formula, and it was double-checked by measuring it directly from Solidworks.

2.3.2.12 Design of the Z-Shaft Extender

Since the motor shaft was not long enough to support the timing pulley, a shaft extender was designed for the motor. The tolerances on the inside hole were designed to be very tight to eliminate any play between the motor shaft and the extender. A setscrew

holds the extender in place. The timing pulley can now be attached to the other end of the shaft extender.

2.3.2.13 Design of the Limit Switches

To avoid the z-axis moving beyond its range of motion, it is necessary to place limit switches at the extremes of motion for safety purposes. The head-plate supports the head platen, which weighs well over 500 lbs. Any interference between this large moving mass and the machine structure could damage the entire CMP machine. Even though the software will not allow the z-axis to approach its limits, having actual limit switches is necessary in case of a software failure.

Mechanical limit switches have limitations in accuracy, maintenance, and reliability. For this reason, optical sensors were selected. Keyence Corp. is a good supplier of optical sensors, and for this application their application engineer suggested the use of self-contained photoelectric sensors, which use super-bright LED's. These sensors come with mounting brackets that were used to attach them at the limits of the z-axis motion.

2.4 MODELING THE DYNAMICS OF THE Z-AXIS

To design the control law for the z-axis, it is necessary to model the dynamics of the system. This was done by writing Newton's equation of motion for each sub-system and determining the equivalent inertia, damping, and friction of the system. A second-order transfer function was used to model the system. Some parameters were very difficult to estimate, such as the total damping and friction in the system. The exact value

for these parameters can be determined by running experiments when the machine is fully assembled. Detailed derivations are shown in the Appendix.

CHAPTER 3: DESIGN OF THE X-AXIS

3.1 BACKGROUND

To allow multi-step polishing using different pads or slurries, the CMP machine must have two separate platens. The polishing head must be able to move from one platen to the next. The x-axis, or the Inter-Platen Motion System, is an essential feature of this machine, and is responsible for the movement of the polishing head from one platen to another. The second task of this system is to provide the “sweep motion” throughout polishing. The sweep motion is the periodic oscillation of the wafer along the radius of the pad, usually at low frequencies relative to the speed of the platens. The main function of the sweep motion is to control the pad wear-rate to make sure the pad wears uniformly. This is important since it directly effects the polishing uniformity of the wafer. The third task of the Inter-Platen Motion System is to facilitate *wafer handling*. Instead of having a separate robot to transfer the wafer to the head for loading, the head itself can move to the load/unload station without the need for a separate wafer handling system.

3.2 CONCEPTUAL DESIGN

3.2.1 Concept Generation

In designing the x-axis, two basic design concepts were generated at the early stages of determining the configuration and overall geometry of the machine. After carefully reviewing each one, the best concept was selected.

3.2.1.1 Concept #1: Linear Configuration

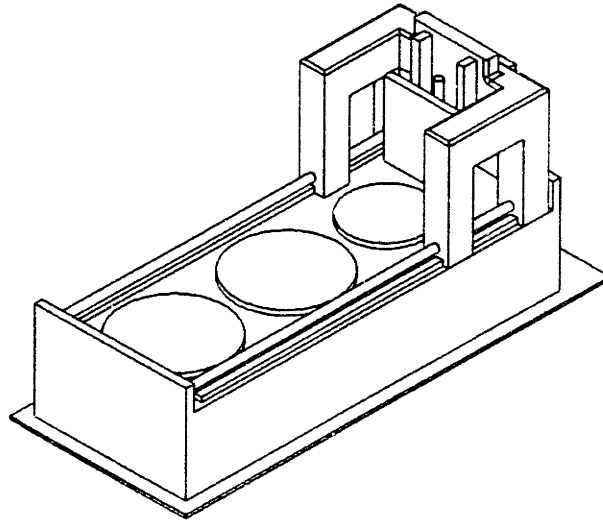


Figure 3.1: Concept #1, The Linear Configuration

In this concept, the platens and the load/unload station are laid out next to each other along a straight line. The polishing head has a *linear motion* to move between them.

3.2.1.2 Concept #2: Rotary Configuration

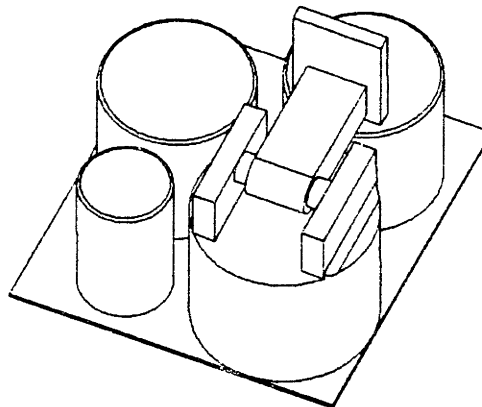


Figure 3.2: Concept #2, The Rotary Configuration

In this concept, the platens and the load/unload station are placed next to each other along an arc. The polishing head rotates to get from one to the other.

3.2.2 CONCEPT SELECTION

One advantage of the linear configuration (concept #1) over the rotary configuration (concept #2) is the reduction in footprint. In concept #1 the polishing head and the supporting structure are placed above the platens (therefore adding to the height of the machine and reducing its footprint), where as in concept #2, a separate base is needed to support the polishing head and provide the rotary motion. Approximating the size of the platens, the two configurations were drawn in AutoCAD for ease of comparison. The footprint of the linear configuration was found to be 15% lower than that of a rotary configuration.

Another advantage of the linear system is that internal moments acting on the wafer due to the frictional forces can be minimized. Frictional forces acting on the surface of the wafer can create large bending moments about the pivot point of a rotary system. This problem does not exist in a linear system, since the frictional forces are seen as normal loads acting on the linear bearings. The 'torque-arm' does not exist, and there are no bending moments created. This idea was previously discussed in Chapter 2 "Design of the Z-Axis".

The disadvantage of concept #1 is its long linear range of travel. A rotary motion is much easier to design and implement. For the approximate size of the platens shown in the previous figure, the range of travel is over six feet long. It is much harder to design linear actuators with such a range, than it is to find motors and gear heads to create a rotary motion. Concept #2 uses a less complicated mechanism to create the required inter-platen motion.

After carefully considering the advantages and disadvantages of each concept, concept #1 was selected. The advantages offered by a linear configuration seem to be greater than those of a rotary configuration.

3.3 DETAIL DESIGN OF THE X-AXIS

The basic function of this system can be divided into the application of the axial force required by the sweep motion, and the supporting of the lateral forces and moments. This means that the remaining degrees of freedom must be constrained, and the system must be allowed to move *exclusively* horizontally.

3.3.1 Supporting the Lateral Forces

3.3.1.1 Conceptual Design

It was previously decided that the Inter-Platen Motion System must be a linear axis of motion. To support the lateral forces, therefore, linear bearings must be used. A number of companies manufacture linear bearings such as THK Inc., and Thomson. Even though the products look similar, the design of the linear bearings differs within each company. The major difference between the linear guides is that some use re-circulating balls (THK's LM Guides), and others use a sliding guide system (Thomson).

After talking to the application engineers at the two companies, and carefully reading their catalogs and looking over the data provided for the performance of each system (such as rigidity, accuracy, run out, smoothness, etc.), it was decided to select THK's LM Guides for the following reasons:

- Rigid in all directions: The LM Guides can support very high radial, reverse radial, and lateral loads. Because of the circular arc grooves, the LM Guides can be preloaded as necessary to increase rigidity.
- Light and smooth motion without any clearance: LM Guides are capable of self-alignment, achieved by the ideal four-row circular arc contact.
- Easy to achieve high running accuracy: LM Guides maintain high running accuracy even if they are installed on a surface finished with poor precision. This is because elastic deformation of the balls can offset the error.
- High positioning accuracy: Because of the rolling guide system, the dynamic and static frictions of LM Guides are very similar to each other. Little control and lost motion is observed.
- High permissible load rating: The raceway groove profile of the LM Guide is similar to the ball. Therefore the permissible load per ball of the groove contact is 13 times greater than that of the plane contact.
- High accuracy over a long period: Because the LM Guide is an ideal rolling contact guide, there is virtually no wear. The original accuracy is maintained over a long period of operation.
- Excellent high-speed performance: When operated at high speed, there are no problems such as scores and scorching that are seen on a slide guide [THK catalog, page 40].

3.3.1.2 Selection of the Linear Guides

To calculate the loads on the linear guides, the forces that act on the wafer were used as the external forces acting on the system, similar to the z-axis. However, in this

case, since the x-axis must be able to move the entire upper structure, the inertial effects also become significant. After calculating the maximum acceleration of the upper structure based on a desired sweep frequency, the loads on the slides can be determined. With knowledge of these loads, the correct linear guides can be selected for the system. Detailed calculations are shown in the Appendix.

3.3.1.3 Spacing of the Linear Guides

Linear guides are designed to endure large normal forces, however, they do not have much rigidity under bending moments. Using two blocks on each rail, and using two separate rails, ensures that there will be only normal forces acting on the guides. Bending moments will be converted into forces acting on each block. The exact same concept will be used here as was on the z-axis: two blocks for each rail separated by a distance A and two rails separated by a distance B.

However, the guidance ratio A/B is now determined by the size of the machine. Dimension A represents the depth of the gantry, which is about 1.5' (slightly larger than the diameter of a 12" wafer), dimension B represents the width of the gantry, which is about 4' (slightly larger than the diameter of the platen). This ratio is then about $1/3$, which is much less than its ideal value of 1.5. This means that the possibility of the drive mechanism jamming is very large. This is a major problem, and it means a single actuator through the center cannot drive the x-axis. The only solution is then to use two actuators on both sides. This will be discussed in greater detail more in the forthcoming sections.

3.3.1.4 Mounting of the Linear Guides

It is extremely important for the wafer to be co-planar with the polishing pad. This is the function of a gimbal mechanism (a universal joint). One of the distinct features of this machine is that the polishing head does not have a gimble mechanism. This is because a gimbal mechanism has an instant center-of-rotation at a point above the surface of the wafer, which will cause the pad to put higher forces on one side of the wafer than on the other. This will result in non-uniform polishing of the wafer. Since a gimble mechanism is not used, this machine has to be very accurate to ensure the wafer will be co-planar with the pad.

The top surface of the lower structure is defined as the reference plane for the entire machine. It is therefore important for the reference plane to be very accurate, since other components will be assembled in reference to that surface. For this purpose, it was decided to make the lower structure out of granite, since it can be machined to be very flat and accurate (many optical machines use granite tables).

The platens were designed to be parallel to the surface of the granite table. The upper structure must also be designed to be parallel to the reference surface. Since the upper structure slides on the linear guides, the mounting of the guides becomes critical. It is important for the linear guides to be *straight*, *parallel* and *co-planar* to each other, and *parallel* to the surface of the platen.

The guides will both be mounted on the surface of the granite table, which is specified to be very flat throughout its length (0.0005" over 108"). This ensures that the guides are *co-planar* with each other, and that they are *parallel* to the surface of the

platen (since the platens are mounted very accurately on the surface of same granite table).

Three dowel pins were accurately placed on the surface of the granite table for one of the linear guides to line up against. This was to ensure the *straightness* of one of the linear guides. Since accurate holes cannot be drilled in granite (only accurate up to 0.005”), stainless steel inserts were placed in the granite table first. Only then accurate were holes drilled on the stainless steel inserts for the dowel pins. Using this method, the dowel pins were positioned to an accuracy of 0.0002”.

To make the guides parallel to each other, one was first mounted on one side (with the help of the dowel pins). The second guide was mounted by first leaving the bolts loose, moving the upper structure in and out several times, and then tightening the bolts in the process. This ensures that the two guides are *parallel*, and offset by a fixed distance (width of the upper structure).

3.3.2 Applying the Driving Force for the X-Axis

3.3.2.1 Concept Selection

As it was previously discussed, the aspect ratio A/B (separation of the blocks / separation of the rails) is about $1/3$, which is much less than its ideal value of 1.5. This means that two separate actuators on both sides must be used to drive the upper structure. The position command is sent to one actuator, and the other is set to always follow the first actuator. Therefore one side leads, and the other side always follows. This is referred to as a ‘master and slave’ control system.

The range of motion is very large (over 6', two diameters of the platens and the load/unload station), as was discussed previously, and the only reasonable linear actuators are the following:

- **Linear Motor**: Linear motors are in general very smooth and accurate, and they can provide high accelerations, but for such a long range of motion and high forces, linear motors would tend to be extremely expensive.
- **Belt-Drive Mechanism**: A belt-drive mechanism is probably the simplest way of providing the linear motion for the upper structure. However, such a system has a lot of compliance, and the belt can be stretched under the high forces. This can create major problems, since this axis of motion has to be very accurate. Also, since the upper structure is driven on both sides, it is necessary to know the exact position of each side, in order to coordinate the two. A belt-drive mechanism is relatively inaccurate (because of its low stiffness) and the upper structure can get jammed if the two sides are not perfectly synchronized.
- **Gear-Pinion System**: The motion of the x-axis has to be very smooth, with no backlash, since it provides the sweep motion while the wafer is being polished. Even though a gear-pinion system is ideal for long ranges of motion, it does not meet the smoothness and no-backlash criteria (gears have backlash, and they are noisy).
- **Motor and Precision Ball Screw**: Ball screws fall into two categories: ground ball screws and rolled ball screws. Because they are easier to manufacture, rolled ball screws are cheaper, but they are much less accurate. Precision ground ball screws have an accuracy of about 0.001" per foot, which meets the criteria for this machine; however, because of the length of such a ball screw, a lead time of about 8 months is

required to purchase these components. This idea had to be abandoned because of the component's lead-time.

- Motor, Ball Screw, and Linear Encoders: Thomson Inc. has rolled ball screws up to 12-feet long in stock. These ball screws, however, are inaccurate. The solution to this problem is to use linear encoders on either side of the upper structure. This way even though the ball screw may not be accurate, the exact position of the ball nut can be determined from the linear encoders. Such a system would be much more accurate and less expensive. This concept was selected and finalized.

3.3.2.2 Selection of the Ball Screws

3.3.2.2.1 Sizing the Ball Screws

The diameter of the ball screw was sized based on its axial load capacity. As it was previously shown, the force along the x direction is only about 200 lbs. on each side. A 1" ball screw (in diameter) would be able to endure several times that load.

The length of the ball screw was determined by the total travel of the machine. After the design of the machine was finalized, the range of travel was checked to be 82" from the overall assembly of the machine in Solidworks. This was the last dimension to be specified.

The pitch of the ball screw was determined by checking the following two criteria: max velocity of the x-axis and the necessary motor torque. The higher the pitch, the faster the ball nut will travel (for a given angular velocity), and a higher driving motor torque will be required. The angular velocity of the ball screw is limited by its whipping, as will be shown in the next section.

3.3.2.2.2 Critical Velocity Calculations

Since the ball screw is very long in this case (82"), vibration becomes an important issue. The natural frequency, or the critical velocity, of the ball screw must be determined to find the limiting angular velocity. Detail calculations are shown in the Appendix. To check this result, Cosmos was used to run a quick vibrational analysis of the ball screw using FEA methods. The critical velocity of the ball screw was found to be very close to that predicted from the formula. Because of the low natural frequency of the ball screw, a *fixed-fixed* support must be used on both ends. This means that the ball screw has to be supported on *four bearings* on each side.

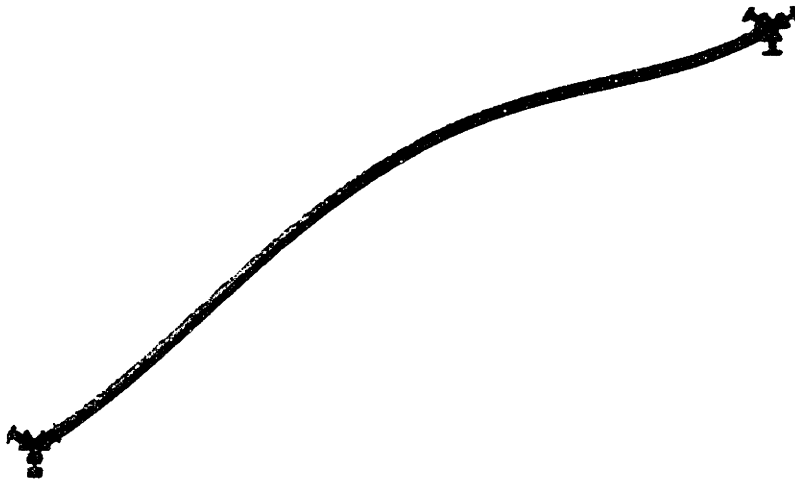


Figure 3.3: Natural Frequency of the Ball Screw (27.2 Hz)

3.3.2.2.3 End Machining of the Ball Screws

The driving side of the ball screw should support the ball screw laterally as well as axially. For this purpose, the ball screw needs a shoulder to sit against the supporting bearings, a thin, smooth section to fit into the bearing bores, a thinner section with threads for a nut to tighten the end shaft against the bearings, and a finally a thinner

section with a flat for the flexible coupling. Two relieves (undercuts) are needed: one to make sure the bearings sit against the shoulder, and one to make sure the nut tightens all the way. The following drawing shows the necessary features needed on the driving end of the ball screw:

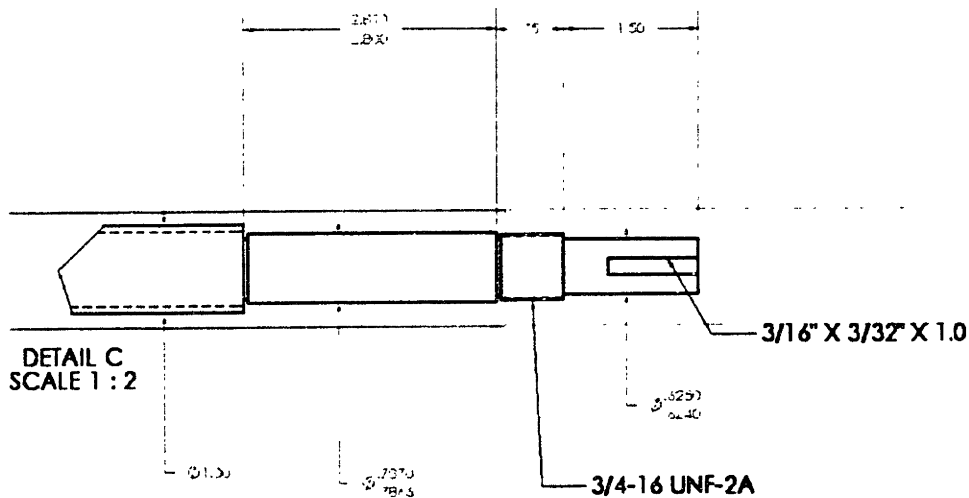


Figure 3.4: Driving End of the Ball Screw

The free end only needs to support the ball screw laterally. Since the ball screw is very long in this case, its axial thermal expansion could create severe problems. The ball screw must be allowed to move axially from one end, otherwise any temperature changes can lead to high internal forces and the possible deformation of the ball screw. At the same time, it is necessary to put the ball screw in tension to reduce whipping and increase its performance. This problem is solved by using Belleville washers at the free end of the ball screw. Using Belleville washers, the tension on the ball screw can be controlled; at the same time, the shoulder of the ball screw is not tightened against the

bearings, allowing it to move in case of thermal expansion. The following drawing shows the necessary features need on the free end of the ball screw:

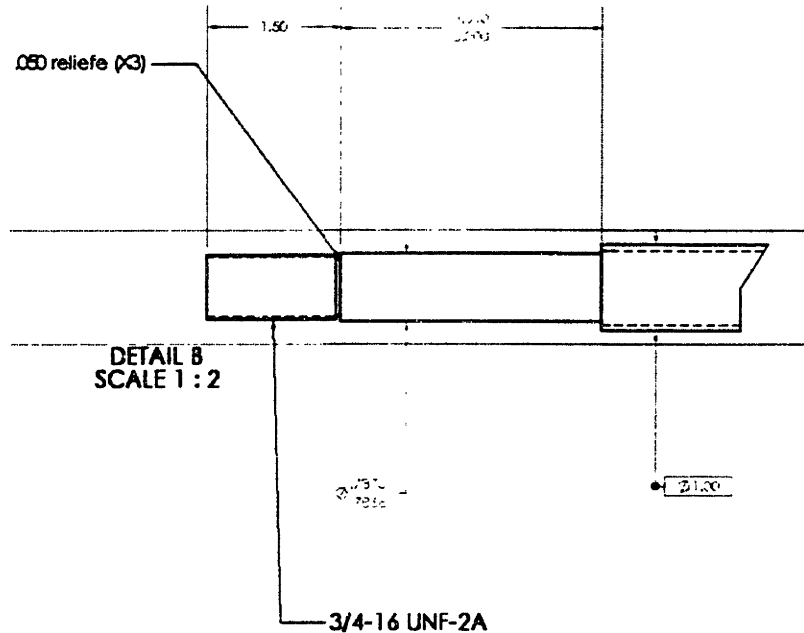


Figure 3.5: Free End of the Ball Screw

3.3.2.3 Selection of the Linear Encoder

The standard solutions for measuring linear position are rotary encoders with rack and pinion and wire-actuated transducers. Their disadvantages are mechanical wear, measuring error due to backlash and aging, high maintenance, and high installation costs. The magnetic length measurement system – consisting of a magnetic strip, a magnetic sensor, and a translation module/display – is the modern solution. However, first an incremental or an absolute encoder must be chosen.

- Incremental Encoder: An incremental encoder will provide the relative distance by simply counting the number of pulses. Even though it is cheaper, once the machine is

turned off, the position of the upper structure will be lost, and it is therefore necessary to use a homing sensor with an incremental encoder. Since it is essential for the two sides of the structure to be at the same position at all times, using an incremental encoder may result in the jamming of the upper structure once the machine is turned on. For this reason, it is necessary to use an absolute encoder.

- **Absolute Encoder:** The core of the system is a flexible synthetic tape containing magnetic particles. A sensor head travels with a small distance along the tape. This sensor scans the tape's magnetic field and transmits the absolute length information to the follower electronics. This system captures movements during power loss, and the current position value is available at any time without having to calibrate the system previously.

A dynamic model was developed to predict the internal forces that would act on the system if the two sides of the x-axis were not perfectly synchronized. The allowed slack between the two sides determines the resolution of the x-axis encoder. It was found that the two sides of the upper structure must always be within 50 microns of each other to avoid jamming. The resolution of the encoder was then sized to be 10 microns. The length of the encoder was determined by the total travel of the machine, which was found to be 82”.

3.3.2.4 Selection of the X-Axis Motor

A brushless DC motor was chosen, since it offers many advantages, such as low maintenance, high torque, and more accurate controllability. Brushless motors provide up to 50% more torque, 15 times the acceleration, 33% shorter length, and 20% lower price than brush DC servos of the same frame size. With the known values of the axial

force exerted on the ball nut, and the pitch of the ball screw, the motor torque was calculated. This was matched by the stall torque of a BM Series Brushless servomotor built by Aerotech Inc. Detailed calculations are shown in the Appendix.

3.3.2.5 Design of the Motor Bracket

The driving end of the ball screw must be supported on bearings, and through a flexible coupling it must be connected to the motor. The motor bracket must provide mounting for the motor and the bearing housing. There must be enough space provided for the flexible coupling. The following part was designed for this purpose:

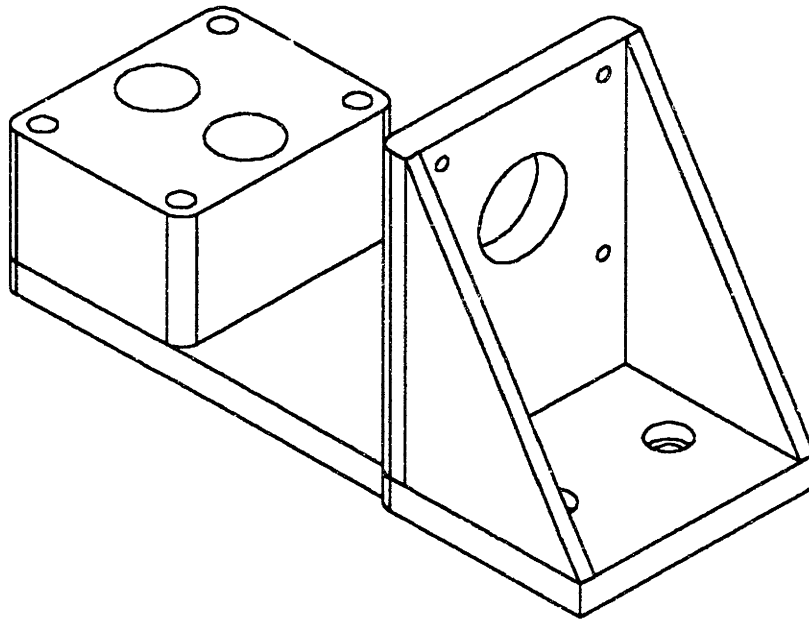


Figure 3.6: Motor Bracket

This bracket is made of individual plates that are all welded together, as opposed to a machined structure. This reduces the cost of construction significantly. It was important to stress relieve the structure (after welding) to release the residual stresses. The final machining of the important surfaces must be done after stress relieving.

Drawings for each plate were provided, and the important tolerances were specified on the final assembly drawing.

In order for the welds not to be seen from the outside, 45-degree chamfers were created at the edges where the plates join. The grooves were then filled up with weld, and the outside surfaces were machined afterwards. The size of the welds (1/4") were smaller than the thickness of the plates (1/2") to make sure the structure would not distort after welding.

The critical dimensions included the tolerances on the diameter and height of the pilot hole, the *height*, *flatness*, and *parallelism* of the mounting surface for the bearing housing, the *flatness* and *perpendicularity* of the mounting surface for the motor, and the *flatness* of the bottom surface of the motor bracket.

3.3.2.6 Selection of the Flexible Coupling

The flexible couplings were selected based on the transmitting torque (max. motor torque), the size of the motor shaft, and the end machining of the ball screw. The clamp type was preferred over the setscrew type. They were purchased from Helical Inc.

3.3.2.7 Selection of the Ball Screw Bearings

Torington Inc. has developed a series of ball bearings specially designed for ball screw applications. Design criteria for these bearings include maximum axial rigidity, low drag torque, and extreme control of lateral eccentricity. Torington also builds the housing unit for these bearings, but it was decided to build the bearing housings, since they are extremely expensive to purchase. As was previously shown, because of the critical velocity of the ball screw, it is required to have fixed supports at each end of the

ball screw. Therefore, sixteen sets (four at each end) of super precision angular contact bearings were purchased from Torrington Inc. These bearings must be preloaded against each other to ensure no play.

3.3.2.8 Design of the Bearing Housing

A bearing housing is an enclosure for the bearings, with two oil seals at each end to keep the bearings lubricated at all times. Once the bearings were selected, the following part was designed to house the bearings:

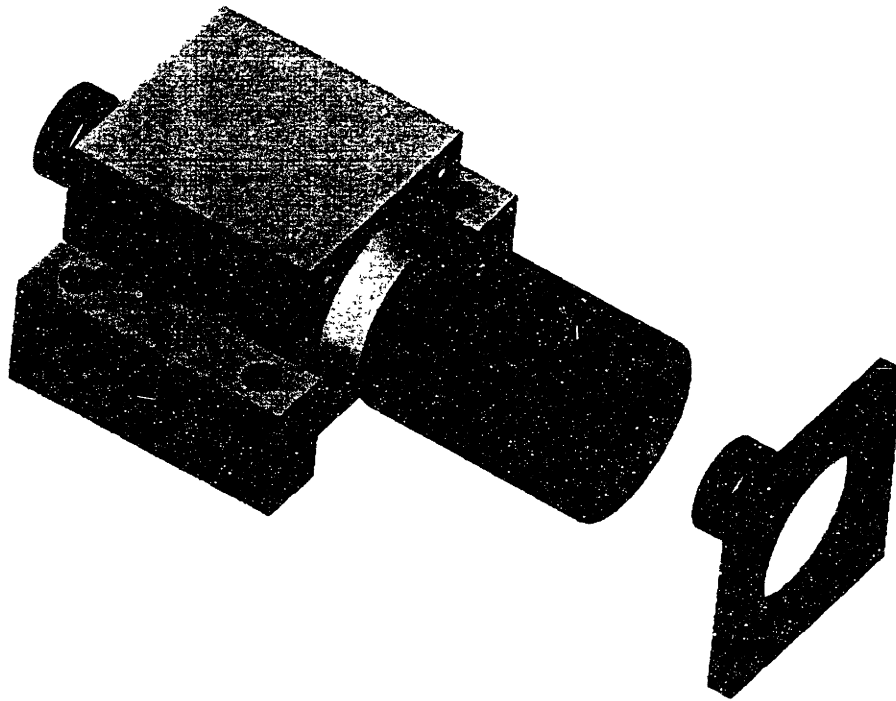


Figure 3.7: Bearing Housing

The housing has a counter-bore whose diameter matches the outer diameter of the bearings, and its depth is the width of four bearings sitting next to each other. One end of the hole has a shoulder for the bearings to sit against. Once the bearings are inserted into

the housing from the other side, a plate bolts on and presses the bearings against the shoulder. This controls the pre-loading of the bearings.

The shoulder of the shaft usually sits against the rotating part of the bearing, and a nut tightens the shaft against the bearing from the other side. But in this case, since there are oil seals in front of the bearings, special spacers were designed to sit between the rotating part of the bearing and the shoulder of the shaft. The insides of the spacers were toleranced to closely fit on the shaft, and the outsides were given the correct tolerance and a surface finish suitable for oil seals.

The important dimensions included the tolerances on the diameter, depth, finish, straightness, and perpendicularity of the bearing enclosure hole, the relief at the end of the hole, the diameter of the shoulder, counter bores for the oil seals, and the flatness of the mounting surface.

3.3.2.9 Selection of the Oil Seals

Lip seals are necessary in the design of bearing housings to ensure that grease will not leak out. Standard size oil seals were selected from Federal-Mogul Corp. based on the size of the ball screw end-shaft. A counter bore was created in the bearing housing for the oil seal to press fit into. The tolerances for the diameter and depth of the mounting hole, and the diameter and the surface finish of the shaft were obtained from the Machinery's Handbook.

3.3.2.10 Design of the X-Sensor Bracket

The x-axis linear encoder has a magnetic strip that sticks to the granite table (lower structure), and a read-head which is attached to the upper structure and moves

over the strip. For the mounting of the magnetic strip, a slot along the edge of the granite table was created on both sides. This feature was designed to ensure the straightness and flatness of the magnetic strip over its length.

This part attaches to the upper structure through the two counter-bored holes, and two tapped holes are provided for the mounting of the sensor head. A pocket is designed into the upper structure (an edge that lines up against the side of the bracket) as an assembly feature, to make sure that the sensor head lies directly above the magnetic sensor.

The critical dimensions include: the flatness and perpendicularity of the mounting surface for the sensor head, the flatness of the bottom surface, the overall width of the part (to fit in the pocket designed into the upper structure), and the location of the sensor holes (to keep a gap of 0.5 mm between the head and the strip).

3.3.2.11 Design of the Bearing Mounting

The bearings at the free end of the ball screw must be raised to the same height as the bearings of the motor side. This requires the design of bearing mountings, which are simply spacers put under the bearing housings.

The large counter-bores in the middle allow access for the tool that tightens the bolts. The four tapped holes on the sides are provided for the mounting of the bearing housing. The important dimensions were the flatness of the bottom, and the flatness and parallelism of the mounting surface for the bearing housings.

3.3.2.12 Design of the Limit Switches

To prevent the upper structure from moving beyond its range of motion, it was necessary to place limit switches at the extremes of motion for safety purposes. The upper structure assembly weighs well over a ton, and any interference between this large moving mass and the machine structure could damage the entire CMP machine. Even though the software will not allow the x-axis to approach its limits, having actual limit switches is necessary in case of a software failure. Similar to the z-axis, Keyence sensors were placed at the extremes of the travel on one side of the x-axis.

3.4 MODELING THE DYNAMICS OF THE X-AXIS

To design the control law for the x-axis, it is necessary to model the dynamics of the system. This was done by writing Newton's equation of motion for each sub-system, and determining the equivalent inertia, damping, friction, etc. of the system. A second-order transfer function was used to model the system. Some parameters were very difficult to estimate, such as the total damping and friction in the system. The exact value for these parameters can be determined by running experiments when the machine is fully assembled. Detailed derivations are shown in the Appendix.

CHAPTER 4: DESIGN OF THE UPPER MACHINE STRUCTURE

4.1 BACKGROUND

The CMP machine can be divided into a lower and an upper structure. The latter is the moving structure of the machine. The x and z axes of motion are mounted on this frame. The lower structure supports the loads exerted on the platens, and the upper structure supports the reaction forces of the polishing head. These forces mainly result from the frictional loads acting on the wafer and the moments created by these forces. The normal polishing load applied by the Force Application System must also be supported by the upper structure.

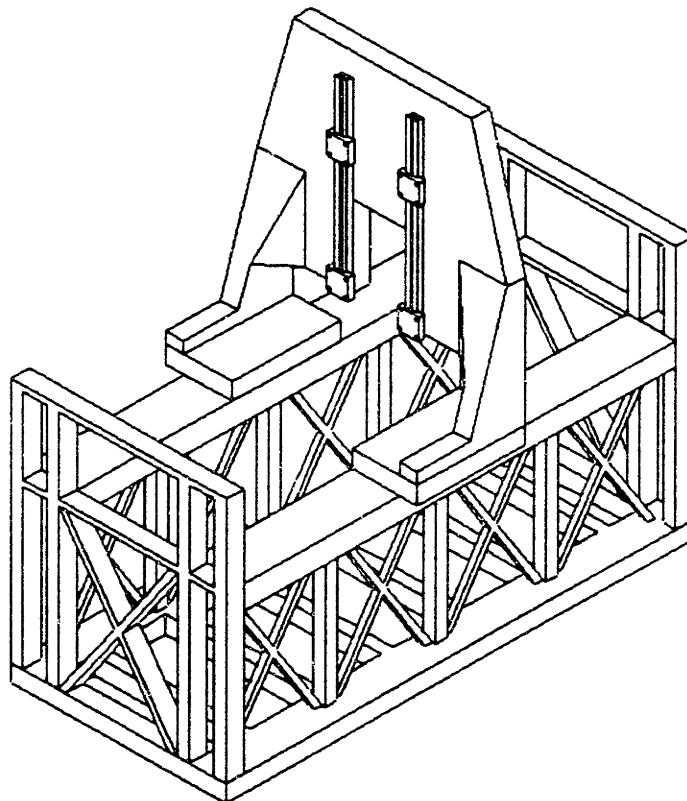


Figure 4.1: Lower and Upper Structure of the CMP Machine (Concept)

4.2 **CONCEPTUAL DESIGN**

In designing the upper structure, a number of concepts were generated at the early stages of design. After reviewing each carefully, the best concept was selected.

4.2.1 Concept Generation

4.2.1.1 Concept #1: The L-Shaped Structure

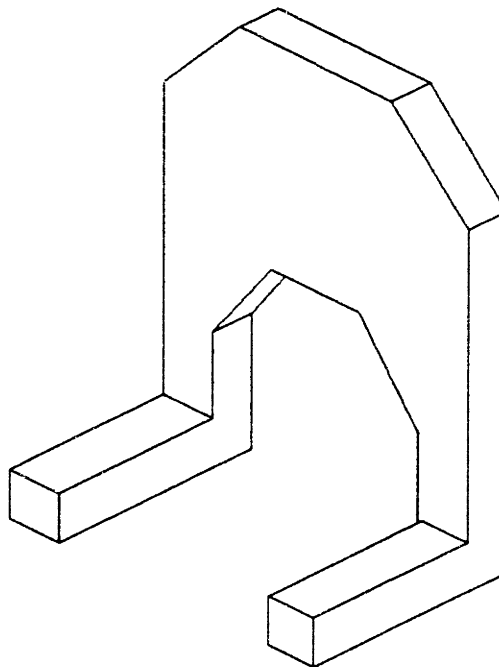


Figure 4.2: Concept #1

This is the simplest possible design for the upper structure. Looking at this drawing from the side, the structure looks similar to the letter 'L'. The x-axis ball screws can drive this system from both sides. The middle cutout is created to allow for the polishing head to move vertically without interfering with the structure.

4.2.1.2 Concept #2: The Reduced-Footprint Design

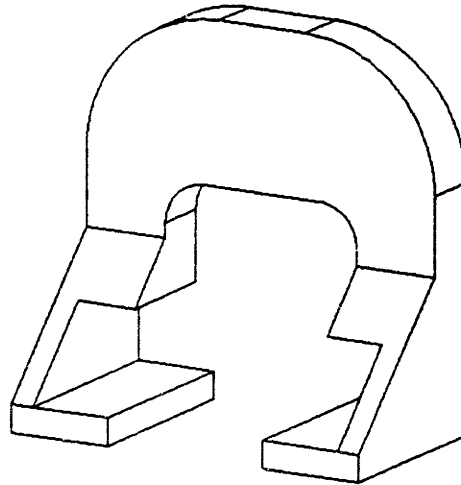


Figure 4.3: Concept #2

In this design, the two sides of the upper structure are tucked under the lower machine structure to reduce footprint. The linear guides are mounted upside down, and the two ball screws drive the system from underneath the lower structure. This is done to avoid exposure of the drive mechanism to the chemical slurry, which can be extremely harmful to the linear bearings and ball screws, since it contains abrasive particles.

4.2.1.3 Concept #3: The Gantry Structure

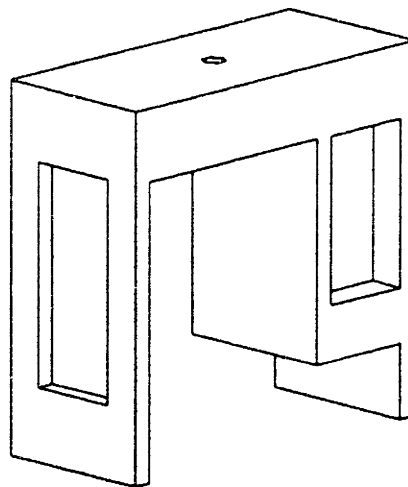


Figure 4.4: Concept #3

This concept is fundamentally different from the previous ones, since the z-axis is now mounted on the side wall. The structure has two full-length walls that are attached to each other through a roof. The x-axis ball screws are attached to the walls, and the z-axis ball screw is attached to the roof. The main idea is to completely eliminate the bending moments (due to the polishing loads) by applying the normal load directly at the center of the wafer. This requires the existence of the roof for the mounting of the ball screw, and the walls for the mounting of the linear guides.

4.2.1.4 Concept #4: The Symmetrical Gantry Structure

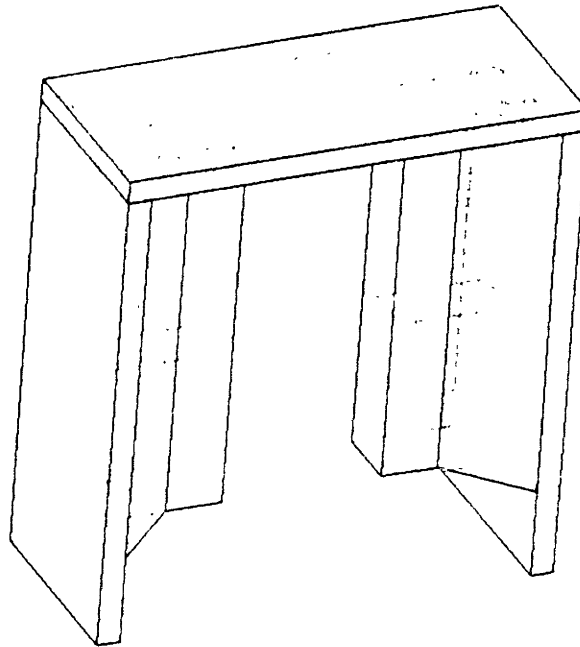


Figure 4.5: Concept #4

This concept is similar to the previous one, except that the linear guides are mounted on separate walls in this case. This creates a symmetrical design in both directions, which has great advantages to offer as will be discussed in the next section.

4.2.2 Concept Selection

Concept #1 is the simplest of all the concepts. However, since the reaction force at the center of the wafer acts at an offset distance from where the ball screw applies the polishing load, large bending moments are created.

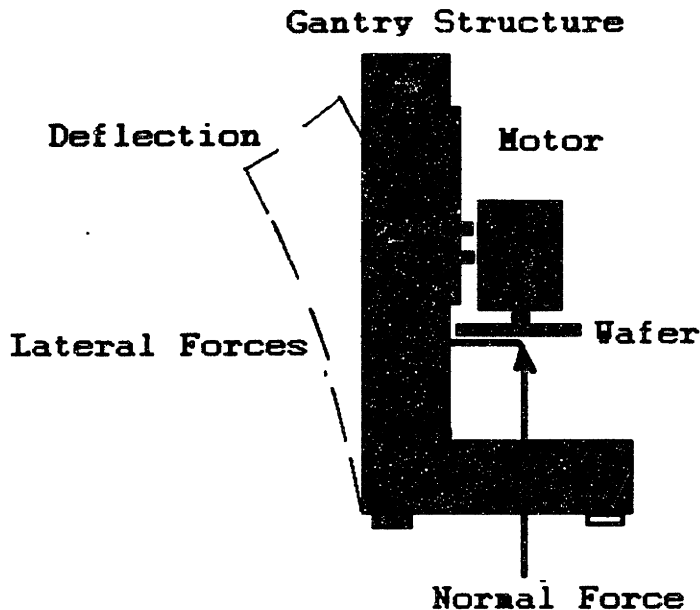


Figure 4.6: Bending Moments Acting on the Upper Structure

The torque-arm cannot be reduced, and since the polishing load is over 1000 lbs., the structure has to be extremely rigid and strong to support the bending moment. Even so, the small deflections will still cause the wafer to form an angle with the pad, which will result in non-uniform polishing of the wafer since a gimble mechanism is not used.

Concept #2 has the advantage of significantly reducing the footprint of the machine. However, this concept has the same disadvantage as concept #1. The main turn off here is the complexity of design. Even though this concept was originally pursued for a while, it was determined that the complexity of design was not worth the reduction of footprint.

Concept #3 is not the simplest design, but it offers a number of great advantages. The main advantage is that since the load is being applied at the center of the wafer, there are no bending moments acting on the structure. The second advantage is that the frictional loads that act perpendicular to the x-axis (along the y-axis), are now seen as normal loads to the linear guides. This allows for an extremely rigid design, without the need of a thick and bulky structure. Also since the deflections are now only in the z-direction, the wafer and the pad will not form an angle in this design.

Concept #4 is similar to the previous concept, except that here the design and analysis of the structure is made much easier through a symmetrical design. The main issue with this concept is the alignment of the two linear guides. In the previous concept, the two guides are mounted on one plane, whereas in this case the two mounting planes must be perfectly parallel to each other. Otherwise the stiffness of the two guides will be significantly reduced, and there will be high internal forces between the two guides. Considering the advantages and disadvantages of the above concepts, concept #3--the gantry structure--stood out as the superior design. The word “gantry” comes from the concept of a “gantry crane,” which has two linear axes of motion. This concept was selected and finalized to be pursued.

4.3 *DETAIL DESIGN OF THE UPPER MACHINE STRUCTURE*

Once the rough geometry of the system has been determined from the conceptual design process, the next step includes creating all of the necessary features and finalizing all dimensions. The first step was to select all of the machine components that attach to this structure. These included motors, linear guides, ball screws, etc., which were

discussed in the previous sections. The function of the upper structure is to provide mounting features for these components.

4.3.1 Exploded View of the Gantry Structure

The following figure shows the final design of the gantry structure. The important tolerances are specified on this drawing. The design and tolerancing of the key features will be discussed in the next section.

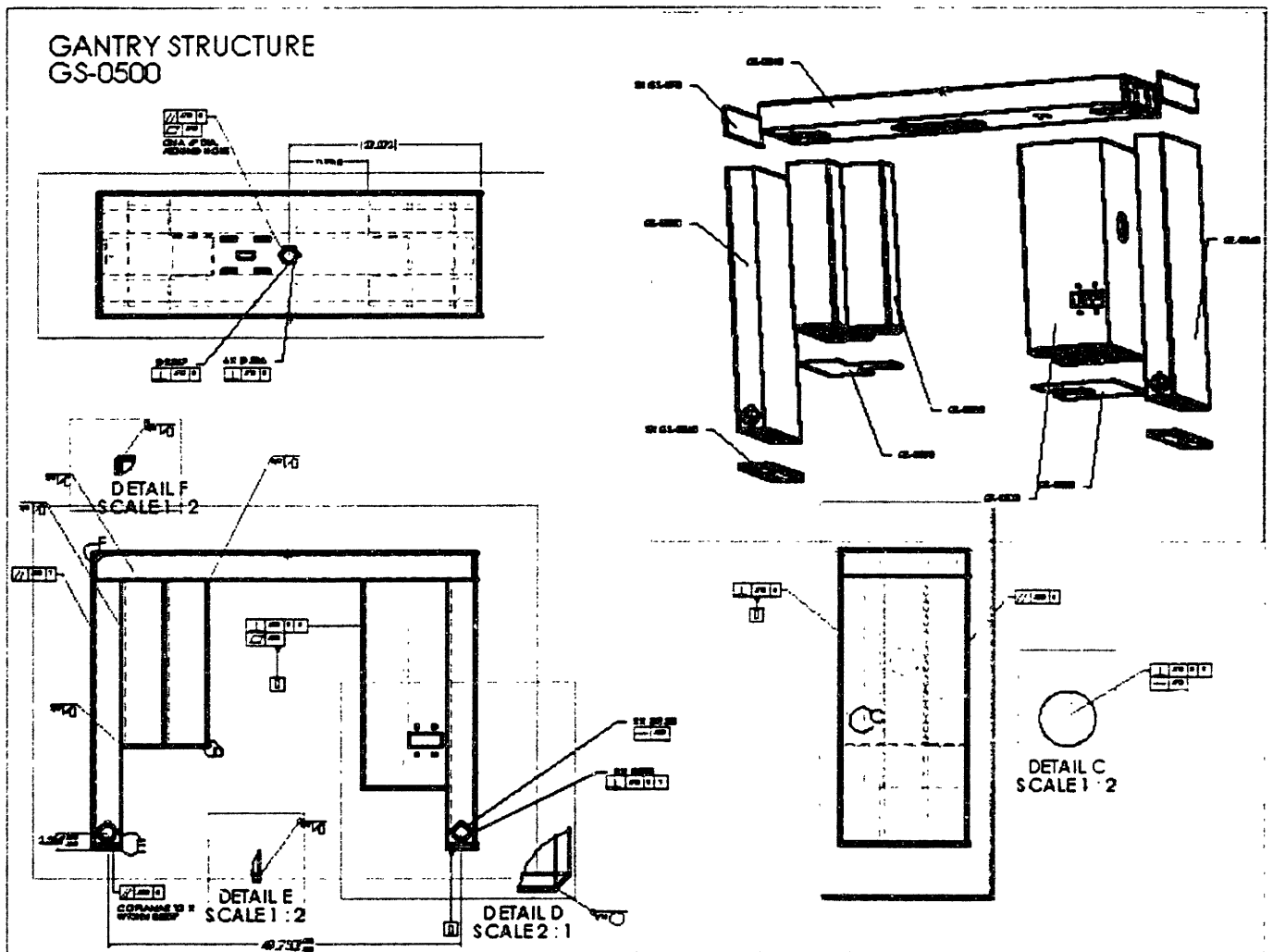


Figure 4.7: Exploded View of the Gantry Structure

4.3.2 Key Features & Tolerancing

4.3.2.1 X-Reference Surface

As previously mentioned, the lower structure is made of granite to create a flat and accurate reference surface for the entire machine. The surface of the pad will be parallel to this surface, and it is therefore important for the upper structure to be parallel to this surface as well. The gantry is mounted on the x-axis linear guides, which sit flat on the granite table. The interaction surface between the upper structure and the linear guides is referred to as the x-reference surface of the upper structure. This surface defines a plane, which is used as the reference for the upper structure. The critical geometric tolerances are measured with respect to this plane, which is sometimes referred to as the x-datum plane. The important tolerances here are the *flatness* of the two mounting surfaces, and the *co-planarity* and *parallelism* of the two sides, as shown on the exploded view.

4.3.2.2 Z-Reference Surface

The z-axis linear guides are mounted on this surface. The function of this surface is to assure both the co-planarity of the two guides, and their perpendicularity to the pad, or in this case the x-reference surface. This is the most important feature of the upper structure, since it determines the orientation of the wafer with respect to the pad. This plane is referred to as the y-datum plane on the figure, and it has a specified *flatness* over its entire surface, and a specified *perpendicularity* to the x-datum plane, as well as the z-datum plane, which is defined as the side of the gantry.

Creating this surface was the most challenging part of the fabrication process. The tubes were first welded together, and then stress relieved. Then the gantry was placed into a large horizontal milling machine, where the tool came in from the side to machine the surface.

4.3.2.3 Z-Reference Edge

The z-reference surface guarantees the perpendicularity of the z-axis from only one direction. The z-axis can also be tilted from the side, and it is therefore important for the linear guides to have a reference edge that will ensure the perpendicularity of the z-axis from the side. This edge is created for one of the rails only, and the second rail will be assembled to be parallel with the first one. The reference edge must be *perpendicular* to the x and z-datum planes, and it must be *straight* throughout its length.

The edge is created by milling the z-reference plane deeper than the remaining surface of the gantry wall, thereby creating a step on the overall surface. Creating this feature was a challenging process, since it was hard to access. The edge could not run all the way up to the intersection of the roof and the side wall. The milling tool did not have access to that junction, and a minimum machining radius had to be specified. Ultimately, the 6" top segment of the edge was not created. This was not a significant change since this was only a reference edge for the mounting of the linear rails.

4.3.2.4 Z-Ball Nut Mounting

This is another crucial mounting feature, which is used to position and orient the z-axis ball screw. The position of the ball screw is measured from the reference y-datum plane (z-reference surface), since the linear guides mount on that surface. This

dimension is critical, and therefore it has a tight tolerance. The other important geometric tolerances include the *flatness* of the mounting surface, and its *parallelism* with the x-datum. It is also very important for the axis of the ball screw to be perpendicular to the x-datum. Otherwise the ball screw will not be parallel with the linear guides, and this will result in high internal forces on the ball screw. The *perpendicularity of the axis* of the through hole, where the ball nut mounts with respect to the x-datum plane, is therefore very important.

4.3.2.5 Z-Motor Mounting

The ball nut is attached to the motor through a timing belt, and consequently there must be a mechanism to tighten the belt. One option would be to use a belt-tightener, which is essentially a suspended pulley that consistently puts the belt in tension. The problem with a belt tightener is that it will significantly reduce the life of the belt, and will cause a high frictional torque. The decision was made to use the motor itself to tighten the belt, by allowing the motor to move back and forth. This explains the long slots (rather than holes) on the roof of the gantry. Since a belt is used for transmitting power, there is no need to have an accurate mounting surface.

4.3.2.6 Z-linear Encoder Mounting

As previously discussed, a small pocket was designed into the head-plate assembly to provide mounting for the z-sensor holder, which holds the encoder read-head. But the actual magnetic strip mounts on the upper structure and it needs an accurate mounting surface. To assure planarity of the linear encoder, the z-reference surface (where the linear guides are mounted) was chosen as the mounting surface. But

to assure the straightness of the encoder, three positioning dowel pins were placed on this surface against which the encoder strip can be lined up. This will ensure the straightness of the encoder. The pins were positioned and toleranced with respect to the edge of the gantry.

4.3.2.7 X-Ball nut mounting

The height of the mounting hole from the x-reference surface is important. The distance between the two x-axis ball nuts is also crucial, and therefore it has tight tolerances. The ball nut through-hole must also be *straight*, and its axis must be *perpendicular* to the x and y-datum planes.

4.3.2.8 X-linear encoder mounting

Similar to the z-axis linear encoder, a small pocket is designed into the gantry structure for the mounting of the x-encoder bracket. It is important for the sensor head to maintain its gap throughout the range of travel, and to be directly above the magnetic strip. The main purpose of the pocket is to create a straight edge against which the x-encoder bracket can be lined up. Also, to maintain the gap, it was necessary to tolerance the depth of the pocket with respect to the x-reference surface. A hole was created behind the pocket to allow for the sensor wires to go into the hollow gantry structure.

4.3.2.9 Cable Carriers and Wiring Holes

The electrical wires and fluid lines from the upper machine structure are transferred to the lower machine structure through two cable carriers. The reason for using *two* cable carriers was to separate the encoder wires from the PWM power amplifier wires to reduce interference and electrical noise. The cable carriers were

selected to have flanges at one end so that they could be bolted to the sides of the gantry. The wires travel through the hollow tubes of the gantry. Several necessary holes were created on the tubes to ensure the wires could run through the different segments of the gantry, accessing all of the machine components.

4.3.3 Design of the Associated Components

4.3.3.1 Design of the Spacer A

Originally, the plan was to mount the linear guides on the surface of the gantry. In such a case, it would have been extremely difficult to correct a design bug or to make any modifications later on. Using spacers under the linear guides added flexibility to the design. Spacer A sits against the z-reference edge, and it provides a similar edge for one of the rails to sit against. A rectangular piece, with a step on its surface (similar to that of the z-reference surface) is used to bring the liner guides closer to the center of the wafer. The *flatness* on both sides of the spacer is important, and the *straightness* of the edge is crucial.

4.3.3.2 Design of the Spacer B

Design of this spacer is very similar to the design of the previous one, except for the reference edge, which is not necessary here. Once one of the rails is mounted accurately, the other one can be assembled to be perfectly parallel to the first. A simple rectangular piece with the appropriate holes is enough to perform the task.

4.3.3.3 Selection of the Cable Carriers

The cable carriers were purchased from the Gleason Power Track Company. The “enclosed” cable carriers were selected (vs. “open”) to ensure that wires wouldn’t be exposed to chemicals. The size of the cable carriers was selected based on the estimated number of wires and tubes that had to go through them. The range of travel determined the overall length of the cable carriers. It was important to keep in mind the bending radius of the cable carriers in placing the mounting features, and in sizing the correct length. On one side, TB flange type brackets were ordered for mounting to the gantry, whereas on the other side SB scoop-type brackets were ordered for mounting to the granite table.

4.3.3.4 Design of the Roof-Cover Plate

The function of this piece is to cover the z-axis power transmission mechanism that is located within the roof of the gantry. It prevents particles from going in, and most importantly, from falling out. This is a simple plate with through holes for four bolts on each corner, and a clearance hole for the z-axis ball screw. The finish was specified to be the same as that of the gantry.

4.3.3.5 Design of the Side-Cover Plates

The side-box on the opposite side of the z-reference surface is not used for anything but structural integrity and symmetry. Two of the tubes were removed from each side to produce empty space for the mounting of the pressure valves and other components. Two side-cover plates were designed to cover these empty spaces. 1/16” sheet metal was cut, bent, and spot-welded to create the desired cover plates. These

plates bolt on to the gantry by several holes from the sides, and they have the same surface finish as that of the gantry. The following picture shows the overall design of the upper structure, and the attaching components.

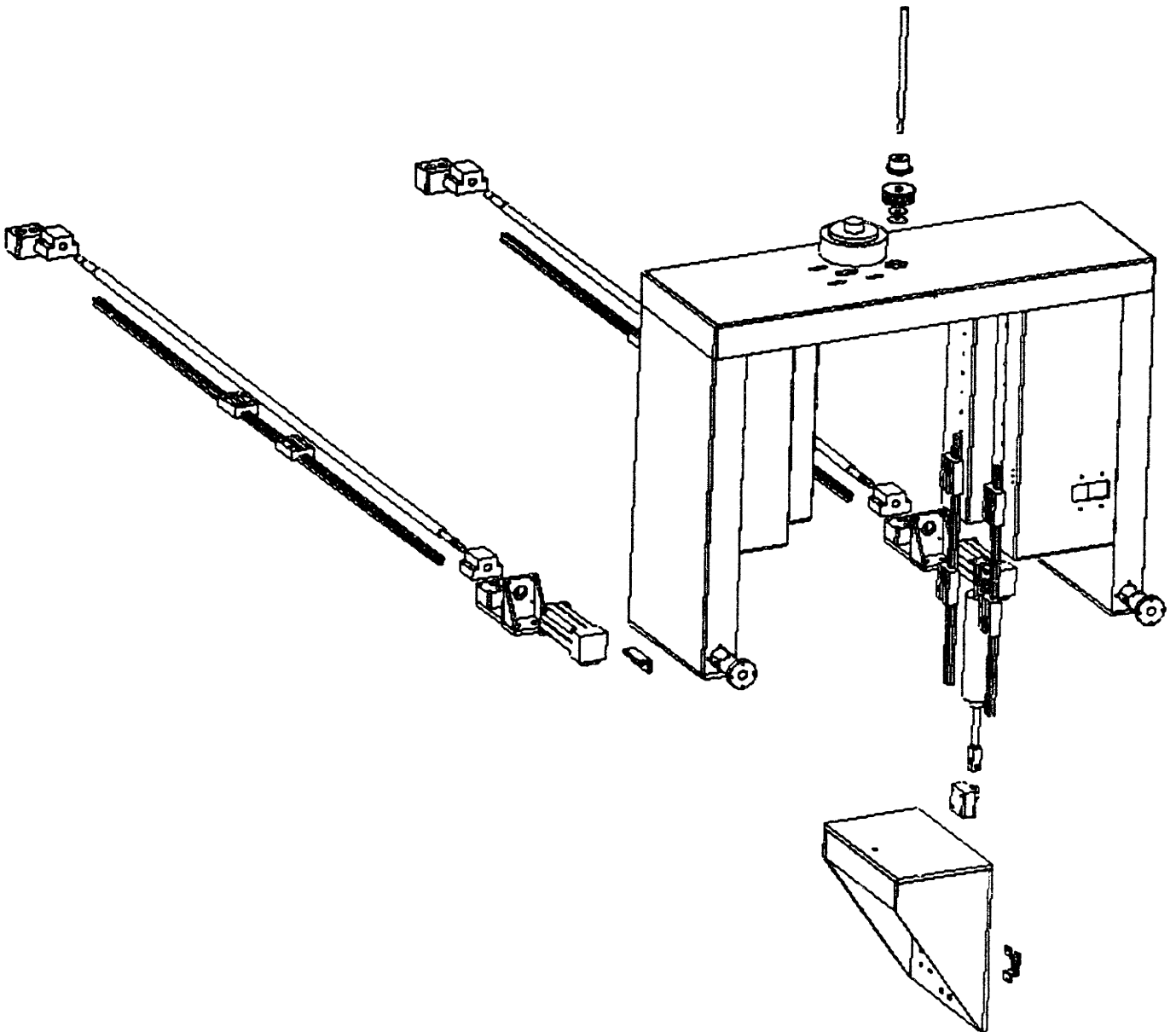


Figure 4.8: Assembly View of the Upper Machine Structure

4.4 FABRICATION PROCESS

How to fabricate this unusual design was a question that took a while to answer. One option was to use *sand casting* to create a single solid part. However this option was questionable due to the enormous size of this structure. Making a solid piece would have also added a tremendous amount of unnecessary weight to the structure. Another option was to make a hollow structure using sheet metal. Pieces of sheet metal could have been bent and welded together to create the final desired geometry. The question here was whether or not a sheet metal structure could have delivered the required stiffness to support the large polishing forces. Additional ribs could have been welded on the inside to provide the required stiffness, but this would have added complexity and cost to the manufacturing process.

The best concept was finally determined to be the use of standard hollow rectangular tubes, welded together, stress relieved, and machined afterwards to create the final desired geometry. The gantry was designed based on the available standard tube sizes. Once the overall size of the gantry was estimated, the next step was to ensure its strength and rigidity, which directly determined the size and thickness of the tubes to be used. This required the performance of FEA analysis.

4.5 STRUCTURAL DESIGN USING FINITE-ELEMENT ANALYSIS

FEA analysis is the most important tool of a mechanical designer. In designing the upper structure, Solidworks was used to draw a particular design, and Cosmos was used to perform the FEA analysis to determine where additional strength is required, and where material can be taken out. Cosmos is nicely compatible with Solidworks, which makes it very convenient to switch between the two programs.

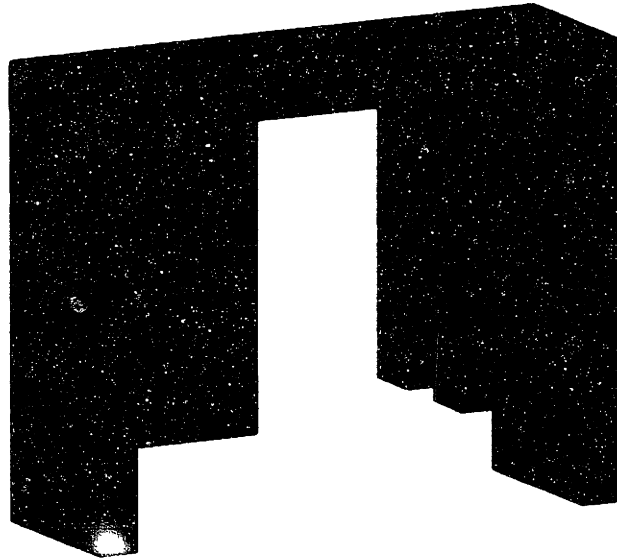


Figure 4.9: Meshed Model of the Gantry

4.5.1 Evolution to the Final Design

The first step to run the analysis was to determine the necessary boundary conditions. In this case, the x-axis linear guides constrain all degrees of freedom except the translation along the x-axis, which is constrained with the ball screw. For the sake of simplicity, the surfaces that come in contact with the linear guides were selected to be fixed in all directions. The next step was to calculate the forces acting on the structure. The frictional loads are negligible in comparison to the normal polishing load. Therefore, the only force acting on the structure was set to be a 1000 lb. load acting on the surface where the z-axis ball screw is attached to the roof of the gantry.

In this case, the FEA analysis was mainly being performed to check the *structural deflections*. Because of the high precision nature of this machine, these deflections can

greatly effect its performance. The goal was to reduce the deflections as much as possible, while maintaining a reasonable weight.

A trial-and-error approach was used to come up with the final design: a concept was generated, and after checking the deflections, the design was modified accordingly. Starting with the simplest possible design, several Solidworks models were analyzed until the deflections were reduced from 1.0 E-4 meters to an acceptable range of 1.0 E-6 meters. To avoid redundancy, details of the design and the FEA analysis have been excluded. Only the FEA model of the final design is presented in this paper to show the final deflections and stresses.

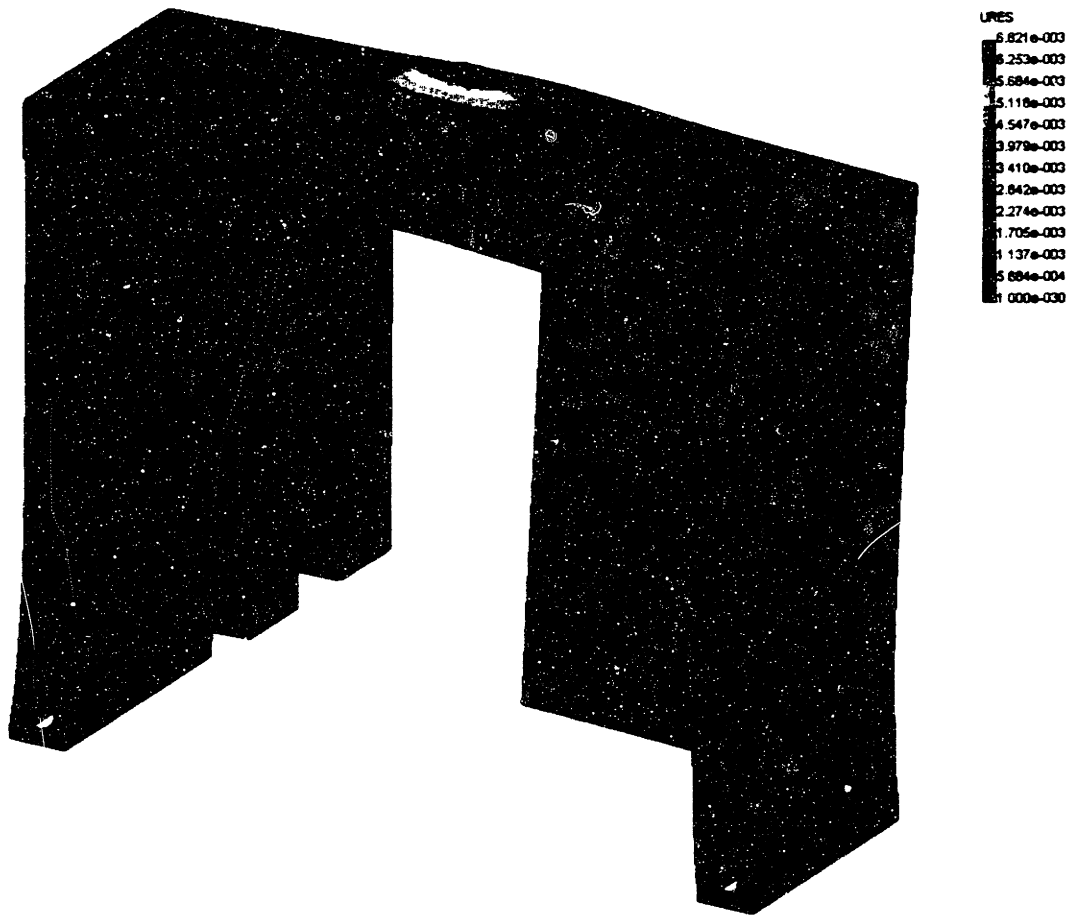


Figure 4.10: Maximum Deflection of the Gantry Structure (6.02E-3 m)

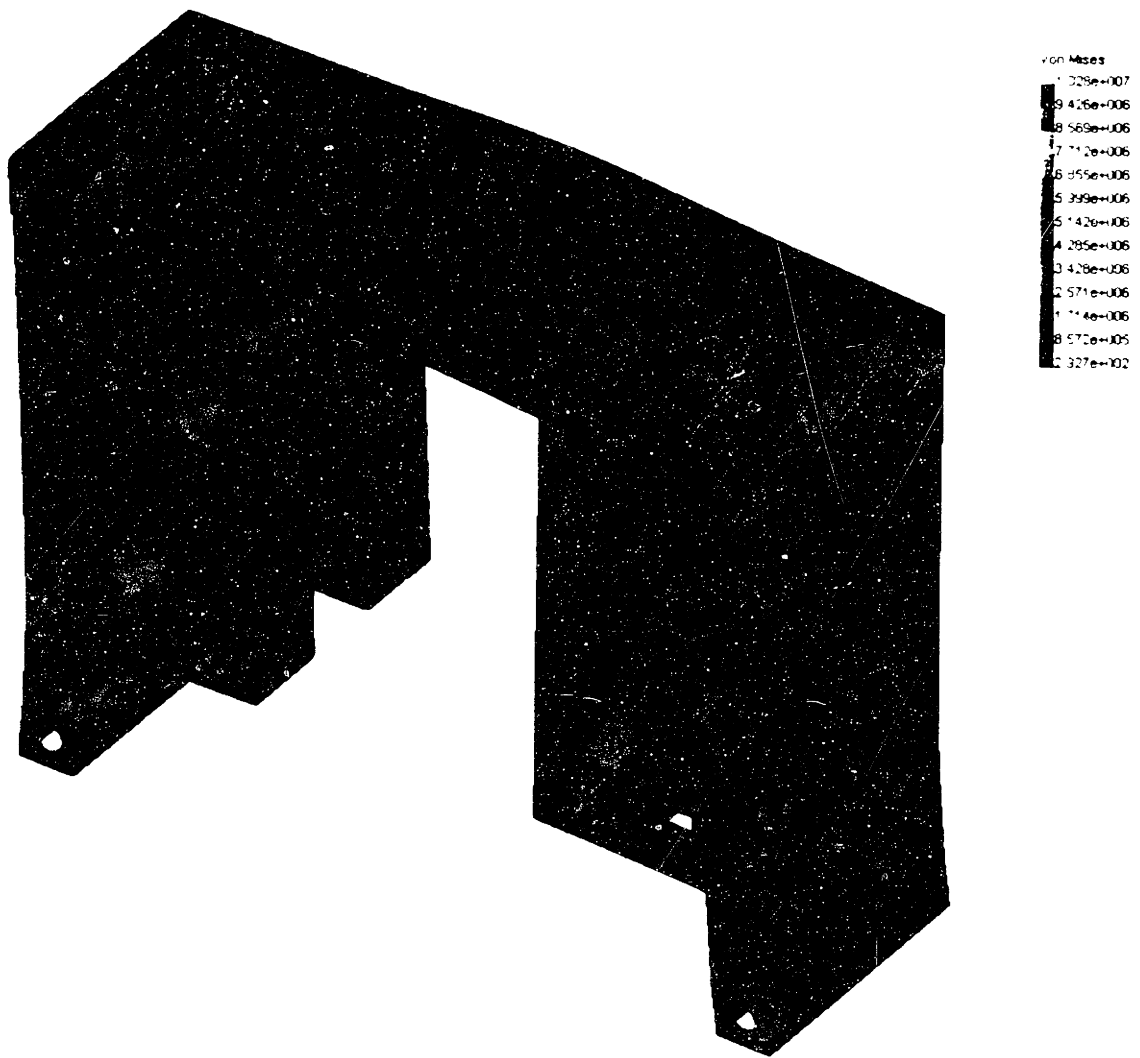


Figure 4.11: Max. Stress on the Gantry Structure ($1.02E7 \text{ N/m}^2$)

4.6 **VIBRATIONAL ANALYSIS OF THE UPPER STRUCTURE**

Using hollow rectangular tubes is a great way of fabricating this structure, but it creates some vibrational concerns. Being a precision machine, one of the most important criteria is to have low mechanical noise. The upper structure, in particular, becomes critical since it has to ‘sweep’ while the wafer is being polished. Hollow tubes, in general, have bad vibrational properties, and therefore a vibrational analysis had to be performed to check the natural frequency of this moving structure. The boundary conditions remain the same – fixed at the interface with the linear guides.

new gantry-freq:: Frequency
Mode Shape: 1 Value = 88.099 Hz

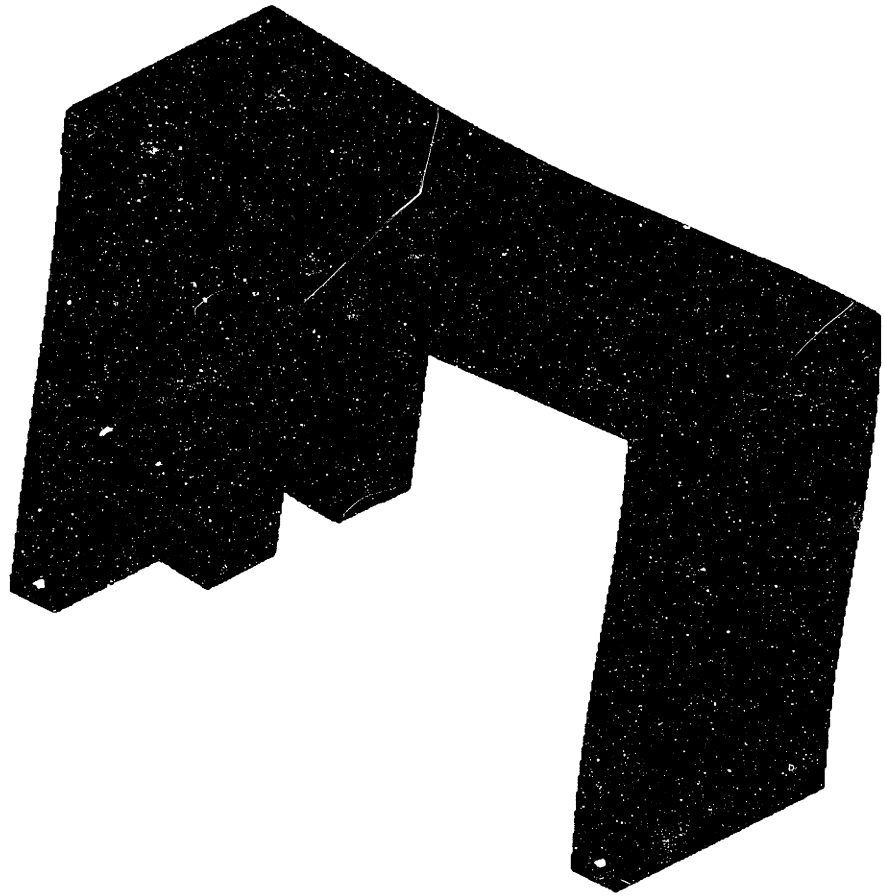


Figure 4.12: Natural Frequency of the Gantry (88.09 Hz)

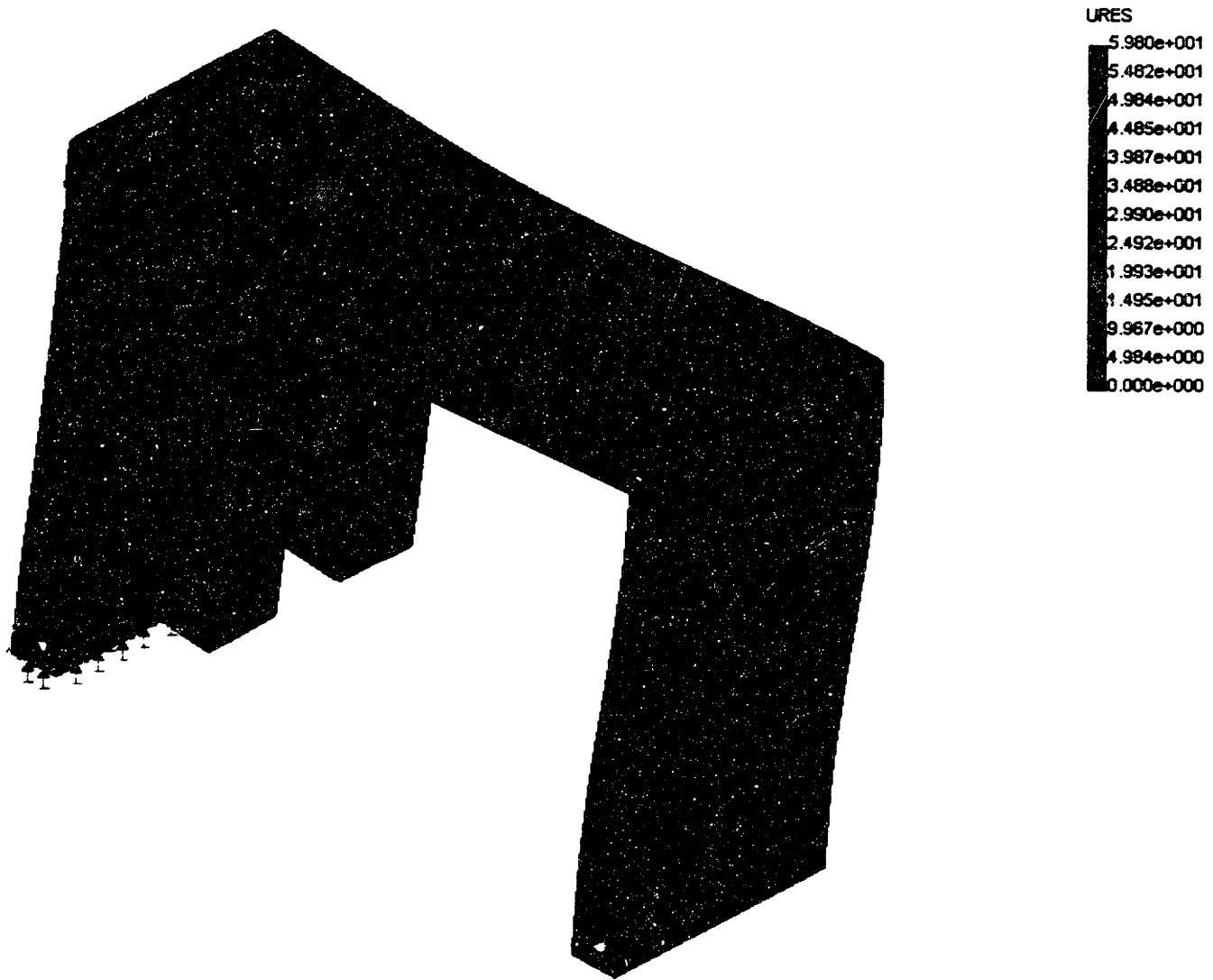


Figure 4.13: Max. Deflection of the Gantry (5.98 E1 mm)

- Load and unload the wafers into the polishing head
- Clean the wafers when moving between the platens
- Clean the polishing head
- Clean the conditioner
- Provide a resting place for the head

To help with the design of this multi-purpose load/unload station, Jamie Nam, the graduate student working on the End-Point Detection of this tool, was asked to work on designing the *cleaning mechanism*. This paper will mainly cover the design of the *load/unload mechanism*. The functions of the load/unload mechanism are listed below:

- Provide a place for the wafer to sit on its front face
- Center the wafer to an exact, repeatable position
- Hold the wafer at that position until the head comes down
- Clear the wafer for the head to grab it from the back

5.2 **EXISTING TECHNOLOGY**

The U.S. Patent # 5804507 describes the design of a popular load/unload station, which has been designed by Applied Materials Inc. The patent shows the setup of the whole machine, and describes the details of the cleaning station as well.

The Applied machine has three heads that simultaneously polish wafers on three platens. The machine has one load/unload station, which is responsible for loading the wafers into each head. The polishing heads do not have an up and down motion, and therefore the load/unload station is required to have a vertical motion to load the wafers into the heads.

The robot puts the wafer face down on a thin elastomeric film (or pad material) on top of the pedestal. Because of the inaccuracies of the CMP robot, the location of the wafer is not exactly known, and therefore it must be centered before loading into the head. Three fork assemblies are disposed around one vertical position of the pedestal to laterally align the wafer. Each fork assembly has a solenoid at the bottom, which will push the forks in an equal distance from the three sides of the pedestal to center the wafer.

Once the wafer is centered, the load station pulls vacuum through the pad material to hold the wafer in its centered position, while the head comes to load it. Once the head is directly above the wafer, the three fork assemblies move away from the wafer, and the pedestal rises until the back of the wafer comes in contact with the polishing head. The head then grabs the wafer by pulling vacuum.

To wash the wafers after they have been polished, the load/unload station sprays water at the wafer from three nozzles around the pedestal. The pedestal is vertically retractable within a washing shroud so that when three washing assemblies attached to the shroud jet rinse fluid toward the wafer, pedestal, or wafer head, the rinse fluid is contained within the shroud.

Wafers must be washed off before they are moved from one platen to another. The Applied machine does the washing via separate cleaning stations located between the platens. The wafer comes in contact with a thin strip of pad material, through which water is shot at the face of the wafer. This way, when the head spins, the whole front face of the wafer gets washed.

5.3 DETAIL DESIGN OF THE LOAD/UNLOAD STATION

In the previous section of this lab, the tasks of the load/unload station were listed. Specific features must be designed in the system for each individual task. Since the load/unload station has a large number of small parts, it would be impossible to discuss the details of individual parts. Instead, a general approach to the overall design will be presented. The load/unload station can be divided into the following main components.

5.3.1 Supporting Surface

Using vacuum, the polishing head grabs the wafer from the back. The CMP robot must therefore put the wafer down on its front face for the head to load it from the back. As discussed previously, the front of the wafer is very sensitive since it may be scratched or contaminated.

One approach would therefore be to provide a ring for the wafer to sit on, so that only the outer edge of the wafer (the 2mm circle on which the circuits are not printed) comes in contact with the ring. An easier way would be to provide a simple circular surface, covered with soft pad material, for the wafer to sit on. The current load/unload stations in the industry use this idea, and they seem to have no problems with scratching and contamination of the wafer. To clean the surface of the wafer, nozzles can be used to shoot water at the surface of the wafer from the openings that are provided in the pedestal.

Another function of the load/unload station is to clean the polishing head. The retainer ring (ring around the wafer in the head) is designed to have actuators that would enable it to move up and down with respect to the surface of the wafer. Therefore, if the retainer ring rises so that it will be at the same level as that of the wafer carrier, a larger

circular surface with pad material can be used to clean the retainer ring. The final design of the supporting surface is shown below.

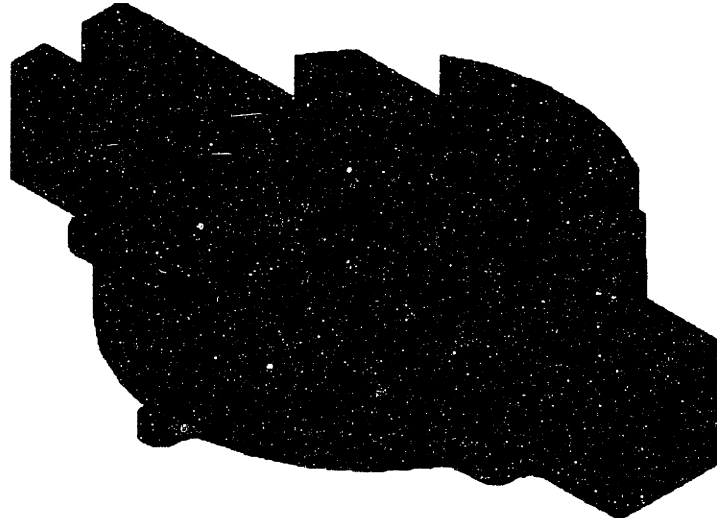


Figure 5.1 : Supporting Surface of the Load/Unload Station (Platen)

5.3.2 Centering Mechanism

CMP robots are not very accurate, and therefore the wafers must be centered accurately once the robot has put the wafer down on the supporting surface. The easiest method for doing so would be to have three arms *rotate* inward towards a center point. Using this technique, there are two possible ways of centering the wafer.

5.3.2.1 Concept 1: Constraining the Wafer in a Repeatable Circle

In this concept, the arms retract to a specific position, thereby defining a repeatable circle which is slightly larger than the wafer. While moving in, the arms push the wafer inside the circle and force it to finally be within the circle defined by the three

points. This way, the wafer will be inside the same circle each time. This is shown on the following figure:

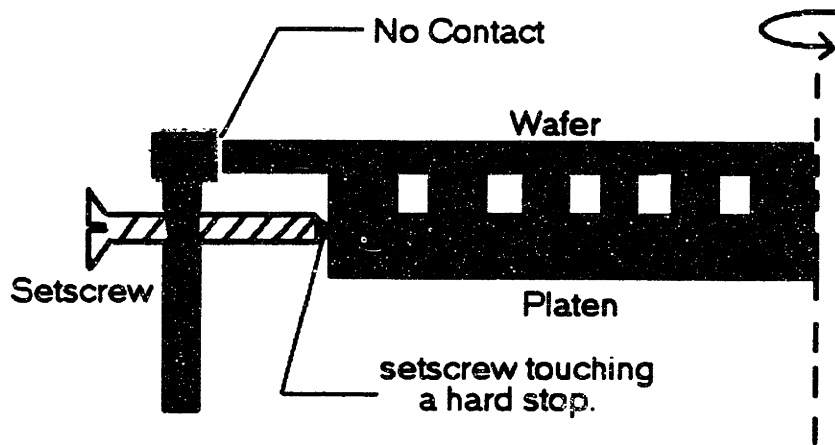


Figure 5.2: Concept #1

The final position of each arm is determined when the set screws at the end of each arm contact the walls of the supporting surface. The set screw can be used to determine the size of the repeatable circle, and to individually adjust of each arm to eliminate the need for high accuracy of each link.

The main advantage of this system is its simplicity. Each arm moves to the exact same position each time via a mechanical stop. Therefore, the need for closed-loop control of each arm is eliminated.

This concept was about to be selected as the final design concept, when a problem was discovered. The three arms define a circle that is slightly larger than the wafer. In addition, the diameter of the wafer itself varies from wafer to wafer. It is possible for a smaller wafer to slip out of the circle by going between two arms.

To eliminate this problem, more than three points must be used. To center the wafer within the desired tolerances, at least eight arms must be used, which would create a very crowded and complex system. The concept was consequentially rejected.

5.3.2.2 Concept 2: Directly Touching the Edge of the Wafer

Here the wafer sits on a surface, which is smaller than the wafer, and the three arms come in at the *exact same rate* to push the wafer towards the center of a circle defined by the motion of the three arms. To improve the performance of this concept, an additional fourth arm is used. This concept is shown below.

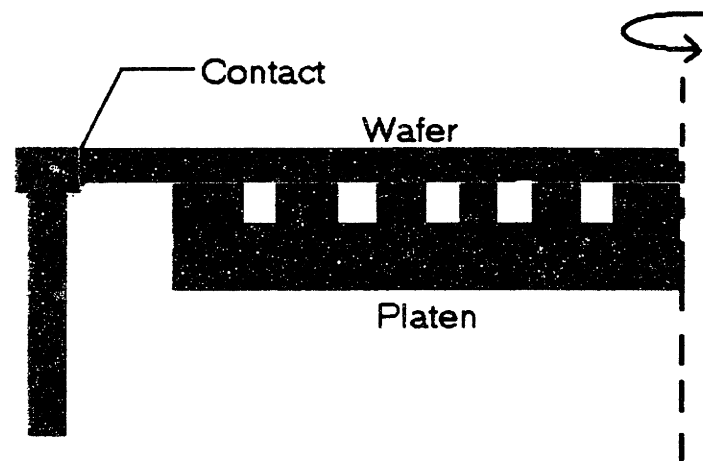


Figure 5.3: Concept #2

Since the arms now directly touch the edge of the wafer at its final position, the previous problem involving the wafer slipping out is no longer present. However, unlike the previous concept, here it is very important for the three arms to come in *exactly at the same rate*, or the wafer will not be centered correctly. This requires a system that would retract the four arms at the exact same time and the exact same velocity. The final design is shown in the figure below.

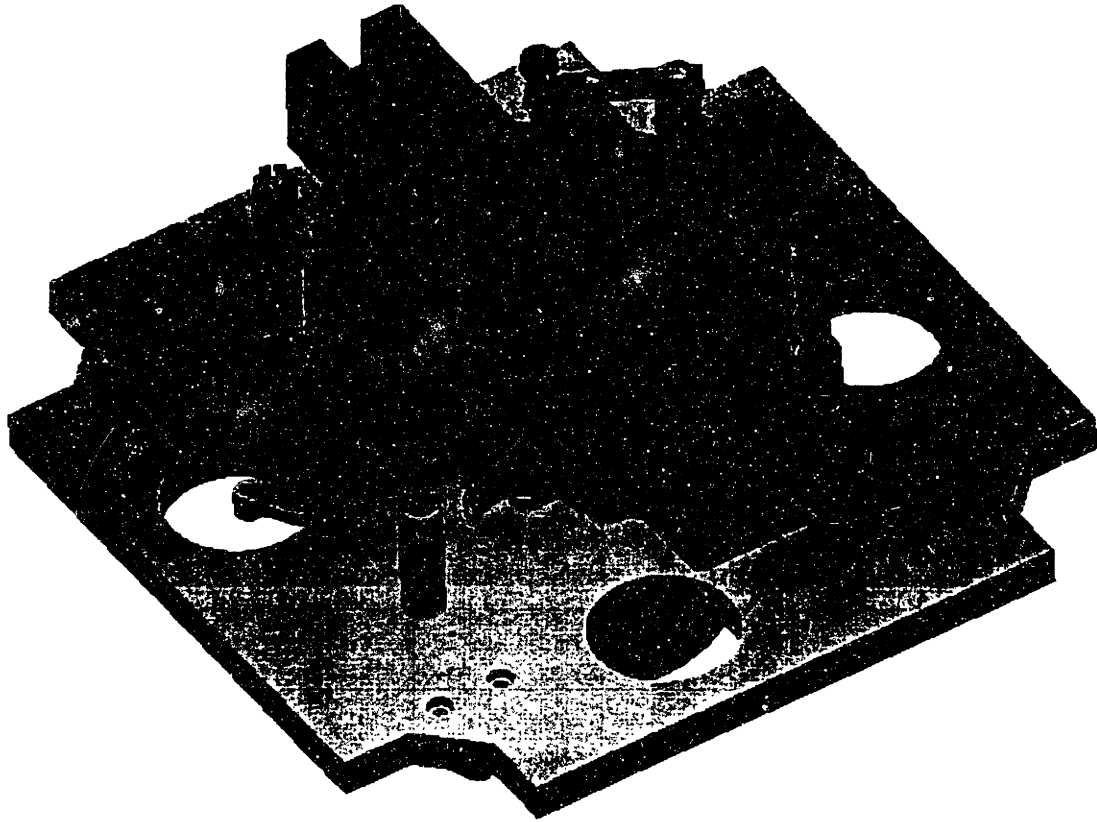


Figure 5.4: Centering Mechanism

5.3.3 Retraction Mechanism

5.3.3.1 **Concept 1: Separate Actuators**

This concept is used in Applied Material's water transfer system. Each moving pin has an associated solenoid. Using individual actuators for each arm seems redundant, and it requires a complex controls algorithm that couples the motion of the arms to make sure they will all come in at the same time

5.3.3.2 Concept 2: Belt Drive

Using a belt drive mechanism, it is possible to use one motor to retract all the arms. The problem is that the belt has some stretching/compliance associated with it, which is large enough to create problems. The centering mechanism will not work correctly if one of the arms slacks due to the stretching of the belt.

5.3.3.3 Concept 3: Kinematic Linkage

The only other way of creating a simultaneous rotation for each arm is to use a four-bar kinematic linkage to connect the arms with a central motor. This will create a “chuck” motion, which will assure the same position for each arm at any given time. This is shown in the following figure:

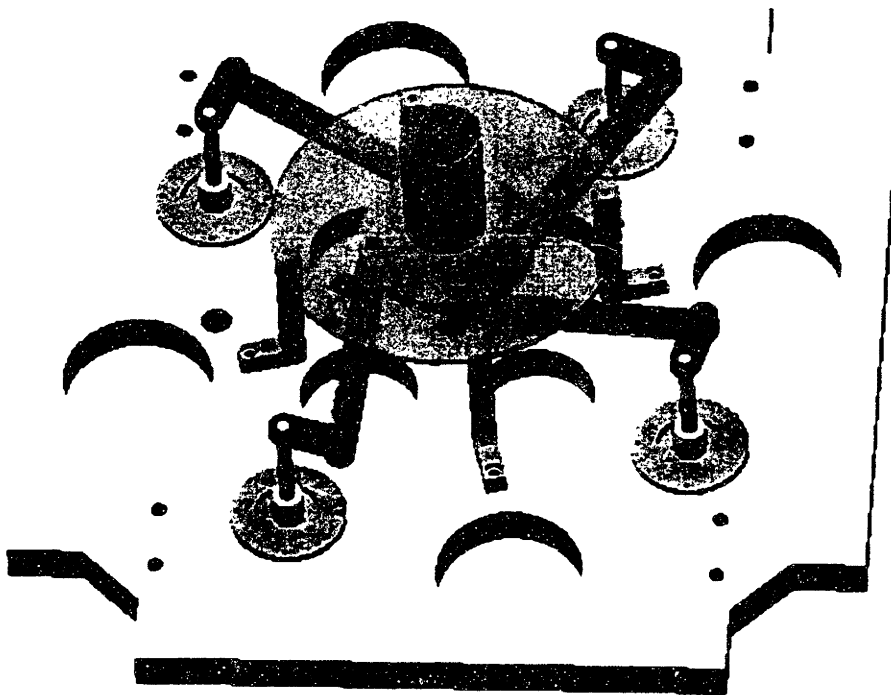


Figure 5.5: Retraction Mechanism

A *tight sliding fit* is created with dowel pins at the joints of each link. The dowel pin is press fitted into one hole, and has a slight clearance in the other hold. There is a Teflon washer between the links to avoid direct contact of the links. Teflon has the least coefficient of friction between all plastics. The rotating shafts are held in place with a pair of angular contact bearings mounted on the base. The linkage system turns one end of the shafts, while the centering arms are attached to the other end of the shaft.

5.3.4 Wafer Holding Mechanism

Once the wafer has been centered, the centering mechanism must clear the back of the wafer for the head to load the wafer. Meanwhile there must be a mechanism to hold the wafer at the same position while the head is coming down. There are two possible ways of holding the wafer.

5.3.4.1 Concept #1: Vacuum

The Applied Materials' wafer transfer station uses vacuum to hold the wafer in place once it has been centered. Once the three pins come in and center the wafer, the load/unload station pulls vacuum through the pad to hold the wafer in place, so that the pins can go back and clear space for the head to come down.

Since there is water and slurry at the surface of the cleaning station, pulling vacuum requires special valves that would not allow the back flow of water. In fact, Applied Materials has a very complicated vacuum system, in which three way valves are used to spray water and pull vacuum at the same time. The complexity of this system is a big disadvantage.

5.3.4.2 Concept #2: Vertical Motion of the Pins

After the wafer has been centered and the pins (at the end of the arms) are in contact with the edge of the wafer, if the pins are free to move down, the head can push them down while grabbing the wafer. This way the pins do not have to move out of the way; they can stay in the centered position and hold the wafer in place while the head comes down. This is shown in the following diagram:

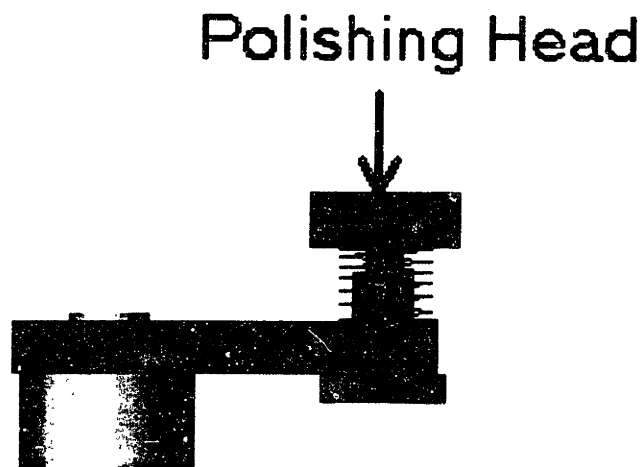


Figure 5.6 Wafer Holding Mechanism

5.4 **OVERALL LOAD/UNLOAD STATION**

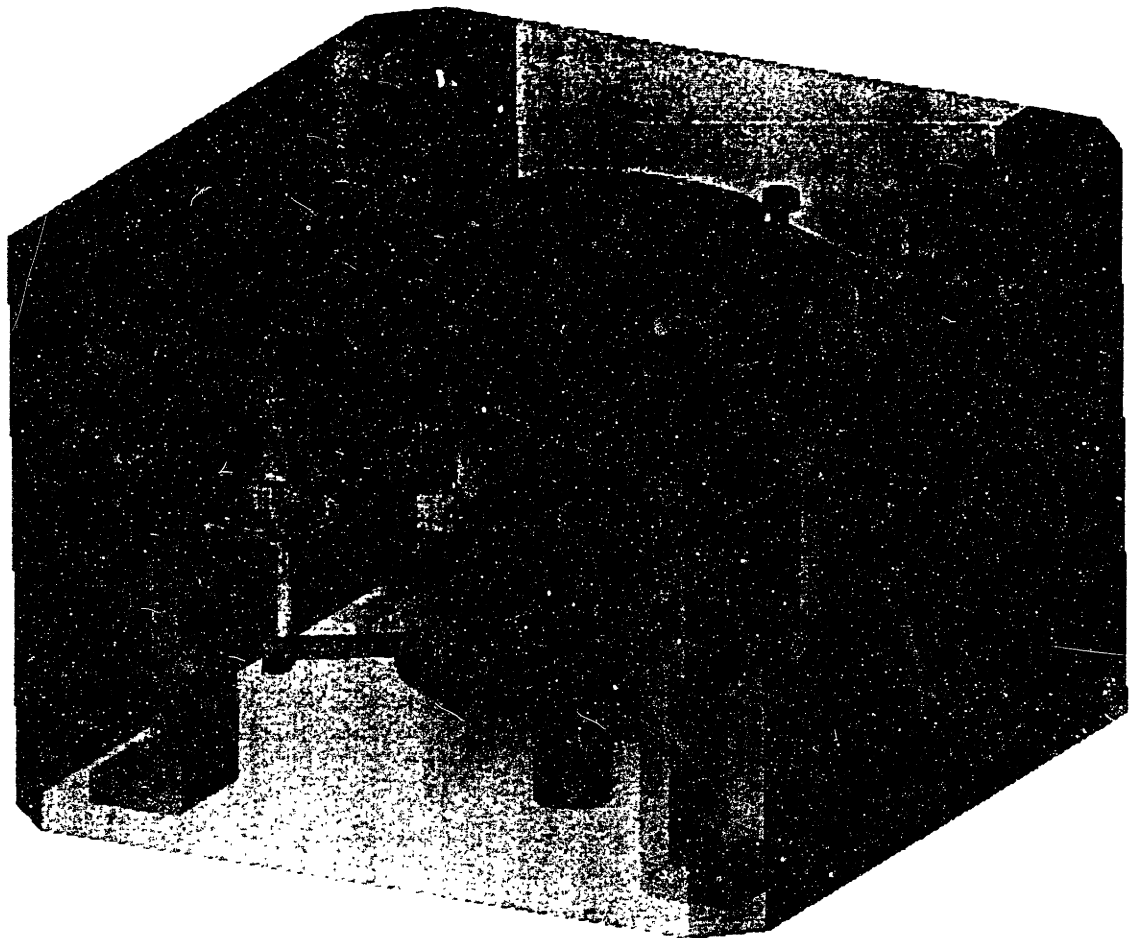


Figure 5.7: Overall Load/Unload Station

The CMP robot places the wafer down on the support surface of the cleaning station. Then the four arms move in and center the wafer. They stay in contact with the wafer, holding it in place, until the head comes down and pushes the pins down to load the wafer.

Water can be shot at the wafer and the head from the support surface. There are also additional nozzles on the sides to shoot water at the sides of the head. The cleaning

station is designed such that the conditioner is also able to access it for cleaning. The splash shield around the cleaning station keeps the water from splashing out.

This design uses the simplest method to satisfy all of the given specifications. It is a complete, yet simpler version of Applied Material's wafer transfer system. The next step is to work on the details of the design, and fabricate the system. The fabrication and testing of the system is discussed in a later chapter.

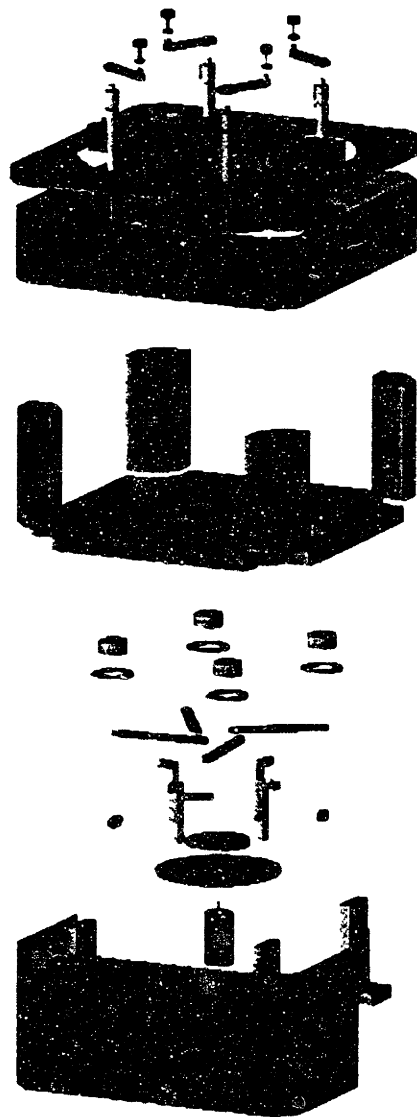


Figure 5.8: Assembly Drawing of the Load/Unload Station

5.5 DESIGN OF THE CONTROLS ALGORITHM

In this section the design and implementation of the control algorithm for the wafer-centering mechanism will be discussed in detail. The basic task is to center the wafer to 0.002" and hold it at that position while the polishing head comes down to grab it. The machine has one Brushless DC Servo Motor that turns a plate, which turns a linkage system that results in the simultaneous motion of the four arms. The final task of the arms is to apply a certain force on the wafer. However, the arms are initially not in contact with the wafer, which turns this into an impact control problem.

5.5.1 Closed-Loop Kinematics Analysis

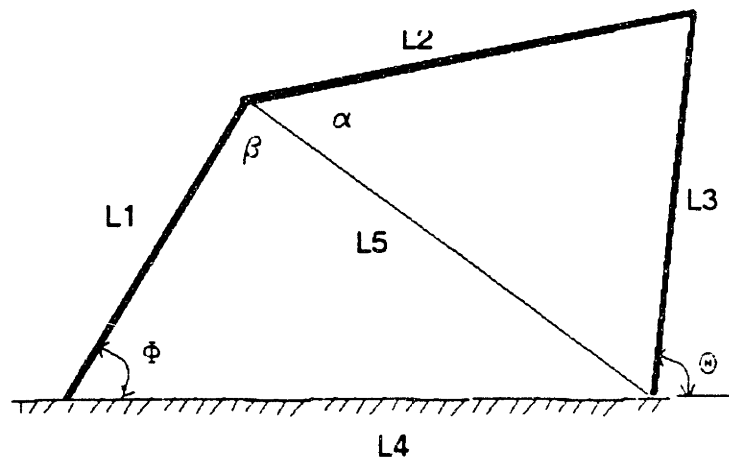


Figure 5.9: Four-Bar Linkage

The linkage system is a simple four-bar with known geometry. The challenge here was to come up with a closed-form solution of θ in terms of ϕ (i.e. θ as an “explicit” function of ϕ) so that it could be used in the control block diagram. By dividing the four-bar into a number of triangles and applying the cosine-law several times to each triangle, the kinematics problem can be solved. To verify the derivation, several points were

selected and checked against the Solidworks model of the tool. For example, at $\varphi = 130.22$ degrees, θ was calculated from the derived relations to be 100.8 degrees. This was then experimentally checked and found to be exactly correct, as shown on the following figure.

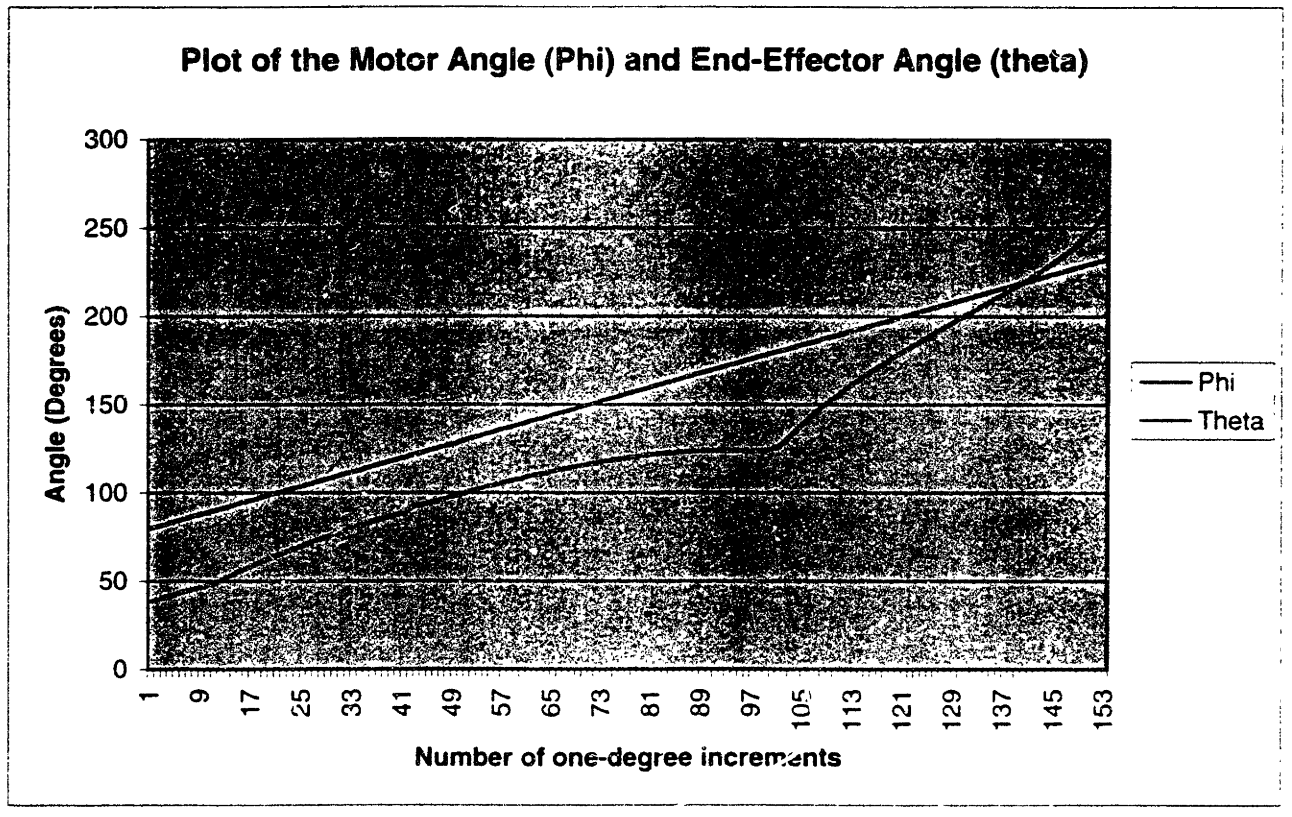


Figure 5.10: Motor Angle vs. Arm Position

5.5.2 Application of Impedance Control in Impact Control

It is not force or position that must be controlled in this problem; rather it is the overall behavior of the system. Impact is a problem here only because velocity is a critical parameter. Using a simple force control with very low gains can lead to low impact forces, but it can also lead to very low velocities. In this problem it is desirable to

minimize the loading time, and to have the arms come in as fast as possible, without damaging the wafer at the moment of impact. In impedance control, virtual damping and virtual compliance can be created at the end-effector, thereby reducing maximum impact force. The two critical parameters, the final *end-effector force*, and its *approach velocity*, dominate the effects of impulse on the wafer. Since the final task of the machine is to apply a certain force on the wafer, the input to the control algorithm is taken to be a desired steady-state force. The approach velocity, however, must also be regulated. This means that a separate controller needs to be added for velocity control. This is similar to impedance control. The following shows the block diagram of the control algorithm.

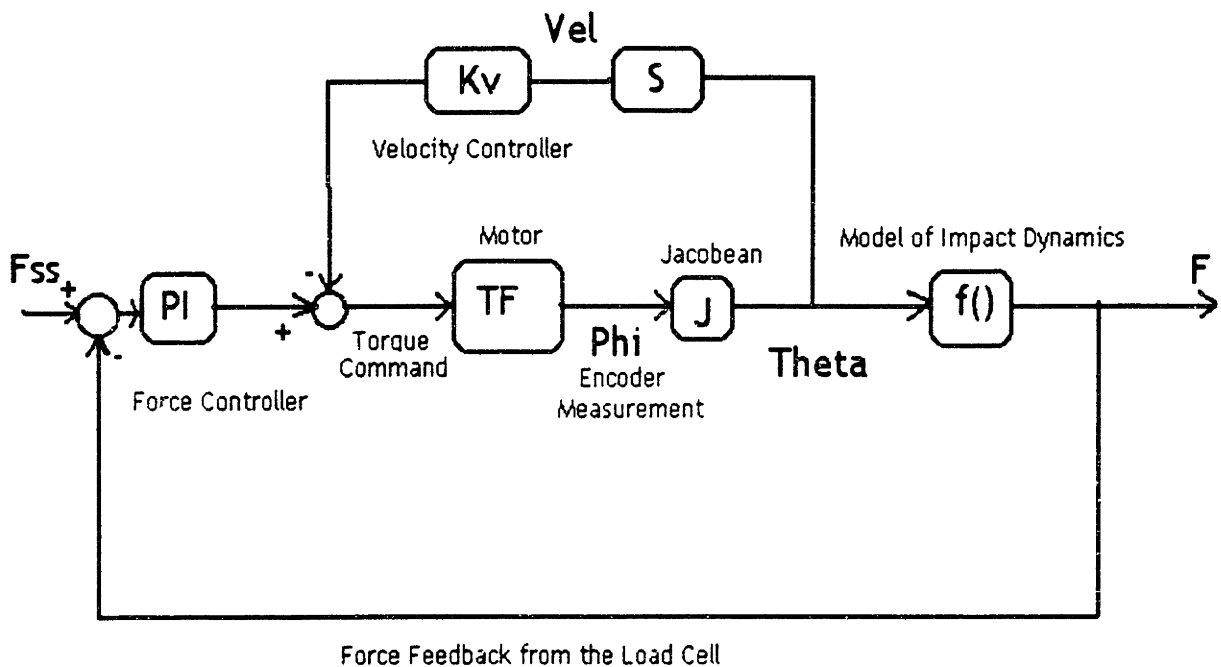


Figure 5.11: Closed-Loop Impact Control

**ORIGINAL
DOCUMENT HAS
MISSING PAGES**

5.5.3 Dynamic Modeling of Impact

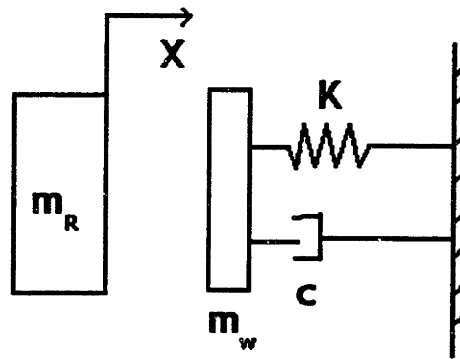


Figure 5.12: Collision Model

A model that accurately predicts the impact dynamics is required for accurate impact simulation and force controller design. In this paper, the simplest impact model is analyzed to give order-of-magnitude estimations for the impact force. It can be derived that $F = C_1X + C_2V$, where F is the impact force, X and V are the robot position, and velocity measured at the point of contact, and C_1 and C_2 are constants that are dependent on system parameters. C_1 represents the compliance of the system, and C_2 represents the system inertia.

5.5.4 Matlab Simulations

Knowing the dynamics and kinematics of the system, Simulink can be used to design and test the control algorithm. As the arms initially come in, there is no contact and therefore the force is zero. The initial impulse on the system represents the first spike in the force diagram. The control algorithm immediately kicks in and retracts the arms back to reduce the impact force. The force is therefore zero again, since the arms have lost contact. The arms come in again and hit the wafer this time with a lower

impulse, and retract again. This process repeats itself several times until the model is finally applying the correct steady-state force on the wafer.

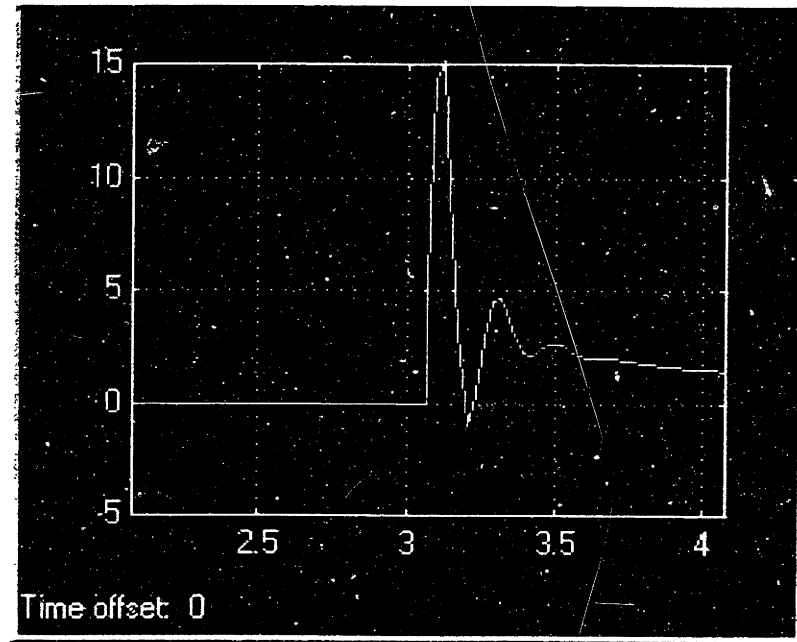


Figure 5.13: Impact Force (N) vs. Time (s)

5.5.5 Results and Discussion

Figure 5.13 shows the open-loop response of the system to a step input. Here the arm is initially not in contact with the wafer, resulting in a force of zero. At the moment of first contact, however, the impact on the wafer becomes significant, resulting in an impact force of 14 lbs. Using lower gains can reduce the overshoot, however, that would result in low velocities, which must be avoided in this machine. We can now apply the designed impact control algorithm previously discussed.

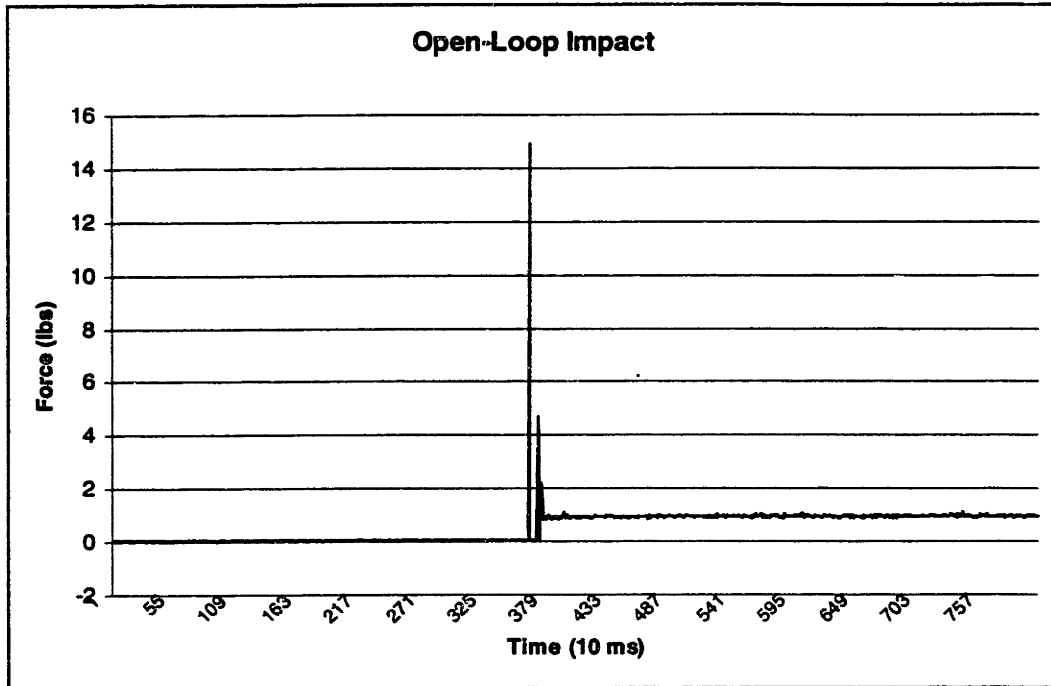


Figure 5.14: Open-Loop Impact

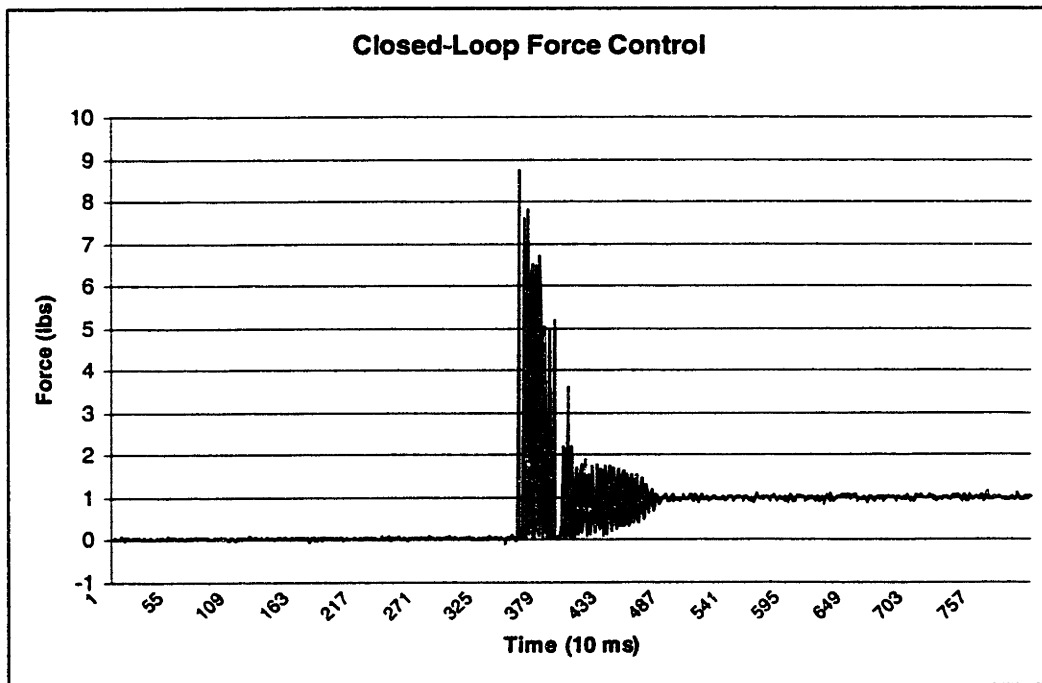


Figure 5.15: Closed-Loop Impact Control

For the same response, and the same parameters, the impact force was significantly reduced to 8 lbs (almost by a fact of 2). The system behaved exactly as predicted by the Matlab simulations. The arms came in with a certain controlled velocity, and upon initial contact they bounced back to reduce the impact force. They came in again and hit the wafer with a lower momentum, and kept doing this until the desired steady-state force was achieved. Thus the impact control mechanism has proven to be quite effective.

CHAPTER 6: AXIOMATIC DESIGN OF THE CMP MACHINE

6.1 INTRODUCTION TO AXIOMATIC DESIGN

Axiomatic design is a power design methodology, which enhances the creativity of the designer. It demands the clear formulation of the design objectives through the establishment of functional requirements (FRs) and constraints (Cs). It provides criteria for good and bad design decisions, which help in eliminating bad ideas as early as possible, enabling designers to concentrate on more promising ideas [Suh 8].

The world of design is made up of four domains: the customer domain, the functional domain, the physical domain, and the process domain. The customer domain is characterized by customer needs or attributes. In the functional domain, the customer's needs are specified in terms of functional requirements (FRs) and constraints (Cs). In order to satisfy the specified FRs, we conceive design parameters, DPs, in the physical domain. Finally, to produce the product specified in terms of DPs, we develop a process that is characterized by process variables (PVs) in the process domain [Suh 15].

The design of the CMP machine is a great application of axiomatic design. Because of its complex nature, the design of this machine required a standard systematic approach. Based on a given set of customer specifications, the design of the CMP machine was decomposed into several sublevels of FRs and DPs. In the following sections, the axiomatic design of the x-axis and the z-axis will be discussed in detail.

6.2 AXIOMATIC DECOMPOSITION OF THE Z-AXIS

6.2.1 FR11136 Allow Wafer Access

DP11136 Z-Axis

	Functional Requirements (FRs)	Design Parameters (DPs)
361	Apply Fz	Z-axis drive mechanism
362	Measure z	Z-position measurement 1
363	Allow z-motion only	Constraining other degrees-of-freedom
364	Control parameters	Z-axis control software
365	Provide mounting for head platen	Head-platen mounting plate

$$\begin{Bmatrix} \text{FR361} \\ \text{FR362} \\ \text{FR363} \\ \text{FR364} \\ \text{FR365} \end{Bmatrix} = \begin{bmatrix} \text{X} & \text{O} & \text{O} & \text{O} & \text{O} \\ \text{O} & \text{X} & \text{O} & \text{O} & \text{O} \\ \text{X} & \text{O} & \text{X} & \text{O} & \text{O} \\ \text{X} & \text{X} & \text{O} & \text{X} & \text{O} \\ \text{X} & \text{O} & \text{X} & \text{O} & \text{X} \end{bmatrix} \begin{Bmatrix} \text{DP361} \\ \text{DP362} \\ \text{DP363} \\ \text{DP364} \\ \text{DP365} \end{Bmatrix}$$

Constraint Table		Impacts:	FR.				
Index	Parent	Description	1	2	3	4	5
-- Operational Constraints --							
C11136a		Support polishing loads			✓		
C11136b		Range of Travel = 8"	✓		✓		
C11136c		Accuracy = 1 micron		✓		✓	
C11136d		Repeatability = 0.1 micron		✓		✓	
C11136e		Z-velocity = 4 in/sec	✓				

FR111361 Apply Fz

DP111361 Z-axis Drive Mechanism

	Functional Requirements (FRs)	Design Parameters (DPs)
611	Apply counter-balance force	Pneumatic Piston
612	Create torque for fine tuning	Z-axis motor
613	Convert torque to Fz	Ball nut
614	Support reaction torque and counter-balance force	Roof of the gantry structure
615	Transfer Fz to moving plate	Ball screw root diameter
616	Support reaction Fz	Bearing of the ball nut
617	Transfer motor torque to ball nut	Pulley and timing belt

$$\begin{Bmatrix} \text{FR611} \\ \text{FR612} \\ \text{FR613} \\ \text{FR614} \\ \text{FR615} \\ \text{FR616} \\ \text{FR617} \end{Bmatrix} = \begin{bmatrix} \text{X} & \text{O} & \text{O} & \text{O} & \text{O} & \text{O} & \text{O} \\ \text{O} & \text{X} & \text{O} & \text{O} & \text{O} & \text{O} & \text{O} \\ \text{O} & \text{O} & \text{X} & \text{O} & \text{O} & \text{O} & \text{O} \\ \text{X} & \text{X} & \text{O} & \text{X} & \text{O} & \text{O} & \text{O} \\ \text{O} & \text{O} & \text{X} & \text{O} & \text{X} & \text{O} & \text{O} \\ \text{O} & \text{O} & \text{X} & \text{O} & \text{O} & \text{X} & \text{O} \\ \text{O} & \text{X} & \text{X} & \text{O} & \text{O} & \text{O} & \text{X} \end{bmatrix} \begin{Bmatrix} \text{DP611} \\ \text{DP612} \\ \text{DP613} \\ \text{DP614} \\ \text{DP615} \\ \text{DP616} \\ \text{DP617} \end{Bmatrix}$$

Constraint Table		Impacts:	FR._____						
Index	Parent	Description	1	2	3	4	5	6	7
-- Operational Constraints --									
C111361a		Apply 750 lbs. of axial load (Fz = 750)	✓	✓				✓	
C111361b		Low noise level and high smoothness.	✓	✓					✓

FR111362 Measure Z

DP111362 Z-Position Measurement System

	Functional Requirements (FRs)	Design Parameters (DPs)
621	Measure motor output	Rotary encoder
622	Provide z-reference	Magnetic strip of linear encoder
623	Determine position relative to reference	Read head
624	Align read head relative to reference	Head mounting
625	Maintain reference alignment	Strip mounting

$$\begin{Bmatrix} \text{FR621} \\ \text{FR622} \\ \text{FR623} \\ \text{FR624} \\ \text{FR625} \end{Bmatrix} = \begin{bmatrix} \text{X} & \text{O} & \text{O} & \text{O} & \text{O} \\ \text{O} & \text{X} & \text{O} & \text{O} & \text{O} \\ \text{O} & \text{X} & \text{X} & \text{O} & \text{O} \\ \text{O} & \text{O} & \text{X} & \text{X} & \text{O} \\ \text{O} & \text{X} & \text{O} & \text{O} & \text{X} \end{bmatrix} \begin{Bmatrix} \text{DP621} \\ \text{DP622} \\ \text{DP623} \\ \text{DP624} \\ \text{DP625} \end{Bmatrix}$$

Constraint Table			Impacts:					FR.				
Index	Parent	Description	1	2	3	4	5	1	2	3	4	5
-- Operational Constraints --												
C111362a		Resolution = 1 micron			✓	✓						

FR111363 Allow Z-Motion Only

DP111363 Constraining Other Degrees-Of-Freedom

	Functional Requirements (FRs)	Design Parameters (DPs)
631	Support normal load (Fy)	Linear guides (recirculating balls)
632	Support radial force (Fx)	Equivalent-loading linear guides
633	Support pitch moment (My)	Separated blocks on each rail
634	Support roll moment (Mx)	Separated rails
635	Support yaw moment (Mz)	Separated blocks and rails

$$\begin{Bmatrix} \text{FR631} \\ \text{FR632} \\ \text{FR633} \\ \text{FR634} \\ \text{FR635} \end{Bmatrix} = \begin{bmatrix} \text{X} & \text{O} & \text{O} & \text{O} & \text{O} \\ \text{X} & \text{X} & \text{O} & \text{O} & \text{O} \\ \text{O} & \text{X} & \text{X} & \text{O} & \text{O} \\ \text{X} & \text{O} & \text{O} & \text{X} & \text{O} \\ \text{X} & \text{O} & \text{O} & \text{X} & \text{X} \end{bmatrix} \begin{Bmatrix} \text{DP631} \\ \text{DP632} \\ \text{DP633} \\ \text{DP634} \\ \text{DP635} \end{Bmatrix}$$

Constraint Table		Impacts:	FR. _____				
Index	Parent	Description	1	2	3	4	5
-- Operational Constraints --							
C111363a		Support 200 lbs. of friction (acting at the center of wafer along x-axis) and the moments induced by that force.	✓				✓
C111363b		Support 500 lbs. of friction (acting at the center of wafer along the y-axis) and the moments induced by that force.	✓			✓	
C111363c		High rigidity in all directions.	✓	✓			

6.2.2 AXIOMATIC DECOMPOSITION OF THE X-AXIS

FR1113 **Set Dynamic Wafer Offset**

DP1113 **X-Axis**

	Functional Requirements (FRs)	Design Parameters (DPs)
131	Apply Fx1	X-axis drive mechanism 1
132	Apply Fx2	X-axis drive mechanism 2
133	Measure x1	X-position measurement 1
134	Measure x2	X-position measurement 2
135	Allow x-motion only	Constraining other degrees-of-freedom
136	Control parameters	X-axis control software
137	Provide cable compliance	Cable carrier

$$\begin{Bmatrix} \text{FR131} \\ \text{FR132} \\ \text{FR133} \\ \text{FR134} \\ \text{FR135} \\ \text{FR136} \\ \text{FR137} \end{Bmatrix} = \begin{bmatrix} \text{X} & \text{O} & \text{O} & \text{O} & \text{O} & \text{O} & \text{O} \\ \text{O} & \text{X} & \text{O} & \text{O} & \text{O} & \text{O} & \text{O} \\ \text{X} & \text{O} & \text{X} & \text{O} & \text{O} & \text{O} & \text{O} \\ \text{O} & \text{X} & \text{O} & \text{X} & \text{O} & \text{O} & \text{O} \\ \text{O} & \text{O} & \text{O} & \text{O} & \text{X} & \text{O} & \text{O} \\ \text{X} & \text{X} & \text{X} & \text{X} & \text{O} & \text{X} & \text{O} \\ \text{O} & \text{O} & \text{X} & \text{X} & \text{X} & \text{O} & \text{X} \end{bmatrix} \begin{Bmatrix} \text{DP131} \\ \text{DP132} \\ \text{DP133} \\ \text{DP134} \\ \text{DP135} \\ \text{DP136} \\ \text{DP137} \end{Bmatrix}$$

Constraint Table			Impacts:							
Index	Parent	Description	FR.							
			1	2	3	4	5	6	7	
-- Operational Constraints --										
C1113a		Support polishing loads						✓		
C1113b		Range of Travel = 78"	✓	✓				✓		
C1113c		Repeatability = 0.1 mm			✓	✓			✓	

Constraint Table			Impacts: FR.____						
Index	Parent	Description	1	2	3	4	5	6	7
C1113d		(X1 - X2) = ± 0.1 mm			✓	✓		✓	
C1113e		Wafer offset oscillation frequency = 1 Hz	✓	✓					
C1113f		X-velocity = 12 in/sec	✓	✓					
C1113g		X-acceleration = 0.2g	✓	✓					

FR11131 Applv Fx1

DP11131 X-axis Drive Mechanism

	Functional Requirements (FRs)	Design Parameters (DPs)
311	Create torque	X-axis motor
312	Convert torque to Fx	Ball nut
313	Support reaction torque	Motor bracket
314	Transfer torque to ball nut	Ball screw root diameter
315	Support reaction Fx	Bearings and bearing blocks
316	Transfer motor torque to ball screw	Flexible coupling

$$\begin{Bmatrix} \text{FR311} \\ \text{FR312} \\ \text{FR313} \\ \text{FR314} \\ \text{FR315} \\ \text{FR316} \end{Bmatrix} = \begin{bmatrix} X & O & O & O & O & O \\ O & X & O & O & O & O \\ X & O & X & O & O & O \\ O & X & O & X & O & O \\ O & O & O & X & X & O \\ X & O & O & X & O & X \end{bmatrix} \begin{Bmatrix} \text{DP311} \\ \text{DP312} \\ \text{DP313} \\ \text{DP314} \\ \text{DP315} \\ \text{DP316} \end{Bmatrix}$$

Constraint Table		Impacts:	FR.____						
Index	Parent	Description	1	2	3	4	5	6	7
-- Operational Constraints --									
C11131a		Apply 100 lbs. of axial load (Fx = 100)	✓				✓		
C11131b		Low noise level, zero backlash, and high smoothness	✓	✓					

FR11133 Measure X1

DP11133 X-Position Measurement System

	Functional Requirements (FRs)	Design Parameters (DPs)
331	Provide x-reference	Magnetic strip of linear encoder
332	Determine position relative to reference	Read head
333	Align read head relative to reference	Head mounting
334	Maintain reference alignment	Strip mounting

FR331	X	O	O	O	DP331
FR332	O	X	O	O	DP332
FR333	O	X	X	O	DP333
FR334	X	O	O	X	DP334

Constraint Table		Impacts:	FR.____			
Index	Parent	Description	1	2	3	4
-- Operational Constraints --						
C11133a		Resolution = 10 microns		✓		

FR11135 Allow X-Motion Only

DP11135 Constraining Other Degrees-Of-Freedom

	Functional Requirements (FRs)	Design Parameters (DPs)
351	Support normal load (Fz)	Linear guides (recirculating balls)
352	Support radial force (Fy)	Equivalent-loading linear guides
353	Support pitch moment (My)	Separated blocks on each rail
354	Support roll moment (Mx)	Separated rails
355	Support yaw moment (Mz)	Separated blocks and rails

FR351	X	O	O	O	O	DP351
FR352	X	X	O	O	O	DP352
FR353	X	O	X	O	O	DP353
FR354	O	X	O	X	O	DP354
FR355	O	X	X	X	X	DP355

Constraint Table			Impacts: FR. __				
Index	Parent	Description	1	2	3	4	5
-- Operational Constraints --							
C11135a		Support 750 lbs. of normal force (acting at the center of wafer) and the moments induced by that force.	✓			✓	
C11135b		Support 500 lbs. of friction (acting at the center of wafer along the y-axis) and the moments induced by that force.		✓		✓	
C11135c		High rigidity in all directions.	✓	✓			

6.3 ***THE OVERALL CMP MACHINE***

6.3.1 Final Design

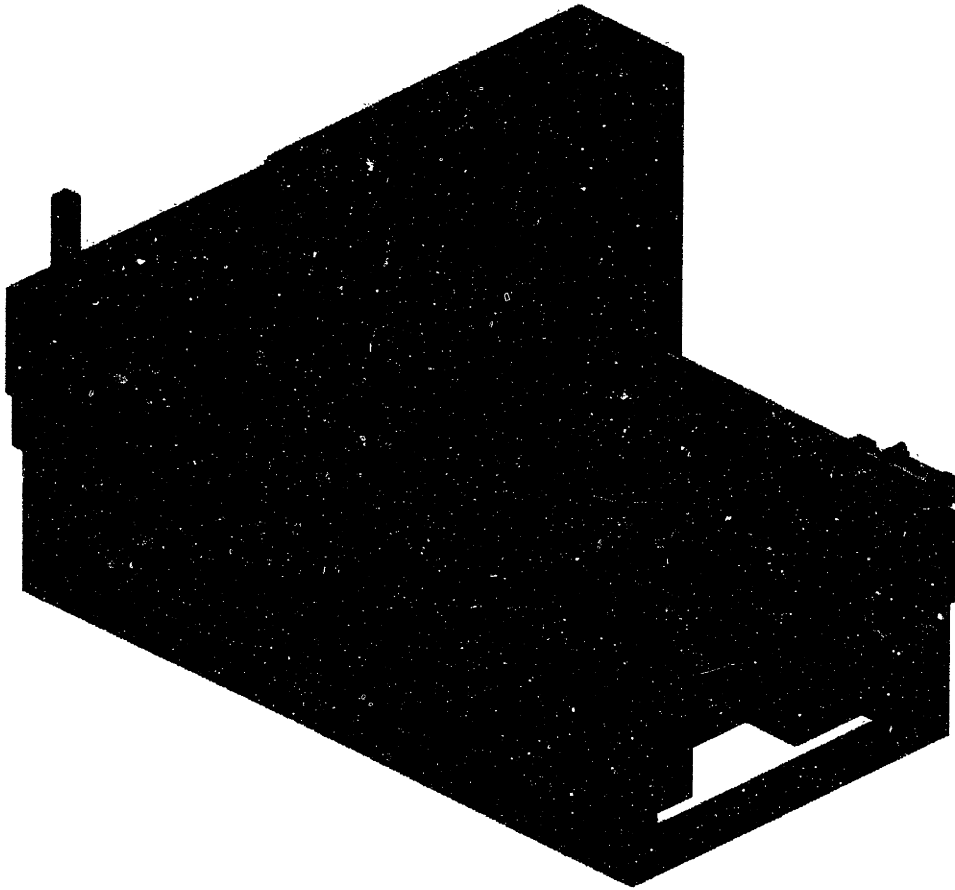


Figure 6.1 : The CMP Machine

The above picture shows the overall CMP machine. This thesis only covers the design of the x-axis, the z-axis, the upper structure, and the load/unload station. The CMP machine consists of many other components, which were discussed in the introduction chapter; they can be seen in the above figure. In addition to the complicated pressure application system of the polishing head, the CMP machine has nine independent axes of motion driven by DC Servo Motors. This paper only covers the design of four actuators.

It is important to understand that even though the three mechanical designers working on this project each worked on specific components, the conceptual design of the machine was developed by a team. The underlying concepts for individual components were discussed at tense design meetings until everyone agreed on the best possible design. Details of the design were the responsibility of the individual designer working on that specific component. The major sections of the CMP machine will be briefly discussed in the next few sections.

6.3.2 Upper Structure

This includes everything above the top surface of the granite table. The upper structure, sometimes called the “the gantry,” refers to the moving structure of the machine. This includes the x-axis, the z-axis, and the actual upper frame of the machine. The design of these systems has been explained in detail throughout this thesis.

6.3.3 Lower Structure

This includes everything below the top surface of the granite table. The lower structure includes the two lower platens, the head platen, the granite table, and the supporting frame. As previously discussed, granite was used in the lower structure because it has the following properties: good surface flatness, high precision and accuracy, good damping, low cost, dimensional stability, and good chemical properties. Granite tables are often used in optical applications because of their high flatness properties. The supporting frame was designed from hollow rectangular tubing. The granite table was supported on only three points to conserve its flatness of 0.0004”

throughout its total length (108"). To eliminate deflections and improved vibrational properties, the granite table was designed to weigh over 8000 lbs.

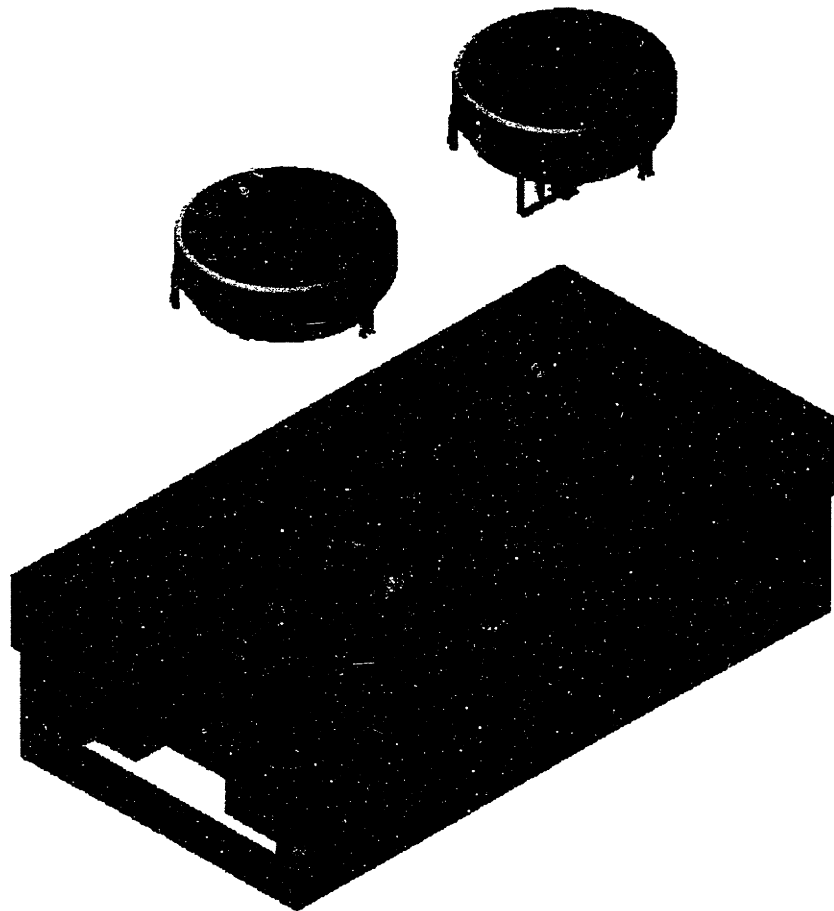


Figure 6.2: Lower Structure Assembly

The platens were designed with extreme precision in mind. The platen motors were custom designed for Navy submarines, and they are among the most mechanically quiet motors ever built. These frameless motors drive the platens, which are sand-casted because of their complicated geometry. The platens have radial flanges to increase stiffness. The platens rest on large diameter ball bearings that are mounted on the granite table. Built in Japan, these bearings are over 3 feet in diameter, and are among the most

precise (2 micron run-out) and most expensive of their kind. Finally, there is a detachable granite disk that attaches to the platens, which is very flat over its length. The following figure shows the platen structure assembly.



Figure 6.3: Platen Assembly

6.3.4 Polishing Head

The polishing head is an important feature of this machine since it directly affects the polishing performance. To manufacture blanket wafers, silicon is grown in the form of single crystals, which are later cut into thin disks. These thin disks are not entirely flat over their length, and most of the incoming wafers are originally bowed. This results in a

non-uniform pressure distribution on the wafer during CMP, which ultimately leads to a non-uniform removal rate.

The polishing head of this CMP machine has the ability to control the pressure profile behind the wafer. This is done by independently controlling the pressure in four separate radial chambers behind the wafer. This idea was implemented using a custom made flexible membrane, which is divided into four separate rings. The polishing head is a compact arrangement of bellows, machined rings, strain gages (force feedback), fluid couplings, etc. as shown in the following figure.

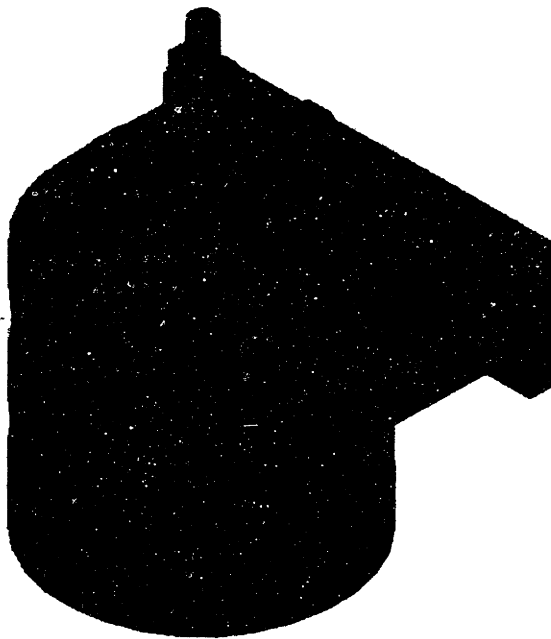


Figure 6.4: Head Platen

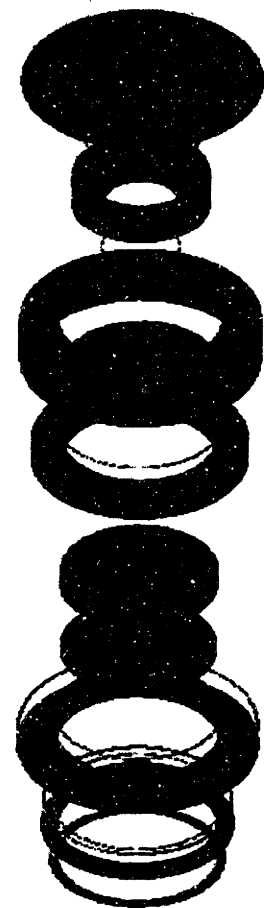


Figure 6.5: Polishing Head Assembly

6.3.5 End-Point Detection

End-point detection is another distinguishing feature of this machine. A major problem with CMP is that wafers are either under-polished (not all of the copper gets removed), or over-polished (too much copper is removed). Under-polishing is not acceptable since it causes shorts between the circuits, thereby necessitating the repolishing of the wafer, which decreases the overall throughput significantly. Over-polishing leads to the 'dishing' phenomenon, which reduces yield.

The end-point detection of this CMP machine takes advantage of the different optical properties of various wafer layers to determine the end of the polishing process. Copper and SiO₂ have drastically different reflectance values (90% Cu vs. 30% SiO₂). An optical sensor is embedded into the lower platen, which scans the surface of the wafer through a window in the pad. The sensor detects the change in reflectance once all of the copper has been removed.

The sensor is capable of local end-point detection since it passes through the entire wafer diameter. The importance of this sensor cannot be overlooked, as it acts as the feedback for the polishing head. The pressure application system can apply more or less pressure at the desired point on the wafer, depending on the reading of the sensor.

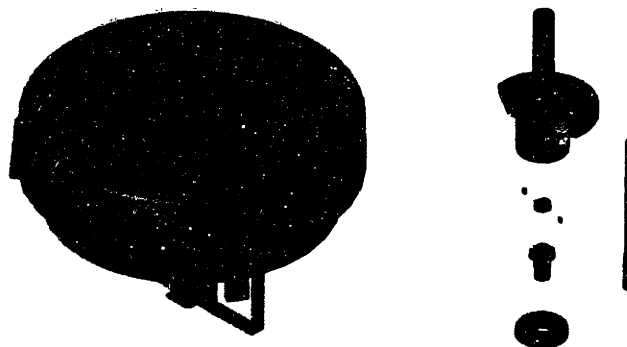


Figure 6.6: End Point Detection Assembly

CHAPTER 7: FABRICATION AND DEBUGGING

7.1 *DEBUGGING*

Once the design of the machine was completed, the computer-generated drawings were sent to outside machine shops for construction. The supplier had to be chosen carefully so that it would have the required equipment to fabricate the large gantry structure (i.e. a large oven was required for stress relieving the gantry). Once the drawings were sent out to the chosen supplier, the technicians often had questions about drawings that had to be answered. In a number of cases there were features the machinist could not create, and therefore the drawings had to be changed accordingly. Such design problems were fixed during the early stages. There were instances in which the problem was discovered during assembly. The part had to be modified in these cases, either at the MIT machine shop or by sending it back to the supplier. Some of these problems are listed below.

Rounds on the Gantry Tubes: When designing the gantry structure, the tubes were assumed to have a sharp 90-degree angle. In reality, these tubes have a 1/2" round on the edges, which led to the following problems:

- One of the holes for attaching the ball nut of the x-axis to the lower leg of the gantry was partly drilled on the round. No modifications were required for this problem.
- The gantry surface supporting the magnetic strip of the z-axis linear encoder had a round on its edge. Epoxy was used to create a sharp edge for sticking down the encoder strip.

Z-Ball Nut Mounting: The supporting surface for the z-axis ball nut should have been toleranced to be parallel with the surface of the granite table (x-datum plane of the gantry). In the gantry drawing, instead of tolerancing the *inner surface* of the roof, which supports the ball nut, the outside of the roof was toleranced to be parallel with the x-datum plane. This problem was solved by injecting Epoxy behind the ball nut once it had been assembled.

Under Cut in the Z-Reference Edge: At the intersection of the z-reference edge with the roof of the gantry, there needed to be a 6" undercut to allow for the milling tool to have access. This problem was solved by leaving out the last 6" of the reference edge.

X-Ball Nut Interference: The gantry leg consisted of three hollow tubes with a through hole for the x-axis ball nut mounting. The hole in the second tube did not line up with the hole of the first tube. When the ball nut was placed in the hole, it did not go through all the way to sit against the supporting surface of the gantry. A thin washer was machined to go between the gantry supporting surface and the ball nut to fill the gap.

Mounting Holes of the Gantry: When assembling the gantry onto the granite table, the gantry holes did not line up with the holes on the blocks of the x-axis linear guides. This was because the holes had not been toleranced from each other (center to center), instead they were only toleranced from the edges. This problem was solved by using a jack to push the walls of the gantry apart so that the holes would line up.

X-Sensor Mounting Bracket: After assembling the x-sensor mounting brackets, it was found that on one side the gap between the sensor head and the magnetic strip was much smaller than it should have been. This was a manufacturing defect, and the part was

made out of spec. The problem was solved by milling away a thin layer from the mounting face of the encoder bracket.

Pneumatic Piston Attachment: A pin joint was used to attach the pneumatic piston to the head plate, so that it would allow the piston to rotate freely. In the current design, the corners where the piston attaches to the “pneumatic piston attachment” do not allow the piston to rotate. This problem was solved by machining two pockets into the “pneumatic piston attachment” to avoid interference with the corners.

Wiring Holes for the X-Axis Encoders: The two holes drilled on the legs of the gantry to allow for the wires of the x-axis linear encoders to go through were too small for the encoder head to pass through. An attempt was made to drill these holes larger. However, drilling a 1” hole through 1/2” thick stainless steel proved to be extremely difficult. Instead of passing the encoder heads through the holes, the wires were cut, passed through the holes, and then reconnected together.

Bearing Housing Hole Defects: The holes on the x-axis bearing mountings were not tapped correctly. The drilled tap hole was probably larger than its standard dimension, thereby resulting in weak treads that were stripped once the bolts were tightened. These holes were drilled and tapped to accommodate a larger bolt size.

Head Plate Reference Edge: The z-axis linear guides were designed to sit against reference edges to be perpendicular to the pad surface. However, the head plate, which mounted on the linear guides, did not have a reference edge to line it up with the guides. To correct this problem, a small rectangular piece of metal was glued to the back of the head plate to create this reference edge. Even though this edge could not guarantee the

perpendicularity of the head plate to the pad surface, it did create a repeatable position for the head plate in case it was disassembled.

Head Plate Access Hole: Once the head plate was mounted correctly, the bolts for the linear rail, resting on spacer B, had to be tightened. However, the head plate was in the way, and therefore a small hole had to be drilled in the head plate to allow access to the rail.

7.2 ASSEMBLY

7.2.1 Assembly of the Z-Axis

The gantry structure and the associated components for the x and the z-axes were among the first components of the machine to be received. The z-axis was ready to be assembled while the lower structure was still being fabricated. The gantry was shipped on a pallet, sleeping on its side. An “A-Crane Gantry Crane” was used to lift it to its upright position, sitting on its two legs. After washing and cleaning the inside of the gantry, the z-axis was ready to be assembled. The following steps were followed in order:

1. Spacer A was bolted to the z-axis reference surface of the gantry, sitting against *the z-axis reference* edge to assure its straightness and perpendicularity. A torque-wrench was used to tighten the bolts, and lock-tight was used to create a permanent attachment. Spacer B was bolted to the z-axis reference surface, using spacer A as a reference.
2. Linear rail A was bolted to Spacer A, sitting against the reference edge of the spacer to assure its straightness and perpendicularity. The bolts were torqued, and

lock-tightened. Linear rail B was assembled using only its first and last bolt. The bolts were not tightened, to allow for the rail to move slightly.

3. The head plate was bolted to the linear guides, by lining up the edge with the linear guide. The head plate was moved up and down several times to assure that rail B was parallel to rail A. The bolts for this rail were then tightened.
4. The Z-Axis ball screw was bolted to the roof, by moving the head plate up and down and tightening the bolts in the process. The z-ball nut timing pulley was bolted to the z-ball nut.
5. The motor was attached to the roof. The z-axis shaft extender was attached to the motor shaft in order to lengthen it. The z-motor timing pulley was attached to the shaft extender. The belt was placed between the two pulleys, and the motor was pulled back to tighten the belt. The z-axis roof plate was bolted to cover the inside of the gantry.
6. The pneumatic piston attachment was attached to the head plate. Thereafter, the piston was attached to the roof from one side, and to the head plate from the other side.

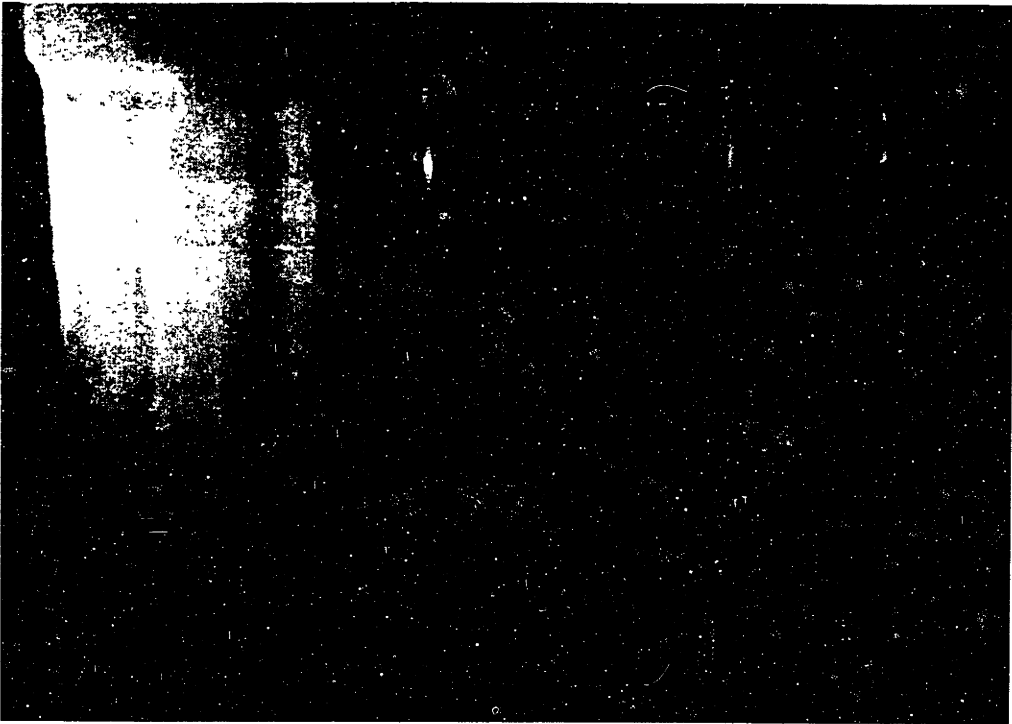


Figure 7.1 : Z-Axis Assembly

7.2.2 Assembly of the X-Axis

Once the granite table had been received, the assembly of the x-axis was begun immediately. Since the assembly of the gantry onto the granite table was very difficult, a dummy gantry was created for assembling the x-axis before the actual gantry could be attached. This was done to test and debug the control algorithm before attaching on the real gantry. An aluminum plate with holes correlating to those of the gantry was used to get this axis of motion running before the final assembly of the upper structure. The following steps were taken:

1. The linear guides were bolted to the granite table on one side. The two separate rails were lined up using a straight edge. A torque-wrench was used to tighten the bolts. The linear guides were also bolted on the other side, leaving the bolts loose to allow for the rails to move slightly.

2. The motor brackets and the bearing spacers were bolted to the granite table on both sides. The bearing housings were separately assembled, and they were bolted to the motor brackets and the bearing spacers.
3. The dummy gantry was bolted to the linear guides. The aluminum plate was moved back and forth several times, and the linear rails were tightened in the process.
4. The ball screws were attached to the bearing housings, and the dummy gantry. Belleville washers were used to properly tension the ball screws.
5. The motors were attached to the motor brackets, and flexible couplings were used to attach the ball screws to the motor shafts.

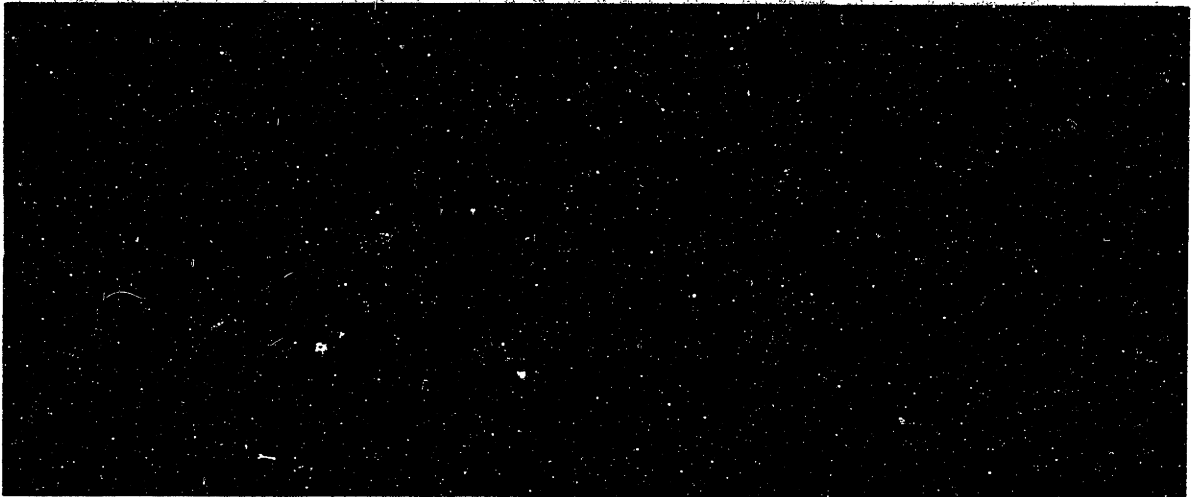


Figure 7.2: X-Axis Assembly Without the Actual Gantry

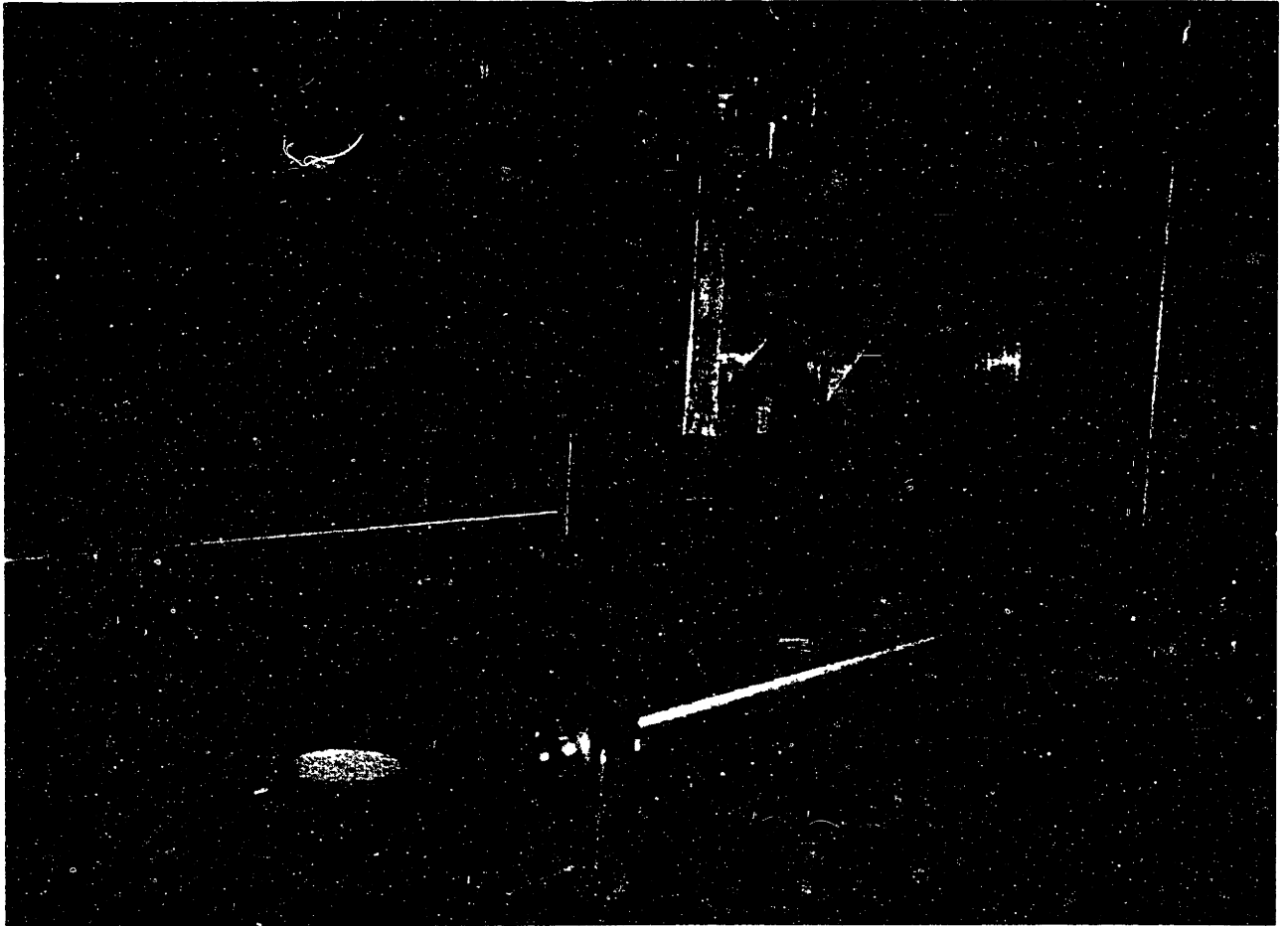


Figure 7.3: X-Axis Assembly

7.2.3 Assembly of the Upper Machine Structure

Once the x-axis was fully assembled and running, the upper machine structure was ready to be assembled onto the lower structure. This proved to be very difficult since the gantry weighed over a ton, and the full height of the machine would hit the ceiling lights. These lights were removed to create room for the gantry. An outside rigging company was hired to get the gantry on top of the lower structure. Using an "A-Crane Gantry Crane," the gantry was lifted and placed above the linear guides. At this position, the connecting bolts were tightened from under the linear guides.



Figure 7.4: Upper Machine Structure Assembly

7.2.4 Assembly of the Load/Unload Station

The load/unload station was easier and quicker to assemble, since it consisted of smaller and lighter components. Dowel pins were press-fitted into the driving linkages, and teflon washers were used at the joints to reduce friction. O-rings were pressed into the shaft grooves, and bearings were used to hold the shafts in place. The motor was secured in place after bolting the motor bracket to the body. The motor shaft was then

attached to “link #1” (a circular disk) which was connected to the remaining four linkages. The following picture shows the final assembly of the load/unload station:

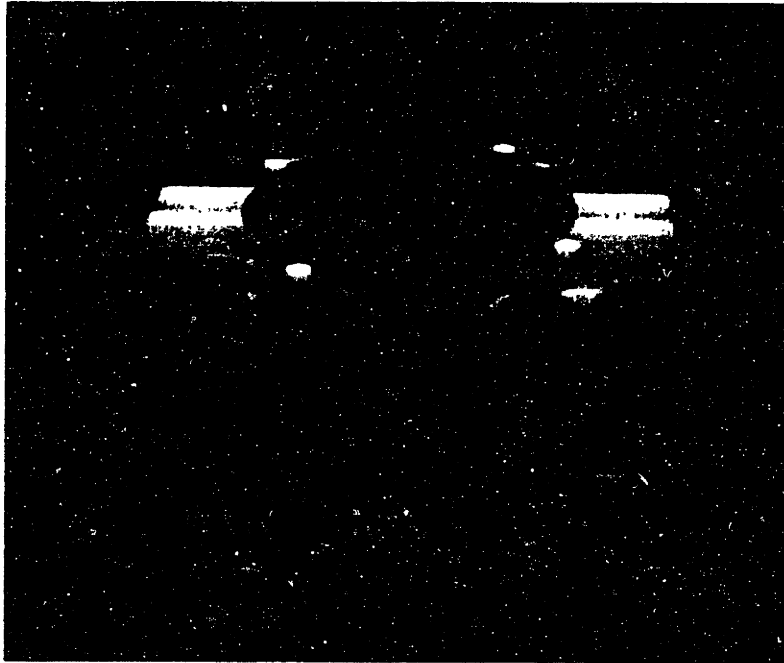


Figure 7.5: Load/Unload Station Assembly

7.3 TESTING

7.3.1 Velocity, Acceleration, and Smoothness

7.3.1.1 X-Axis Smoothness

To measure the x-axis smoothness, the gantry was moved by an arbitrary distance of 500 mm. The position, velocity, and acceleration of this motion were collected and plotted as functions of time. The control system was designed to provide a *trapezoidal velocity profile* for the movement of the gantry. As seen from the figure, one side of the trapezoid is steeper than the other side. This means that in order for the gantry to come to a smooth stop, it requires a high take off acceleration and a low deceleration rate. This can also be seen from the acceleration graph, where the positive acceleration is much

higher than the negative acceleration. The maximum velocity of the gantry in this case is 4.8 in/sec (120 mm/sec), which is about 1/3 of its maximum velocity (12 in/sec). The maximum acceleration is also 0.06 g's (600 mm/s²) which is about 1/3 of its maximum acceleration (0.2 g's). Looking at the acceleration graph, the smoothness of the x-axis motion is about 0.02 g's.

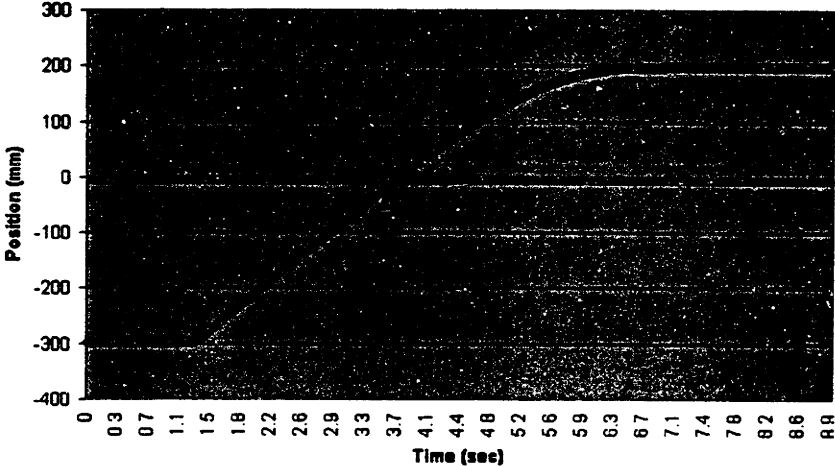


Figure 7.6: X-Axis Position

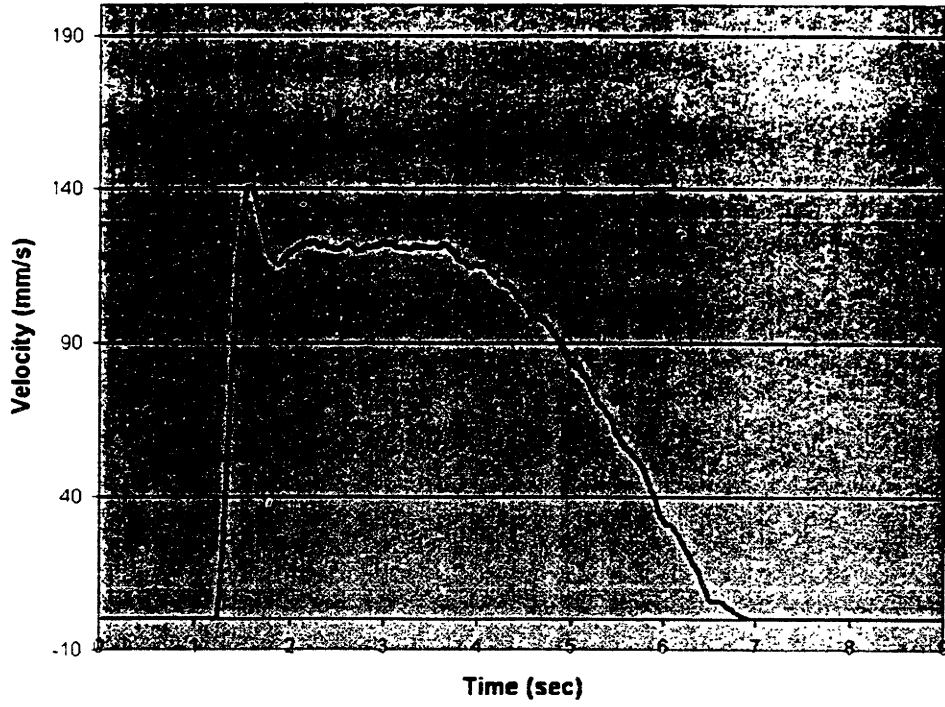


Figure 7.7: X-Axis Velocity

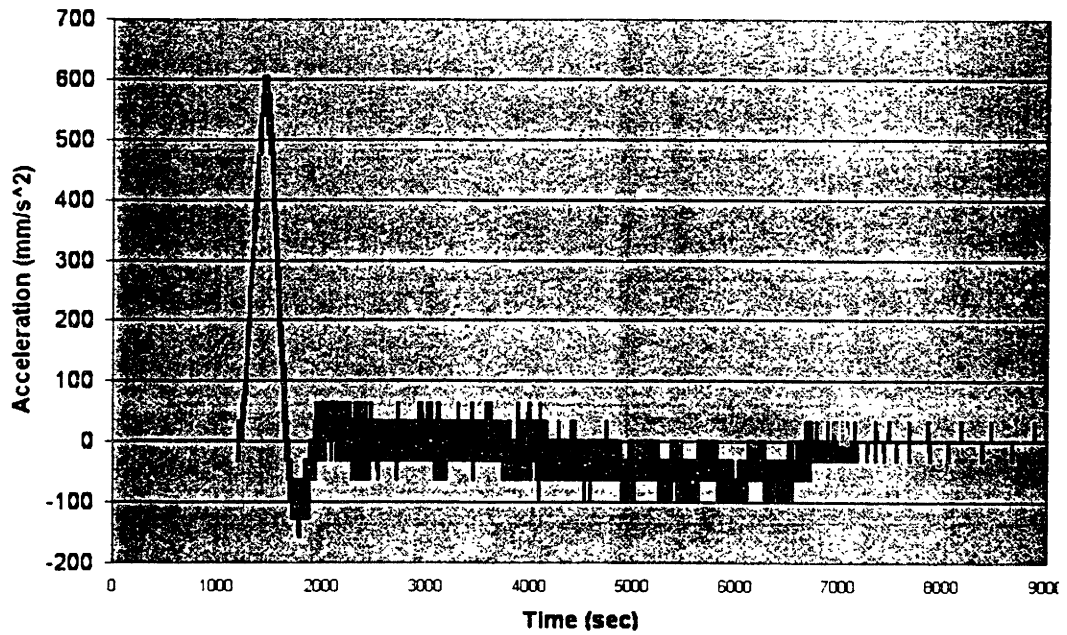


Figure 7.8: X-Axis Acceleration

7.3.1.2 Z-Axis Smoothness

The same procedure was followed to measure the z-axis smoothness. The head plate was moved to an arbitrary distance of 100 mm. The position, velocity, and acceleration of this motion were collected and plotted as functions of time. The control system was similarly designed to provide a *trapezoidal velocity profile* with a high acceleration and a low deceleration. The maximum velocity of the head plate in this case was 1.18 in/sec (35 mm/sec) which is about half of its maximum velocity (2.5 in/sec). The maximum acceleration is also 0.019 g's (190 mm/s²), and the smoothness of the z-axis motion is about 0.003 g's.

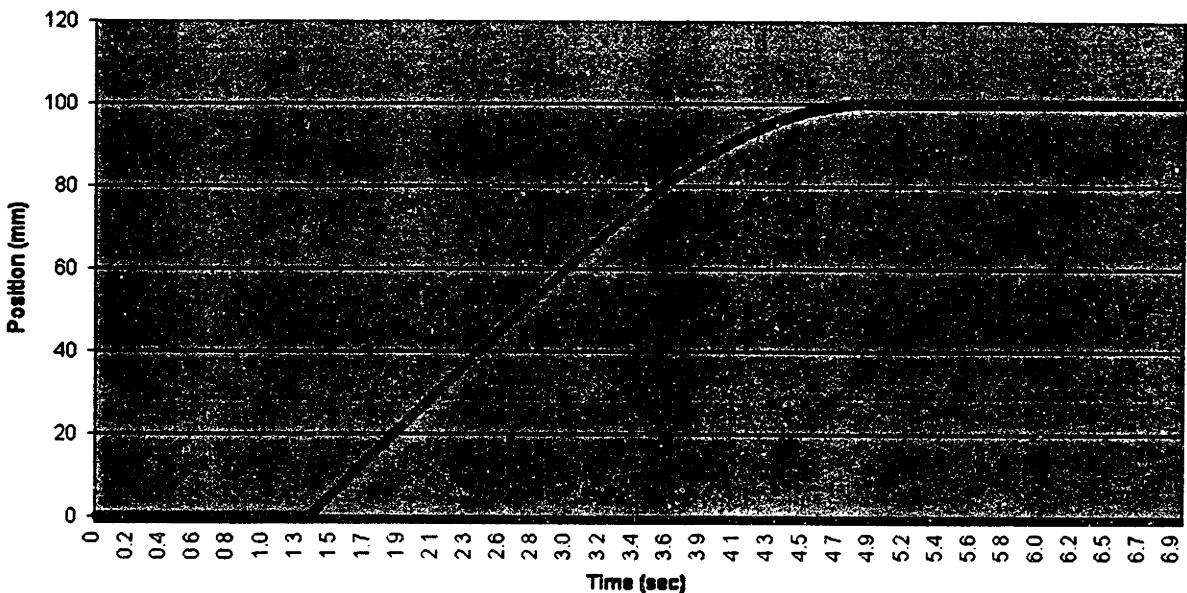


Figure 7.9: Z-Axis Position

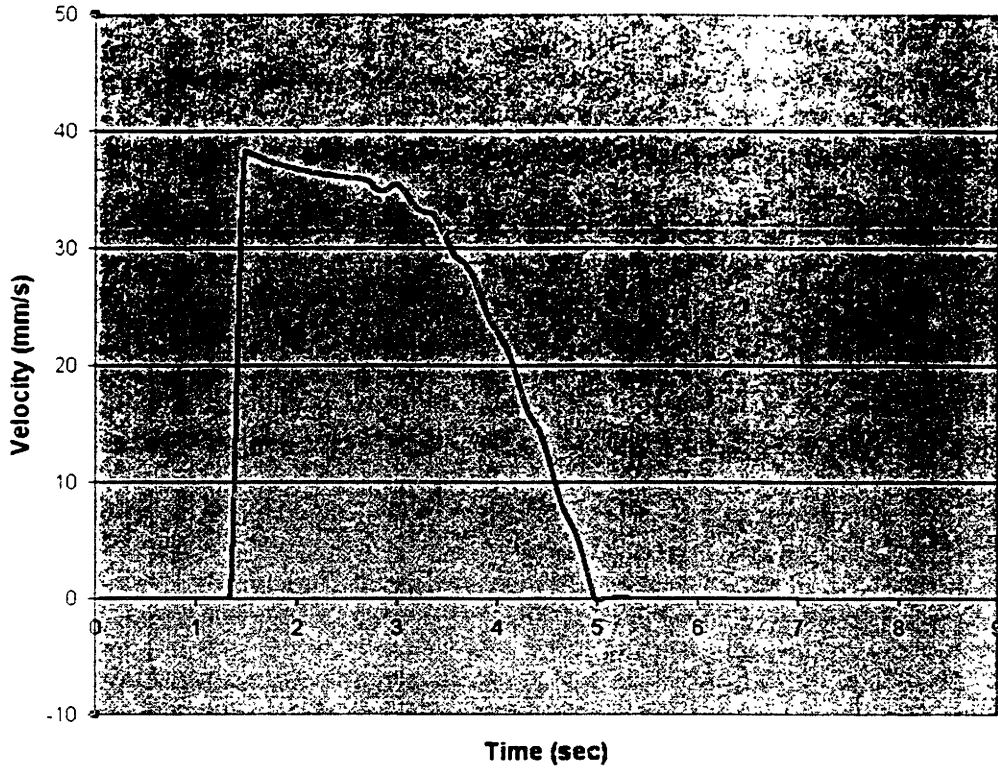


Figure 7.10: Z-Axis Velocity

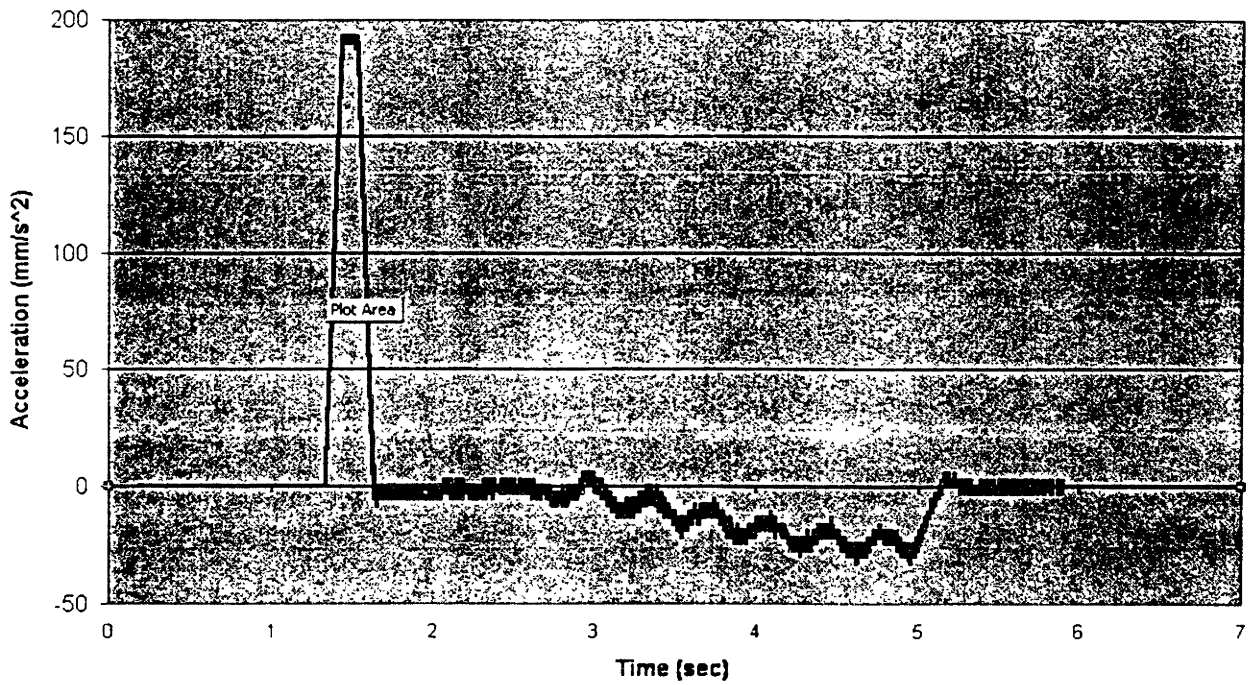


Figure 7.11: Z-Axis Acceleration

7.3.2 Frequency Response Analysis

Knowing the dynamics of the system plays a key role in designing the control algorithm, and understanding the behavior of the drive mechanism. The exact values of some parameters, such as friction and damping, can only be determined by running experiments on the fully-assembled system. One approach is to disturb the system with a step-input and plot the output to determine the necessary parameters. However, if the order of the system is unknown, this approach will not work. In such a case it becomes important to identify the transfer function of the system. As previously mentioned, the x and z axes were initially modeled as second order systems. In reality, however, these systems behave quite differently.

To determine the transfer function of a drive mechanism, it is necessary to plot its corresponding Bode diagram. This requires measuring the magnitude of the output of the system over its input (in dB's), while running the system at different frequencies. This is done by performing a "sweep frequency analysis," in which the input command has a variable frequency that increases with time (i.e. input $X = A \sin \omega t$, where $\omega = c.t$). This analysis was done on the x -axis to identify the system. The importance of the information provided in the following figure cannot be over looked. The peaks here correspond to the resonance frequencies of the x -axis. These frequencies must be kept in mind while determining the bandwidth of the controller.

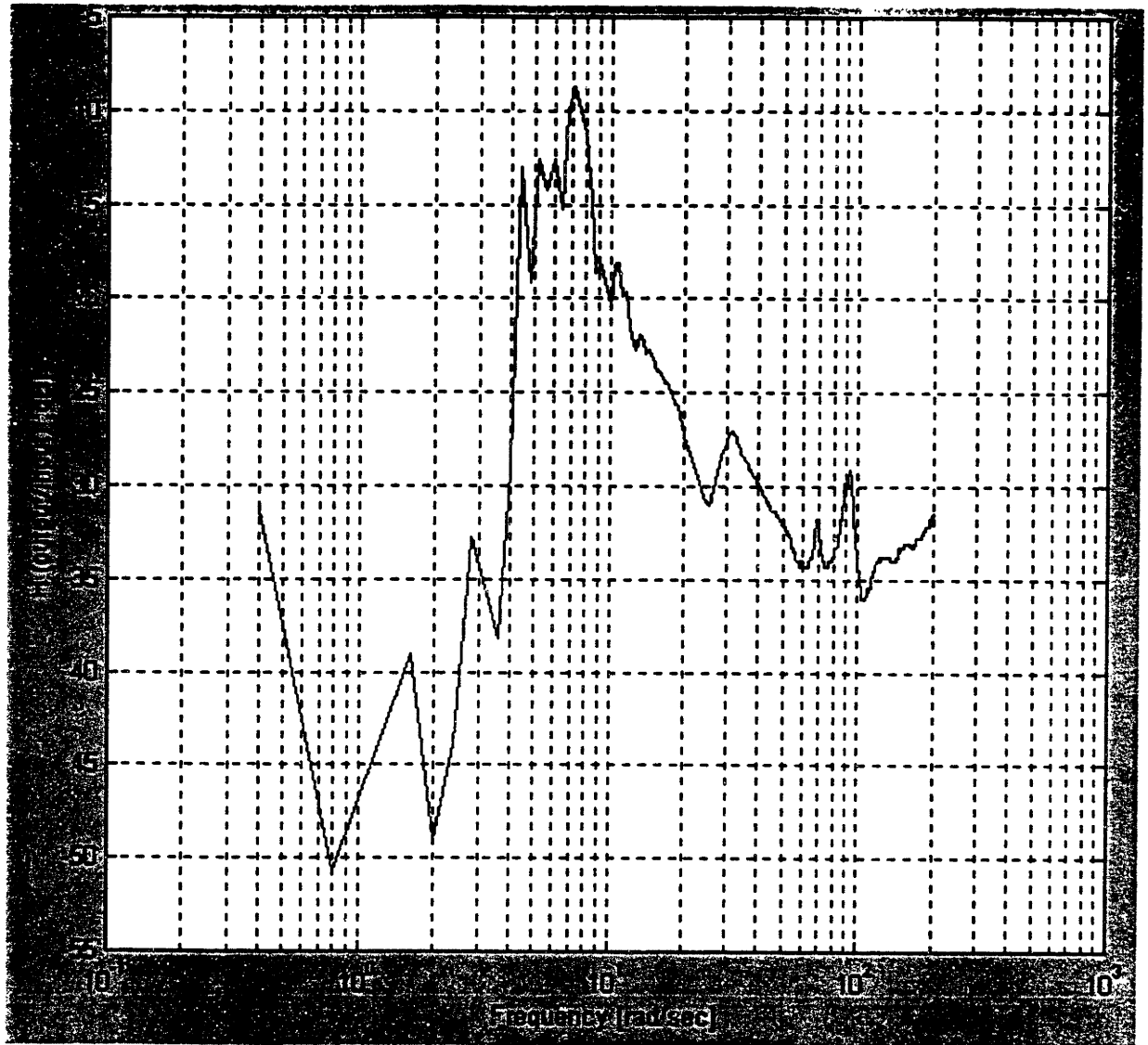


Figure 7.12: Frequency Response of the X-Axis

7.3.3 Accuracy, Resolution, and Repeatability

Another important test to run on the CMP upper machine structure determines the *accuracy, resolution, and repeatability* of the two linear axes of motion. The resolution of the x and z-axes is determined by the resolution of their linear encoders. Once the system was connected, the z-axis linear encoder could read positions *of up to 10 microns*,

while the z-axis linear encoder could read positions of up to 50 nm. The repeatability and accuracy of the two axes are expected to be higher than their resolutions. A dial-gauge was used to check for the repeatability of these drive mechanisms. The following data was collected for each axis of motion.

7.3.3.1 X-Axis Repeatability

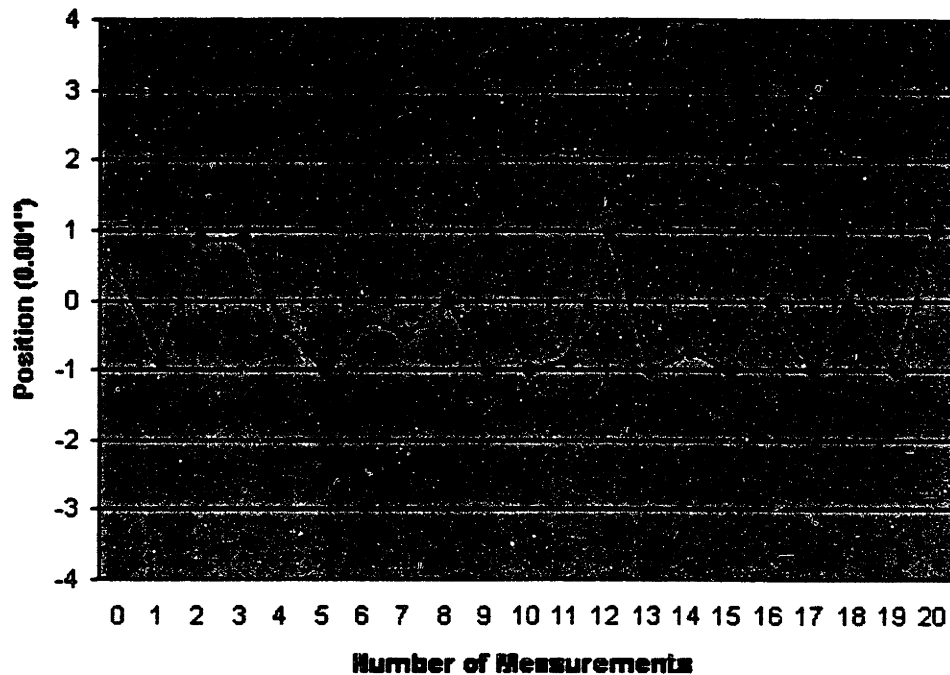


Figure 7.13: X-Axis Repeatability Measurements

The dial-gauge was set to zero at a certain position along the travel of the x-axis. The gantry was moved 500 mm away from the gauge, and it was then returned to the same position. Twenty data points were collected for the same experiment, and every time the gantry repeated its position to + 0.001". The average of the above data points is - 0.298 mils, and the standard deviation is 0.755 mils. The repeatability of the x-axis, which is three times its standard deviation, is about 0.0023".

7.3.4 Z-Axis Repeatability

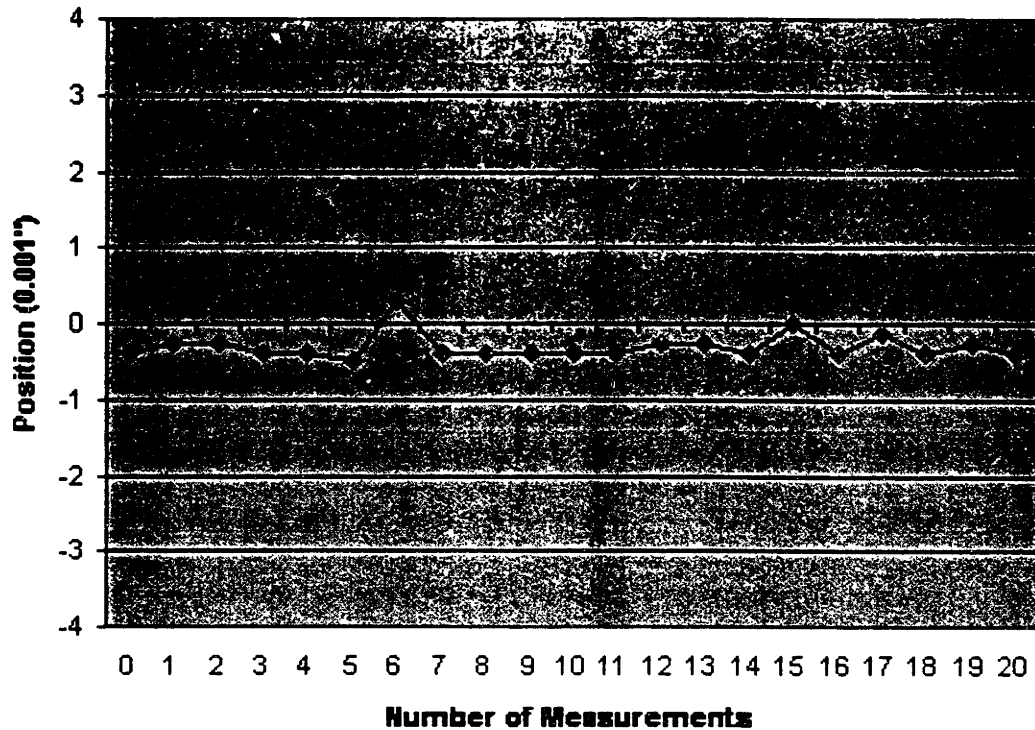
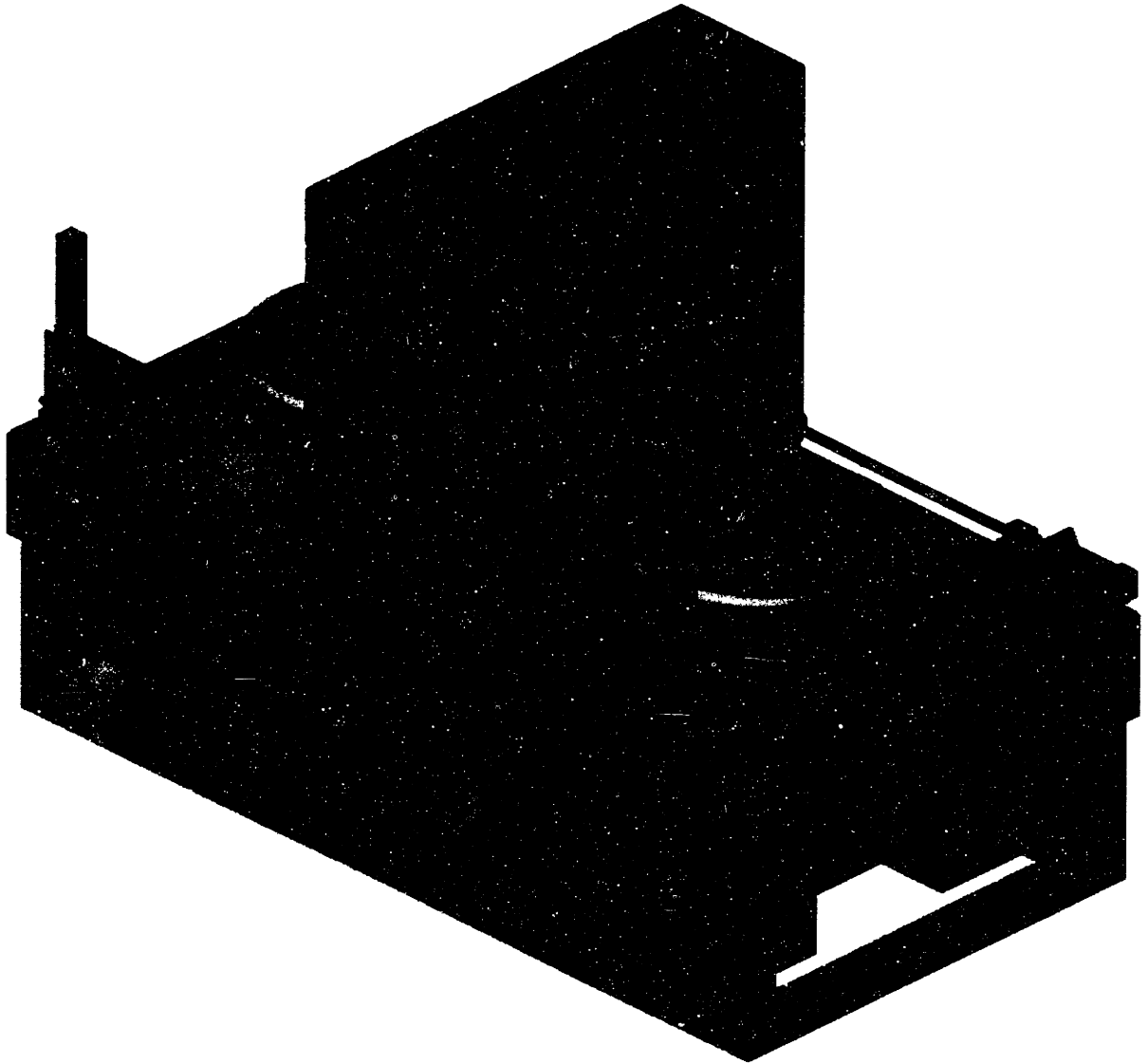


Figure 7.14: Z-Axis Repeatability Measurements

The same procedure was followed for testing the repeatability of the z-axis. The head plate was moved back 100 mm from the dial gauge, and it was then returned back to the same position. Twenty data points were collected for the same experiment, and every time the head plate repeated its position to $+0.0005$ ". The average of the above data points is -0.289 mils, and the standard deviation is 0.173 mils. The repeatability of the z-axis is about 0.00051 ".



The CMP Machine

Birthrate: January 2000

Birthplace: MIT, Cambridge, MA

APPENDIX

Sample Design Calculations

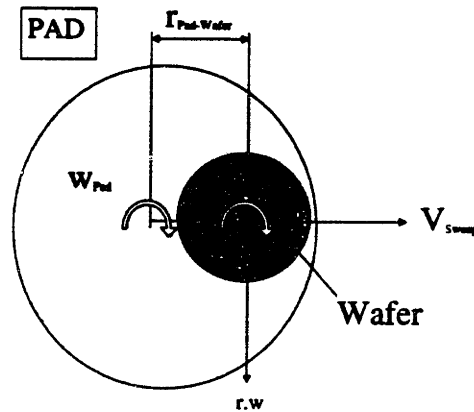
Wafer-Pad Kinematics

$$\vec{V}_{Relative} = \vec{V}_{Pad} - \vec{V}_{Wafer}$$

$$\vec{V}_{Pad} = \vec{\omega}_{Pad} \times \vec{r}_{Pad-Wafer}$$

$$\vec{V}_{Wafer} = \vec{V}_{Sweep} + \vec{\omega}_{Pad} \times \vec{r}_{Wafer-Pad}$$

$$\Rightarrow \boxed{\vec{V}_{Relative} = V_{Sweep} \hat{i} - (\omega_{Pad} r_{Pad-Wafer}) \hat{j}}$$



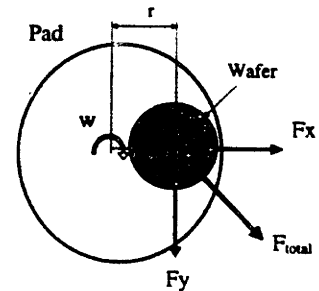
External Forces Acting on the Wafer

$$|\vec{F}_{Total}| = \mu P_{max} A_{Wafer}$$

$$\vec{F}_{Total} = |\vec{F}_{Total}| \cdot \left\{ \begin{array}{l} \vec{V}_{Relative} \\ |\vec{V}_{Relative}| \end{array} \right\}$$

$$\vec{F}_{Total} = \mu P_{max} A_{Wafer} \frac{V_{Sweep}}{\sqrt{(r\omega)^2 + V_{Sweep}^2}} \hat{i} - \mu P_{max} A_{Wafer} \frac{(r\omega)}{\sqrt{(r\omega)^2 + V_{Sweep}^2}} \hat{j}$$

$$\Rightarrow \boxed{F_x = 100\text{lbs}, F_y = 200\text{lbs}, F_z = 750\text{lbs}}$$



Velocity and Acceleration of X and Z Axes

$$\omega = 2\pi f$$

$$X = A \sin(\omega t)$$

$$\dot{X} = -A\omega \cos(\omega t)$$

$$\ddot{X} = A\omega^2 \sin(\omega t)$$

f = Sweep Frequency = 1 Hz

A = Sweep Amplitude = 5 cm

$$\Rightarrow \boxed{\dot{X}_{\max} = 12 \text{ in/sec} \quad \ddot{X}_{\max} = 0.2 g's}$$

$$\dot{Z} = \frac{Z}{t}$$

Z = Z-Travel = 8"

T = travel time = 3 sec

$$\Rightarrow \boxed{\dot{Z}_{\max} = 2.5 \text{ in/sec}}$$

X-Axis Ball Screw Calculations

$$T_{\text{BallScrew}} = F_x + m_{\text{Gantry}} \ddot{X}_{x\text{-axis}}$$

$$\omega_{\text{BallScrew}} = \frac{\dot{X}_{\text{Gantry}}}{\xi}$$

$$\omega_{\text{Critical}} = (4.8 \times 10^6) C_s \frac{d_r}{L^2}$$

$$\omega_{\text{BallScrew}} < \omega_{\text{Critical}}$$

d_r = Ball screw root diameter (0.880")

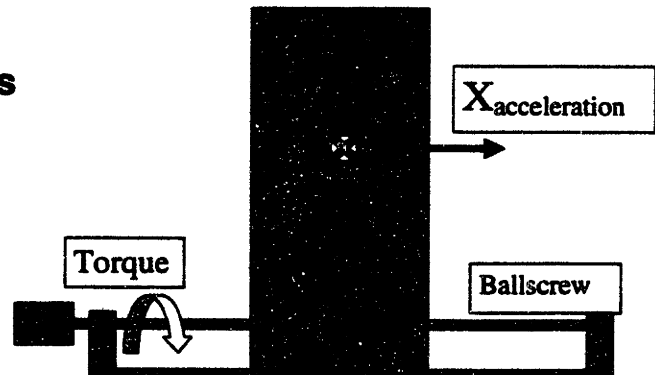
C_s = Support Constant (2.4 for fixed-fixed)

L = Length of the ball screw (72")

$T_{\text{BallScrew}}$ = Axial Load on the ball screw

ξ = Lead of the ball screw (1 in/rev)

$$\Rightarrow \boxed{T = 200 \text{ lbs, } \omega_{\text{ballScrew}} = 600 \text{ RPM, } \omega_{\text{critical}} = 1300 \text{ RPM}}$$



Z-Axis Ball Screw Calculations

$$T_{\text{Ball screw}} = F_z$$

$$T_{\text{Buckling}} = \frac{\pi^2 EI}{L^2}$$

$$T_{\text{Ball screw}} < T_{\text{Buckling}}$$

$$\omega_{\text{Ball screw}} = \frac{\dot{z}}{\xi}$$

$$\Rightarrow T_{\text{ball screw}} = 1000 \text{ lbs, } T_{\text{buckling}} = 6,300 \text{ lbs}$$

Z-Axis Motor

$$\tau_{\text{Motor}} = \left(\frac{\xi F_z}{2\pi\eta} \right) \frac{Z_2}{Z_1}$$

Z_1 = # of teeth of small pulley

Z_2 = # of teeth of large pulley

η = Ball screw Efficiency (90%)

ξ = Ball screw lead (16mm/rev)

$$\Rightarrow T_{\text{motor}} = 2.9 \text{ N.m}$$

15.1 X-Axis Motor

$$\tau_{\text{Motor}} = \frac{\xi F_x}{2\pi\eta}$$

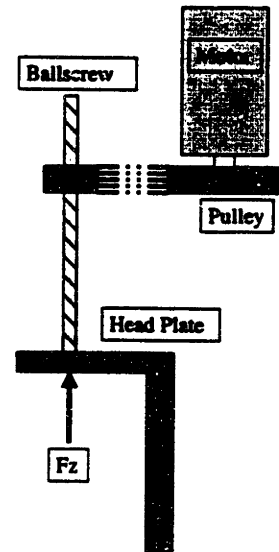
$$\Rightarrow T_{\text{motor}} = 2.5 \text{ N.m}$$

Z-Axis Timing Belt

$$L_{\text{Belt}} = \frac{t}{2}(Z_1 + Z_2) + 2a + \frac{1}{4a} \left\{ \frac{(Z_2 - Z_1)}{\pi} \right\}^2$$

a = center-to-center distance

t = pitch of the belt



X-Axis Dynamics Modeling

$$\tau_{Motor} = \tau_{Friction} + J_{Equivalent} \ddot{\theta}_{motor} + B_{Equivalent} \dot{\theta}_{motor}$$

$$J_{Equivalent} = J_{Motor} + J_{Flexible-Coupling} + J_{Ballcrew} + J_{Gantry}$$

$$J_{Gantry} = \frac{m_{Gantry}}{\xi^2}$$

$$B_{Equivalent} = B_{Motor} + B_{Flexible-Coupling} + B_{Ballcrew} + B_{Gantry}$$

$$\frac{X(S)}{\tau_{motor} - \tau_{friction}} = \frac{0.9357}{S^2 + 0.000172.S}$$

$J_{Equivalent}$ = Equivalent Inertial of the X-Axis (0.004323 Kg-m²)

$B_{Equivalent}$ = Equivalent Damping of the X-Axis (0.000172 N-m/rad/sec)

$T_{friction}$ = Frictional Load on the Motor (0.1500 N-m)

Z-Axis Dynamics Modeling

$$\tau_{Motor} = \tau_{Friction} + J_{Equivalent} \ddot{\theta}_{motor} + B_{Equivalent} \dot{\theta}_{motor} + \left\{ \frac{N_{polishing-load} - P_{Piston} A_{Piston} - m_{Head-plate} g}{\xi} \right\} \frac{Z_2}{Z_1}$$

$$J_{Equivalent} = J_{Motor} + J_{pulley1} + \left(J_{pulley2} \right) \frac{Z_2}{Z_1} + J_{Head-Plate}$$

$$J_{Head-Plate} = \left(\frac{m_{Head-Plate}}{\xi^2} \right) \frac{Z_2}{Z_1}$$

$$B_{Equivalent} = B_{Motor} + B_{Timing-Belt} + B_{Ballcrew}$$

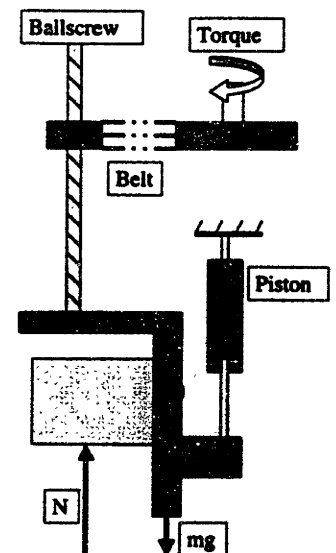
$J_{Equivalent}$ = Equivalent Inertial of the Z-Axis (0.00366 Kg-m²)

$B_{Equivalent}$ = Equivalent Damping of the Z-Axis (0.000172 N-m/rad/sec)

$T_{friction}$ = Frictional Load on the Motor (0.1500 N-m)

P_{piston} = Pressure Applied by the Piston

$N_{polishing-Load}$ = Desired Polishing Load on the Wafer



$$\delta_{gantry} = \frac{PL^3}{192EI} \text{ (Fixed-Fixed Support)}$$

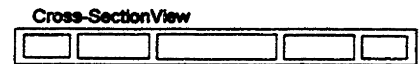
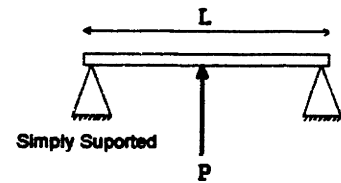
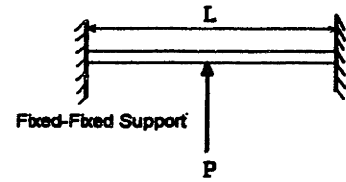
$$\delta_{gantry} = \frac{PL^3}{48EI} \text{ (Simply Supported)}$$

I = moment of Inertia of the Gantry Roof (36 in⁴)
E = Modulus of Elasticity of Stainless Steel (30e6 psi)
P = Z-Axis Load (1000 lbs)
L = Free-Length of the Gantry Roof (21")

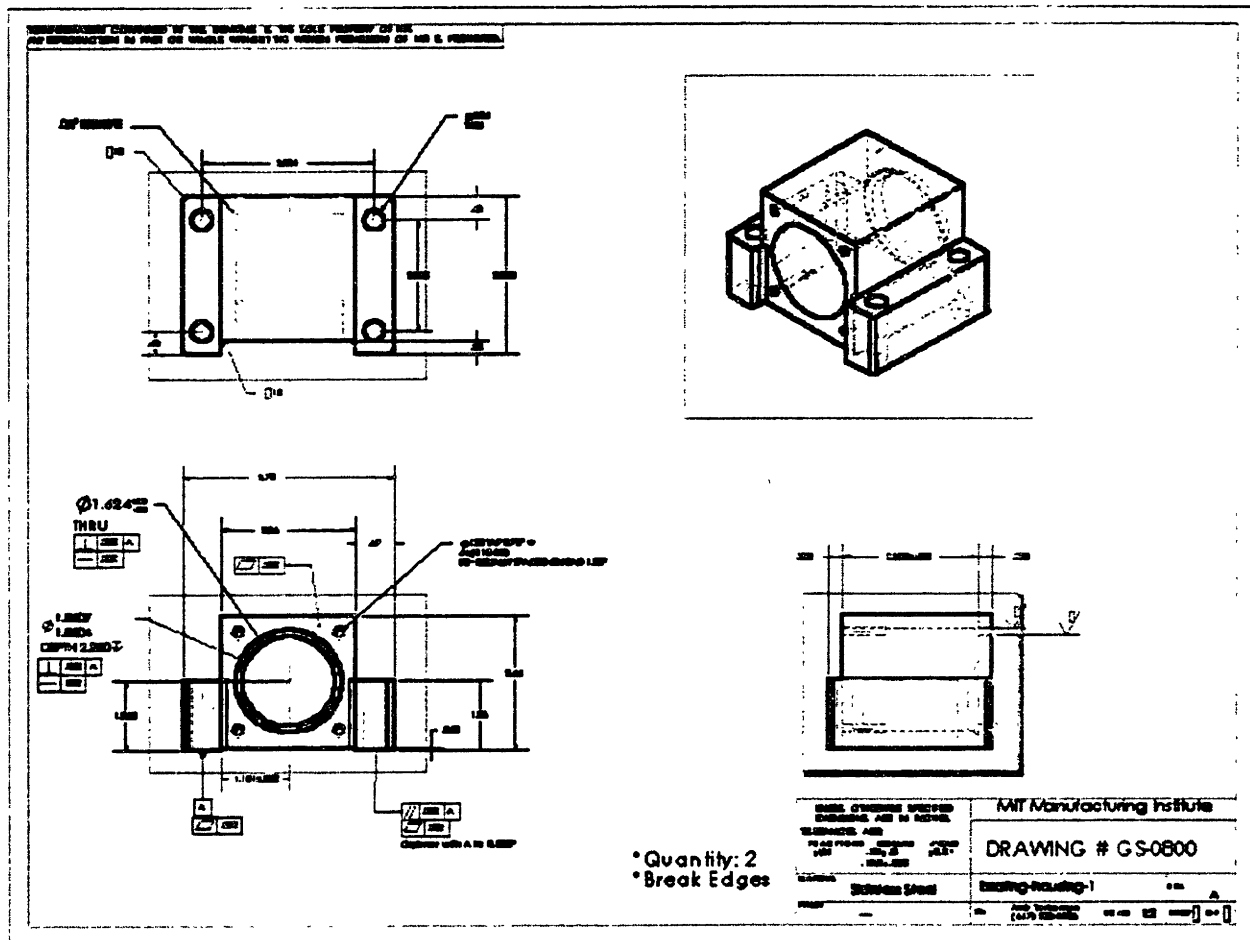
$$\Rightarrow \delta_{\text{simply-Supported}} = 0.0042 \text{ mm}, \delta_{\text{fixed-fixed}} = 0.0014 \text{ mm}$$

Check Results with FEA-Analysis of the Gantry Structure:

$$\delta_{\text{FEA}} = 0.0061 \text{ mm}$$



Sample Engineering Drawing



References

- [1] Robert J. Lineback. "Fab Strategies: Why CMP is becoming essential." *Semiconductor Business News*, November, 1998.
- [2] Ruth Dejule. "CMP Grows in Sophistication." *Semiconductor International*, November, 1998.
- [3] Arthur H. Altman. "Applying Run-By-Run Process control to Chemical-Mechanical Planarization and Assessing Insertion Costs Versus Benefits of CMP." Ph.D. Thesis, MIT, Electrical Engineering Department, 1995.

THESIS PROCESSING SLIP

FIXED FIELD: ill. _____ name _____

index

biblio

► COPIES: Archives Aero Dewey Eng Hum
Lindgren Music Rotch Science

TITLE VARIES: ► _____

NAME VARIES: ► Hesem

IMPRINT: (COPYRIGHT) _____

► COLLATION: _____

► ADD: DEGREE: _____ ► DEPT.: _____

SUPERVISORS: _____

NOTES:

cat'r:

date:

► DEPT: M.C.

page: 5134
► F37

► YEAR: 2000 ► DEGREE: S.M.

► NAME: TERKINGTON, Almir